AD-A034 264 ADVISORY GROUP FOR AEROSPACE RESEARCH AND DEVELOPMENT--ETC F/G 20/4
FLOW OF SOLID PARTICLES IN GASES,(U)
OCT 76 G RUDINGER
UNCLASSIFIED AGARD-OGRAPH-222 NL

1 OF 1
AD-A
034 264

END
DATE
FILMED
2-16-77
NTIS

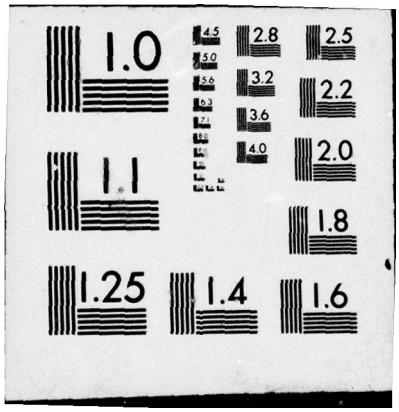
1.0
1.1
1.25
1.4
1.6
1.8
2.0
2.2
2.5
2.8
3.2
3.6
4.0
4.5
5.0
5.6

FLOW OF SOLID PARTICLES IN GASES

ADVISORY GROUP FOR AEROSPACE RESEARCH AND DEVELOPMENT, PARIS, FRANCE

OCTOBER 1976

AGARD-AG-222

AGARD-AG-222

AGARD

ADVISORY GROUP FOR AEROSPACE RESEARCH & DEVELOPMENT

7 RUE ANCELLE 92200 NEUILLY SUR SEINE FRANCE

AGARDograph No. 222

on

Flow of Solid Particles in Gases

by

G.Rudinger

NORTH ATLANTIC TREATY ORGANIZATION

DISTRIBUTION AND AVAILABILITY ON BACK COVER

NORTH ATLANTIC TREATY ORGANIZATION

ADVISORY GROUP FOR AEROSPACE RESEARCH AND DEVELOPMENT

(ORGANISATION DU TRAITE DE L'ATLANTIQUE NORD)

AGARDograph No.222

FLOW OF SOLID PARTICLES IN GASES

by

George Rudinger
Adjunct Professor of Mechanical Engineering
State University of New York at Buffalo
Buffalo, New York, USA

Edited by

A.Auriol
Directeur de l'Institute Franco-Allemand de Recherches
de Saint-Louis, France

This AGARDograph was prepared at the request of the Fluid Dynamics Panel of AGARD.

THE MISSION OF AGARD

The mission of AGARD is to bring together the leading personalities of the NATO nations in the fields of science and technology relating to aerospace for the following purposes:

- Exchanging of scientific and technical information;
- Continuously stimulating advances in the aerospace sciences relevant to strengthening the common defence posture;
- Improving the co-operation among member nations in aerospace research and development;
- Providing scientific and technical advice and assistance to the North Atlantic Military Committee in the field of aerospace research and development;
- Rendering scientific and technical assistance, as requested, to other NATO bodies and to member nations in connection with research and development problems in the aerospace field;
- Providing assistance to member nations for the purpose of increasing their scientific and technical potential;
- Recommending effective ways for the member nations to use their research and development capabilities for the common benefit of the NATO community.

The highest authority within AGARD is the National Delegates Board consisting of officially appointed senior representatives from each member nation. The mission of AGARD is carried out through the Panels which are composed of experts appointed by the National Delegates, the Consultant and Exchange Program and the Aerospace Applications Studies Program. The results of AGARD work are reported to the member nations and the NATO Authorities through the AGARD series of publications of which this is one.

Participation in AGARD activities is by invitation only and is normally limited to citizens of the NATO nations.

Published October 1976

ISBN 92-835-1228-6

Printed by Technical Editing and Reproduction Ltd
Harford House, 7–9 Charlotte St, London, W1P 1HD

FOREWORD

During the meeting of the AGARD Fluid Dynamics Panel in Rome, Italy, September 1974, one day was devoted to the topic of Multiple Flow of Solids and Gases to review the activities in this field in various countries. Five survey papers were presented by representatives of France, West Germany, United Kingdom, Belgium, and the United States. Subsequently, the undersigned was invited to prepare an AGARDograph based on these presentations.

The papers were prepared by the individual authors and are collected here in the order in which they were presented at the meeting. Minor updating and clarifications were incorporated in cooperation with these authors. The final text, was established with the concurrence of the Editor, Ing. Gen. A. Auriol, Directeur de l'Institut Franco-Allemand de Recherches de Saint-Louis, France.

Several topics are discussed in more than one paper. Therefore, cross references were inserted in the text to facilitate comparison of different points of view. These identify the papers consecutively by A to E and the appropriate subsections. In addition, a subject index was prepared to allow quick location of specific topics.

It is a great pleasure to thank the Fluid Dynamics Panel of AGARD for the invitation to prepare this material and to acknowledge the cooperation of the authors of the papers, of Ing. Gen. A. Auriol, and of Mr. J. A. Lawford and Mr. M. C. Fischer, Executives of the Fluids Dynamics Panel. The help of Textron Bell Aerospace Company and the State University of New York at Buffalo, New York, in the preparation of the manuscript is greatly appreciated.

George Rudinger

Buffalo, New York
September 1976

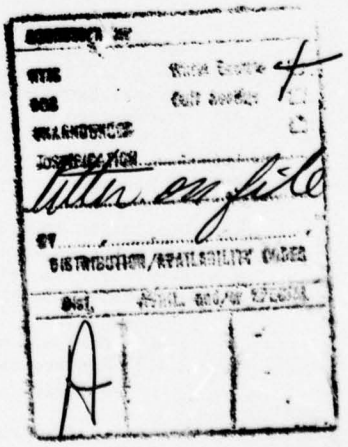

CONTENTS

REPORT DOCUMENTATION PAGE			
1. Recipient's Reference	**2. Originator's Reference** AGARD-AG-222	**3. Further Reference** ISBN 92-835-1228-6	**4. Security Classification of Document** UNCLASSIFIED
5. Originator	Advisory Group for Aerospace Research and Development North Atlantic Treaty Organization 7 rue Ancelle, 92200 Neuilly sur Seine, France		
6. Title	FLOW OF SOLID PARTICLES IN GASES		
7. Presented at			
8. Author(s)	G.Rudinger Editor: A.Auriol		**9. Date** October 1976
10. Author's Address	Adjunct Professor of Mechanical Engineering State University of New York at Buffalo Buffalo, New York, USA		**11. Pages** 95
12. Distribution Statement	This document is distributed in accordance with AGARD policies and regulations which are outlined on the Outside Back Covers of all AGARD publications.		
13. Keywords/Descriptors	Solids flow Gas flow Multiphase flow	Gas dynamics Reviews Research projects	

14. Abstract

During a meeting of the AGARD Fluid Dynamics Panel held in Rome, Italy in September 1974, one day was devoted to a review of activities in various countries in the field of multiple flow of solids and gases. Five survey papers were presented by representatives of France, West Germany, United Kingdom, Belgium and the United States.

This AGARDograph includes edited versions of these five papers, which are printed in the order of their presentation at the meeting. The papers are: French Contribution to Aerodynamics of Gas-Particle Mixtures (P.Kuentzmann); Gas Flows with Solid Particles: Research and Development in Germany (W.Wuest); Review of Research in the UK in the field of Multiple Flows of Solids and Gases (R.A.Duckworth); Flow of Solid Particles in Gases: Activities at the Von Kármán Institute for Fluid Dynamics (J.J.Ginoux and M.Riethmuller); Fundamentals and Applications of Gas-Particle Flow (G.Rudinger). The AGARDograph also includes cross-references between papers, and a subject index.

This AGARDograph was prepared at the request of the Fluid Dynamics Panel of AGARD.

A. FRENCH CONTRIBUTION TO AERODYNAMICS OF GAS-PARTICLE MIXTURES

Paul Kuentzmann
Chef de Groupe de Recherche à l'O.N.E.R.A.
Office National d'Etudes et de Recherches Aérospatiales (ONERA)
92320 Chatillon, France

SUMMARY

Mixed gas-particle flows were studied in France mainly for particular applications. Three examples, concerning the aerospace field, are presented; they concern rocket propulsion, laser anemometry and capture of droplets. From the main problems encountered in these studies, it has been possible to shed some light on the most important fundamental problems.

A precise knowledge of the particle size distribution is essential in most cases, and improvements in optical techniques are desirable. Velocity measurements, satisfactory for small concentrations, should be extended to larger ones. Temperature measurement methods for both phases exist. Interactions between particles should be better known.

Two-phase flows, the importance of which is expected to increase in the future, should be at first the subject of two types of research: fundamental studies of elementary mechanisms and development of new experimental means.

1. INTRODUCTION

1.1 General

Gas-particle mixtures belong to the category of dispersions, that is of media made of a continuous fluid phase and of another phase distributed among discrete volume elements. There exist, a priori, five possible combinations according to the nature of the two phases; they can be classified by considering first the fluid phase:

- Liquid fluid phase:
  - Solid dispersed phase: suspension
  - Liquid dispersed phase: emulsion
  - *Gaseous dispersed phase: foam*
- Gaseous fluid phase:
  - Solid dispersed phase: suspension, smoke, fluidized bed
  - Liquid dispersed phase: mist, fog

We shall concentrate here on aerodynamic phenomena, i.e., on dispersions in which the fluid phase is gaseous. Mixtures in which the fluid phase is liquid, the dispersed phase being liquid or solid, can be treated by the same methods as the gas-particle mixture; but the properties of liquid-gas mixtures can be more varied.

A detailed listing of gas-particle mixtures can be established according to the two following parameters: the volume fraction occupied by the condensed phase, and the mean dimensions of the dispersed elements. This classification is given in the following table.

Classification of the mixtures of gas and particles (1).

Particle State	Name of the Mixture	Partial Volume Occupied by the Condensed Phase	Mean Size of the Particles
Liquid	Fog	$\ll 1$	$< 0.1\mu m$
	Cloud	$\ll 1$	$> 0.1\mu m$
	Aerosol	$\ll 1$	very small droplets or particles
Solid	Aerosol	$\ll 1$	very small droplets or particles
	Smoke	$\ll 1$	$< 0.1\mu m$
	Suspension of dust	$\ll 1$	$> 0.1\mu m$
	Fluidized dust	~ 1	$\gg 1\mu m$

For high volume concentrations, the action of the condensed phase on the gaseous phase, and interactions between particles, are important, so that we are led to analytic processes and to experimentations quite different from those concerning low concentrations (see also E 3.2, 4 and 7).

For low volume concentrations, to which we shall limit ourselves, we must first consider the mean dimensions of the particles: it is known that the action of the gaseous phase on the condensed phase depends strongly on this parameter.

The flow of a gas-particle mixture is controlled by the exchanges occurring between the two phases: exchange of momentum due to mechanical entrainment of the particles, exchange of heat resulting from thermal

nonequilibrium between the phases, and exchange of mass if there is evaporation, condensation or combustion.

Problems related to mass transfer between phases will not be considered here: we shall only consider problems where the condensed phase is driven only by aerodynamic mechanisms. We shall not limit ourselves to solid particles, as many applications concern liquid particles, these two classes of problems being often treated by similar means.

1.2 Outlook of National Work

There does not actually exist in France any university laboratory specialized in the field of gas flows with a low concentration of particles. This type of flow is however studied in applied fields at the Paris VI University and at the Atmospheric Physics and Pollution Laboratory (Prof. Bricart). The National Center of Scientific Research (CNRS) does not conduct any specific research in this field; in its activity report, multiphase flows are mentioned in the category of rheological flows.

On the other hand, in some institutes of applied research and some industrial companies, some effort is made, usually under the pressure of specific problems. This situation makes it difficult to draw any overall conclusion regarding fundamental studies; that is why we shall start from technical problems, and then attempt to emphasize the fields in which fundamental knowledge appears insufficient.

The dispersion of the lines of effort and their technical specialization explains the small number of publications permitting a study of gas-particle flows. Professor Fortier gathered in a single volume the texts of lectures given at the Paris VI University within the framework of the Higher Hydrodynamics and Aerodynamics Certificate (1). The general equations of multi-phase media are established, and the laminar flow of a fluid around a spherical particle is derived. Applications considered concern mainly turbulent flows in long cylindrical ducts, with a view to determining concentration variations and pressure drop. More recently, we summed up the work initially oriented towards the operation of rocket engines (2). Equations for both phases are written for a suspension with general assumptions on liquid or solid particles, distributed according to their diameter, the mass exchanges being taken into account and the gaseous medium being multi-reactive. A limited number of applications is given in the field of aerodynamics.

The applied problems we are going to examine concern flows within solid-propellant rocket motors, those encountered during implementation of laser anemometry, and droplet accretion on obstacles. All these problems belong to the aerospace field, and the mechanisms brought into play are varied enough to permit a synthesis of a fundamental nature.

Before reviewing these applications, let us mention that some work is carried out in France on high-concentration mixtures, in particular with a view to study the transport of powdered matter (Experimental Fluid Mechanics Laboratory, Orsay University, Prof. Fortier) and the phenomena of sedimentation and particle removal from a wall (Aerothermodynamics Laboratory of CNRS, Meudon-Bellevue, Prof. Bernard).

2. FLOW OF COMBUSTION PRODUCTS IN SOLID PROPELLANT ROCKET MOTORS

2.1 Problem Statement

Flow in rocket motors often present a two-phase character, as in the case of liquid-propellant motors, during combustion of propellant droplets in the combustor; this problem, which involves mass transfer, lies outside the scope of this paper. In most solid-propellant motors, a dispersed metallic charge is introduced into the propellant in order to increase its performance. The metal is found in the combustion products in the form of tiny oxide particles which may account for up to 40% of the mass flow. Figure 1 shows alumina particles picked up in the jet of an experimental nozzle.

The formation of this condensed phase is not to be discussed here; we are only concerned with the aerodynamic aspect of the phenomena occurring in the motor combustor and nozzle. Practically, the influence of particles is being felt in the following characteristics:

- Performance - Thermodynamic calculations made in order to predict performance assume that kinetic and thermal equilibrium of the phases is achieved locally, and thus do not take into account the two-phase aspect of the flow. The experimental specific impulse of metallized propellants is further away from its theoretical value than for non-metallized propellants; it thus appears necessary to explain and predict the influence of the interaction between phases on performance. The loss of specific impulse seems highly dependent on the operating parameters of the motor, in particular on its scale; for small motors it may exceed 5%, which justifies the attention paid to this problem. Figure 2 gives, as an example, the variations of the specific impulse discrepancy $\delta I/I$ as a function of the ratio between curvature and aperture radii at the throat of a biconical nozzle.

- Wall Interference - This kind of problem includes the accretion of part of the condensed phase within the combustor, when the motor is rotated about its longitudinal axis, formation of an alumina layer on the nozzle, and erosion of part of the nozzle by particle impact. Figure 3 shows the thickness e of the alumina layer deposited at the distance s from the beginning of the convergent part of a small test motor nozzle for zero and 10 revolutions per second.

- External Aerodynamics - Among problems related to jets, those concerning their radiolectric behavior and erosive effects are of particular interest. Photographs of rocket exhaust jets (3) show that the condensed phase tends to concentrate along the jet centerline, but the available photographs are not suitable for reproduction (see also E, Fig. 13).

- Combustion Instabilities - For determining the stability range of the motor, it is mandatory to know the acoustic loss due to the condensed phase; this loss is directly dependent on the mean particle size.

This paper is limited to problems concerning steady internal aerodynamics, in the combustor and the nozzle.

2.2 Work Already Performed

The problem of the flow of a two-phase mixture within the motor may be approached theoretically by using general equations. However, we should first give a sufficiently fine description of the condensed phase and, in view of the complexity of the calculation, define the simplifications that will permit a faster processing of the equations.

A difficulty pertaining to the problem concerns the characteristics of the condensed phase. Considering the experimental results obtained (3), we may state that the particles are nearly spherical and very broadly distributed in size. Figure 4 gives the distribution of the particle diameters d_p obtained experimentally by analysis of a sample of particles picked up within a rocket motor jet. Moreover, the alumina particles are liquid during most of the expansion, and their collisions entail an increase and a local variation of their size distribution; this effect is reinforced by particle segregation in zones with high velocity gradient, which implies also a non-uniform distribution of the condensed phase in combustion products.

Calculation emphasizes that the effects are about proportional to the square of the particle mean diameter; so it is essential to determine experimentally the particle size distribution. Two techniques are used in France: capture and optical measurement.

The capture technique was developed at length at ONERA. The particles are captured mainly in the jet, far from the outlet section; this measurement gives an idea of the particle size distribution after solidification and during the whole motor operating time (tests never exceeded 10 seconds). A careful statistical analysis of a sample of deposited particles permits a calculation of the various mean diameters of the distribution law.

Measurements of the same type were also performed by capture within the combustor and the nozzle. In spite of the difficulties due to the liquid state of the trapped particles, the results prove the reality of particle size increase. The capture technique is rather difficult to handle; moreover, the statistics established this way are relatively inaccurate at extreme values of the diameter, and the mechanism of particle deposition on capture plates is not well known.

Another technique was more recently developed by a joint effort of SEP (Societé Européenne de Propulsion) and CERT (the ONERA-dependent research center at Toulouse); it is based on radiation scattering by a particle cloud, and rests on the classical Mie theory (4). First measurements concerned a rocket motor jet and provided encouraging results, emphasizing in particular the evolution of the particle distribution during motor operation. Figure 5 gives a general view of the instrumentation, Fig. 6 an example of results. This method is being improved, on the one hand with regard to calibration with particles of known size, on the other by extending the measuring range and the processing method. It is also envisaged to measure the particle size distribution inside a motor equipped with a window.

The quality of aerodynamic calculations depends on available data on the size distribution of the condensed phase. In spite of the progress still to be made in this field, many calculation schemes have already been developed. Apart from a few exceptions (3), size increase and collisions between particles are neglected and, according to the additional simplifications made, the calculations are more or less realistic (Fig. 7).

A first approach consists in studying the movement of a particle of given size in a reference flow defined by a two-phase equilibrium calculation of this type, performed by the Aérospatiale Company. It shows that the particle trajectories do not noticeably depart from the flow streamlines except in the zones of high-velocity gradient: in the vicinity of a slope discontinuity of the duct meridian of the nozzle and in the nozzle. More complete flow schemes are at present being developed in various companies working on propulsion - Aerospatiale, SEP, SNPE (the National Society for Powders and Explosives) - for the study of the various interesting zones, mainly the nozzle. Only a single particle size is at first considered, the flow is usually assumed laminar, various laws for drag and thermal exchange are considered, and radiation phenomena are ignored.

Experiments were also performed by Aérospatiale by simulating the flow of combustion products in a combustor by a gas-particle mixture and by determining the drag on a jet-thrust-measuring ground facility for various nozzle shapes and various loading ratios; these tests are of fundamental interest, as the experimental conditions are well known, though they do not represent exactly the real phenomena (5).

The study of wall phenomena is directly linked to aerodynamic calculations, which should permit the prediction of impacts in the various zones of the motor. Moreover it is necessary to predict the behavior of particles trapped in the boundary layer in order to determine the deposits. These problems seldom have been approached, and then only from very simplified capture calculations in which the trajectory is being studied in a reference gaseous flow.

2.3 Problems Still to be Solved

The main cause of uncertainty is the incomplete knowledge of size measurement of the condensed phase and the mechanisms of particle collisions and accretion. The calculation schemes must take these phenomena into account to be realistic. The role of turbulence on the condensed phase should be clarified. So it seems that, for the moment, the research work should concentrate more on the development of measuring methods and on fundamental studies than on the improvement of calculation methods.

3. LASER ANEMOMETRY

3.1 Problem Statement

Among aerodynamic measuring methods, the optical ones are particularly interesting as they present the advantages of not disturbing the flow, of being usable in difficult conditions and of providing nearly point measurements. Among them, laser anemometry was the subject of many improvements during the last years. The principle is now well known and can be explained either by a calculation of the Doppler frequency of the light scattered by the moving particles, or by the crossing of the particles through the interference fringes created by interaction of two incident laser beams. The analysis of the frequency of the signal received by the detector provides the velocity of the particles entrained by the flow.

In its practical utilization in aerodynamics, this method raises a problem of interpretation, as we have to deduce the fluid velocity from the particle velocity. These two velocities are the same if the particles are small enough to follow instantaneously the velocity fluctuations of the gaseous phase. It is thus important to define precisely the tolerable particle size, or to establish the corrections permitting the passage from the measured velocity to the fluid velocity (see also C.7, D.5, and E.9).

With powerful enough lasers it is possible to work with particles that are normally in suspension in any flow. Injection of smoke can also be envisaged.

3.2 Work Already Performed

Laser anemometry was simultaneously developed at the Saint Louis Franco-German Institute (I.S.L.) (6) and at ONERA (7); good experiments were performed with both types of instrumentation. The two crossed-beam instruments are different with regard to signal analysis, which is performed by counters at ISL and by a spectrum analysis at ONERA. The ISL instrument permits the elimination of spurious signals and seems to be better adapted to the measurement of rather low turbulence rates during relatively short times. The ONERA instrument offers a better space resolution thanks to a smaller measuring volume; high turbulence rates can be measured, but only over relatively long times.

The first ISL experiments concerned the turbulence rate in a small free jet at low speed; the rates measured for the axial velocity fluctuations in the jet agree well with determinations done with the hot wire technique, as seen in Fig. 8. The velocity field around a two-dimensional wing profile was then established, but without comparison with other methods, in order to determine the possibilities of the instrument; measurements of the two velocity components in the leading-edge area were obtained. Results of the exploration of a thin boundary layer compare favorably with the Blasius theoretical profile. During these various experiments, ISL made an effort to know the size distribution of the particles and natural dust in suspension in the experimental installations: the main method used is that of very fine sieves, obtained by chemical treatment of brass whiskers, able to remove particles 1 μm in diameter; it is not however sure that the biggest particles are collected by the sieve, and that they are not responsible for the difficulties encountered in the study of low-velocity flows.

The ONERA techniques were applied to the study of a flow behind a step in the S8B wind tunnel. The mean velocity profile at mid-step compares favorably with pitot measurements and with those performed with a hot wire in a similar incompressible flow. The turbulence rate is established up to a high level, and corresponds approximately to that provided by the hot-wire method; the differences observed between these two types of measurements are found in the turbulence profile, as seen in Fig. 9. The mean velocity profiles and the turbulence rate profiles in the boundary layer of the supersonic flow in front of the step were also recorded; results for mean velocity are in good agreement with the pitot measurements. During the experiments, the air used in the wind tunnel was thoroughly filtered before its passage through the test section. A check on dust size distribution by the whisker-capture method confirmed that the particles were of submicron size, but the quality of the comparisons did not justify further investigation by this technique.

Before the development of laser anemometry, ONERA had worked on photographic techniques (8). The study concerned internal aerodynamics in the end part of a solid-propellant motor, and used a two-dimensional model, fed with compressed gas through porous walls and with 20 μm-dia. particles at some points of the walls. Illumination of the test section by a continuous laser permitted the determination of the mean particle trajectory (Fig. 10); this trajectory is well defined for 20 μm particles, but we could detect a rapid dispersion of 1 μm particles after their emission at the wall. Illumination of the test section by a pulsed laser, either in its natural or Q-switched mode, permits in principle the visualization of the successive particle positions, and thus the calculation of the velocity components; the values obtained for 1 μm particles are highly dispersed, which may be explained by flow turbulence.

3.3 Problems Still to be Solved

In the application of laser anemometry to classical aerodynamic studies, the flows include very few particles in suspension. The action of the condensed phase on the flow is negligible, and the main problem is to determine the limit size under which the particles follow the flow fluctuations without delay. In this type of experimentation, we partially control the particle size distribution, for instance by thorough filtering of the gas; water-vapor condensation has to be avoided. A check of particle size can be made either by capture or by optical measurements, but the quality of the results obtained is more generally established by comparison with other physical measurements, such as hot wire, if the velocity is sufficient, or pressure. That is why the aerodynamic studies conducted at ISL and ONERA have not yet shown the need to go further with problems specific to the condensed phase.

If we attempt to apply laser anemometry to flows with moderate particle content, or with particles of more than 1 μm diameter, we must expect to encounter new problems with regard to signal analysis and interpretation of results. Velocity measurements then cannot be separated from those of particle size and concentration.

4. PARTICLE CAPTURE

4.1 Problem Statement

Particle capture was already mentioned at the occasion of condensed-phase size measurement and of flow in rocket motors. We shall now examine activities related to aircraft icing and to rain effects. The flows considered are lightly loaded with droplets of about 20 μm diameter for icing and of 1 mm diameter for rain.

The theoretical study of laws governing icing sheds some light on several physical phenomena. The first mechanism concerns the capture itself of droplets by the obstacle; we then have to determine their movement within the aerodynamic field around the obstacle, and the similitude conditions of this problem were established quite a long time ago (9). The second phenomenon to be studied is that of water and ice distribution over the aerofoil; lastly we have to treat the problem of thermal equilibrium of the wall in an icing atmosphere. There has been no study in France on the latter two points, and the results used are American or British. Rather general similitude conditions are thus available, and permit the reproduction in the wind tunnel of given flight conditions. The tests performed have an industrial character and aim to be able to fix experimentally the icing conditions at the given values.

With regard to rain erosion, we are mainly concerned with capture conditions, and results remain qualitative. Again, the point is to be able to reproduce given physical characteristics.

4.2 Work Already Performed

Icing and rain erosion are studied at ONERA at the Modane Wind Tunnel Department. Icing studies were recently reactivated for new French or European aircraft. In particular the Concorde was the occasion of an important series of tests, following doubts expressed abroad (10). Experimentation was carried out in the large S1-MA wind tunnel on a 1/6 scale model (Fig. 11). The application domain of similitude conditions was extended from 1/6 to 1/12 scale by studies of a more fundamental character on simpler geometries (cylinders, classical delta wings). The results obtained made it possible to qualify satisfactorily the icing similitude technique. Icing problems on aircraft engines are also carried out at the French Engine Test Center (CEPr).

High-speed (Mach 2) rain erosion tests are performed at the Landes Test Center (CEL) on aeronautical structures and on missiles (11). The elements under study are placed on a trolley moving on a single or dual-rail track, 600 and 400 m long, and accelerated by solid propellant motors in a cloud of droplets created by ejectors (Fig. 12). Approximate similitude conditions are used to reproduce damage observed in flight; parameters to be adjusted are exposure time, rain intensity, droplet size and trolley speed. This installation is operational, and work is in progress to increase the velocity range.

4.3 Problems Still to be Solved

The main practical problems concern droplet production and dimensional control to make sure that the test conditions are satisfied.

In the ONERA icing installations, the droplets are produced on a atomization grid by air break-up action; the influence of adjustable parameters (water flow rate, air pressure) was determined empirically. The artificial-rain generating station at CEL was made by the Bertin Company, under the direction of the official Launching Range Instrumentation Service (SECT), and is made of atomization manifolds; drop size is controlled by water pressure.

Qualification of mists made this way appeared as a difficult problem. The measuring method used for rain erosion is that of drop capture on an oily plate; the photograph of the sample is then analyzed by traditional means of counting by size classes. Icing was the objective of various measurements; the technique of capture on an oily plate, also implemented at CEPr, was first employed and based on a statistical analysis, using a catalogue developed by the British firm Hawker-Siddeley; precision of the results is limited by the various assumptions which have to be made regarding the spherical shape of the collected droplets, absence of droplet accretion and evaporation, nonmiscibility of oil and water, and existence of a known ratio between the diameter of the observed image and that of the actual droplet. A photometric method was tried, but the instrument, initially developed by the ESRI Company and improved with regard to optics and electronics, did not give satisfactory results. An instrument developed by the Bertin Company, using droplet capture in a softened layer, measured imprints left after evaporation, but these measurements do not agree well with those obtained with oily plates. Thus, there remains an uncertainty about the size analysis of the mists produced, and new measuring methods are currently investigated.

Icing and rain-erosion tests of industrial character do not seem to raise specific two-phase aerodynamic problems. The influence of some phenomena related to liquid particles (deformation, accretion) is ignored. On the other hand, progress in techniques for measuring mist sizes would be highly appreciated (see also B 3.5, C.4 and 5, and E.9).

5. SUMMING UP THE PROBLEMS

We shall not attempt to present a synthesis of the problems that appeared during the survey of previous applications. Knowledge of size distribution is always necessary; this problem being assumed solved, the incidence of mechanisms related to particles on the results seems to depend on the application considered; that is why we shall only enumerate the fields where progress in our knowledge would be useful.

5.1 Knowledge of the Condensed Phase

There exist many classical means for measuring the size distribution of a condensed phase; let us mention, for the record, filters (large particles), diffusion batteries for pollution (fine particles or aerosols), suspension of particles in an electrically conductive liquid (Coulter counter), separation devices

(cyclones). These methods are not applicable to the flows considered, which usually contain a small amount of particles broadly distributed in size. The only methods used are either direct capture methods or indirect ones based on the optical properties of the suspension.

5.1.1 Particle Capture

According to the nature of particles, the capture element may vary widely: whiskers (particles in suspension wind tunnels -- ISL), glass or quartz plates (alumina particles of combustion products of metallized propellants -- ONERA), oily plates or plates coated with a plastic film (liquid particles -- Bertin Co.). In all cases, exposure times should be strictly controlled.

Statistical analysis of the sample requires powerful enlarging means, when particles are submicroscopic (use of a scanning electron microscope -- ONERA). Automatic processing of the image is often out of the question in view of particle superposition, and manual processing is always long and difficult.

Interpretation of results is possible only if the movement of particles in the aerodynamic field is known and the capture efficiency calculated. This problem requires the knowledge of the drag laws, little studied for particles of complex shape or for clusters (soot). When the particles are small and the flow turbulent, the deposition mechanism is poorly understood.

It is desirable to calibrate the collecting devices in conditions near those of actual utilization. We then must have at our disposal particles of given shape and size distribution, and possibly of uniform size; these materials are still not available in sufficient quantities, especially for microscopic sizes.

The capture technique was for a long time the only one available, and gave valuable information in most applications. It is however limited with regard to precision for extreme size values, in particular for very broad distributions. In spite of progress accomplished, it remains rather difficult to handle and provides only mean measurements in time and/or space.

5.1.2 Optical Methods

We can count among these methods photographic techniques, holography and processes making use of light transmission or scattering, in particular by a cloud. Photographic techniques are, for example, used to determine the size of droplets formed by an injector; their use remains limited to relatively large diameters not requiring too big an enlargement which is incompatible with a sufficient depth of field.

Holography was applied to the study of an icing cloud at ISL, for application to test chambers at CEPr (12) (Fig. 13). Results are promising regarding the particular problem envisaged. The field of application of this technique seems however limited to particle diameters of more than 5 μm and low concentration if the hologram quality is not to be altered, and at velocities no higher than 100 m/sec. Processing is relatively slow, as for capture. The holographic method is thus only interesting for certain fields of application, and progress remains to be needed to make its practical application easier.

Processes making use of transmission and scattering properties of a suspension were the object of quite a few applications in industrial fields, which should be mentioned in spite of their non-aerodynamic character. Measurements of the optical absorption coefficient of a mist were performed at the Research Division of EDF (the French Electricity Board) with a view to study two-phase phenomena in steam turbines; preliminary studies concerned the determination of mean diameters in the 0.02-10 μm range in various experimental conditions (13). Applications are under way or envisaged at the Hydraulic Binders Industrial Research Center (continuous control of cement mixers) and at the Coal Board Research Center (measurement of the dust content in mine galleries).

The study of light scattering by a particle cloud should permit a fine particle-size determination, and was the object of an application in chemical propulsion. First results shed light on several classes of problems, which limit the accuracy of the results. The first category of problems concerns the analysis of scattering; whereas the theory for single scattering cannot be questioned, we can express doubts on the role of multiple scattering in case of relatively high particle concentrations and on that of non-homogeneity of the spatial distribution of the condensed phase in the flow. The diffraction coefficients of the particle material should be precisely known, which is not always possible for materials formed at high temperature. Optical characteristics of the set-up should be thoroughly checked, as they control the useful measuring range. Lastly, deriving size distribution from measurements is an arduous numerical problem. Progress may be expected by making for instance, simultaneous measurements of scattering and attenuation, or by working with several wavelengths. Thus, this method is in full development and it is still too early to define its limits.

5.1.3 Synthesis

There is no universal method for determining size distribution of a condensed phase, in view of the extreme variety of the particles, of their size range and of their concentration in the flow. All existing methods are rather difficult to handle and do not offer the expected accuracy. In these conditions, capture and optical processes should be considered for the moment as complementary means. Only optical methods present an interesting potential for development; progress to be expected in the knowledge of the condensed phase rests on the research efforts in the field of applied optics.

5.2 Velocity Measurements

Regarding velocity determination, the two main problems concern the measurement itself and its use in aerodynamic studies.

The only methods envisaged here are the optical methods developed in classical aerodynamics. Photographic techniques, an example of which is given in Section 3, seem to be the only ones applicable to particles with a diameter of the order of 10 μm and relatively low concentration in the flow: laser anemometry

requires very low concentrations for signal analysis.

Regarding interpretation, for tests performed for the aerodynamic study of homogeneous flows in which the particles are being used only as tracers, perturbation by the condensed phase is to be avoided; the point is, in this case, to know if the particles are small enough to follow all the fluctuations of the gaseous phase. This problem is theoretically solved for spherical particles and a turbulent, homogeneous and isotropic flow.

The study of real two-phase flows, i.e., with a particle content sufficient to act on the gaseous flow, has not been experimentally approached. The application of laser anemometry to mixtures with a high concentration of particles will probably be difficult, and the interpretation of measurements will only be obtained if the local concentration of the condensed phase is determined and if the various forces acting on the particles are known.

The drag laws currently used in France are taken from the literature and are convenient for most applications where particles are solid and spherical. Complementary fundamental research would be useful in the following fields:

-- behavior of an isolated particle in a viscous fluid flow with velocity gradient (Aerothermics Laboratory, CNRS),

-- drag laws for liquid particles, taking into account deformations due to high velocity gradients, and internal circulation,

-- effects of the surface state on the solid particle drag,

-- study of unsteady entrainment, with a view to applications to turbulent flows,

-- drag laws of non-spherical particles and of clusters.

Velocity measurements were, up to now, only treated for practically homogeneous flows. An important effort remains to be made for two-phase flows in both the experimental and fundamental fields (see also C.8.1).

5.3 Temperature Measurements

Temperature measurements are especially interesting for very hot flows; their interpretation raises a particular problem when concentration and temperature gradient are high enough for differences to appear between the temperatures of the two phases. In particular, this is the case in the expansion of combustion products in rocket motors.

Gas temperature T_g and particle mean temperature T_p have been measured at ONERA in a rocket jet (14). Gas temperature is determined by absorption of two monochromatic radiations in the near infrared range. Temperature of the condensed phase is deduced from the jet emission characteristics, assumptions having to be made regarding homogeneity of the particle distribution within the flow and the particle size distribution. Figure 14 gives an example of the pressure p and particle temperature obtained as functions of the test time t; temperature differences between the phases are emphasized.

Analysis of the phenomena implies the knowledge of thermal exchange laws between gas and particles. The main laws used result from a compilation of the literature, and complements should be established for unsteady mechanisms and non-spherical particles.

Temperature and velocity measurement problems are different as it is possible to measure the gas temperature directly. The interest in temperature measurement is only obvious in particular applications. Let us lastly remark that the influence of thermal phenomena on two-phase flows is usually smaller than that of dynamic phenomena (see also E.6.1).

5.4 Interaction Between Particles

This problem concerns only two-phase flows with rather high particle content. They are however of great practical interest, in particular for two of the applications previously mentioned: rocket motor internal aerodynamics and droplet capture.

When the particles are solid, their collision tends, on the one hand, to limit the velocity differences between particles (see also E, Fig. 8) and, on the other, to ensure their diffusion within the flow. From a theoretical point of view, the movement of each class of particle should be studied by examining the momentum exchanges between that class and all other particles. This interaction term is established by a statistical analysis of the impacts, and this calculation implies a good knowledge of the elementary collision mechanism, a knowledge not yet acquired in a sufficiently general manner.

The problem becomes more difficult, but also more important, when we consider liquid particles. Collisions entail accretions and possibly breakdowns, appearing as a continuous evolution of the condensed phase, particularly unfavorable for aerodynamic predictions. The elementary mechanisms of coalescence are little known, and we can predict neither the collision efficiency nor the size of the particles formed when accretion is followed by breakdown.

Interactions between particles seem to have to be studied first at the level of elementary phenomena, which will probably entail implementation of new facilities. Macroscopic equations for both phases will then have to be written (see also E.5). Radiative exchanges, in particular, that have not been mentioned, should be predicted with the available optical theories (see also B.2.4 and E.3.3).

6. CONCLUSIONS

Aerodynamic problems of gas-particle mixtures were mainly approached in France in connection with particular applications, which explains the relative paucity of works of fundamental character and the wide diversity of the techniques implemented. Theoretical approaches remained rather general, so that fundamental phenomena are imperfectly known. Flow analyses should be complemented in the fields already studied, and expanded to high-concentration suspensions. Progress will depend on development of experimental means, and mainly of optical methods whose performance should be improved and implementation simplified.

Applications present a variable degree of success depending on the nature of the particles, their size distribution and their concentration; the most difficult problems are raised by liquid particles, broad distributions, high concentrations and high temperatures. In the present situation, new applications seem to appear in the field of energy exchanges: to raise the efficiency of thermal machines and of transformation cycles, fluids are sought that possess extreme physical properties, in particular with regard to transformation temperatures and heats. We could thus imagine using "two-phase fluids" made for example of capsules of coated mineral salts in suspension within a fluid with low freezing point and low viscosity. It will be possible to optimize these fluids with a composite structure, whose behavior will be controlled at all levels of the cycle by the laws of two-phase flows.

7. REFERENCES

(1) Fortier, A., "Mécanique des Suspensions," Masson et Cie, 1967.

(2) Kuentzmann, P., "Aérothermochimie des Suspensions," Mémoires de Sciences Physiques, Gauthier Villars, 1973.

(3) Kuentzmann, P., "Pertes d'Impulsion Specifique dans les Fusées à Propergol Solide," Publication ONERA, No. 151, 1973.

(4) Seguin,J., "Fonctionnement Interne des Propulseurs," Granulométrie d'Alumine par Laser. Rapport de Synthèse,Internal Document SEP TP/SA 17609/73, Nov. 1973.

(5) Carrière, R., "Recherche de l'Influence de la Géometrie d'un Convergent de Tuyère et de l'Intégration de la Tuyère sur l'Impulsion Spécifique d'un Propergol," Internal document S/DEE-1 No. 473306, Sept. 1973.

(6) Masure, B., Gautier, B., Haertig, J., Hancy, J. P., "La Vélocimétrie Laser: Description et Application a l'Etude des Ecoulements Gazeux," Rapport ISL Co. 1/73, Oct. 1973.

(7) Boutier, A., "Laser Anemometry in a Highly Turbulent Supersonic Flow," ONERA, T. P., No. 1348, 1974.

(8) Boutier, A., Philbert, M., "Velocity Measurements in Gas and Liquid Flows with an Interferential Velocimeter," ONERA, T.P., No. 1059, 1972.

(9) Brun, M., Ed., Vasseur, M. M., "La Mécanique des Suspensions," Journal des Recherches du CNRS (Laboratoires de Bellevue) No. 3, 1947.

(10) Charpin, F., Fasso, G., "Essais de Givrage dans la Grande Soufflerie de Modane sur Maquettes a Echelle Grandeur et Echelle Réduite," L'Aéron. et l'Astron., No. 38, 1972.

(11) Alexandre, J. P., Friou, A., "Simulation des Effets de Pluvioérosion a Grande Vitesse," L'Aéron. et l'Astron., No. 43, 1972.

(12) Royer, H., "Etalonnage d'un Brouillard Givrant par Holographie," Rapport ISL S/73, Jan. 1973.

(13) Mouren, J. M., "Etude Optique des Gouttes Formées par Condensation Homogène de Vapeur d'Eau dans un Jet Supersonique," Thèse de 3e Cycle de Sciences Physiques (Géophysique), Université de Paris VI, 1971.

(14) Crabol, J., "Charactéristiques Thermiques d'un Jet de Fusée Contenant des Particules d'Alumine," Publication ONERA, No. 133, 1970.

(15) Laug, M., Luneau, J., Srut, G., "Mésure de Granulométrie dans les Ecoulement Diphasiques," Colloque d'Aérodynamique Appliquée AAF, Faculté des Sciences de Bordeau - Talence, 6-8 Nov. 1974.

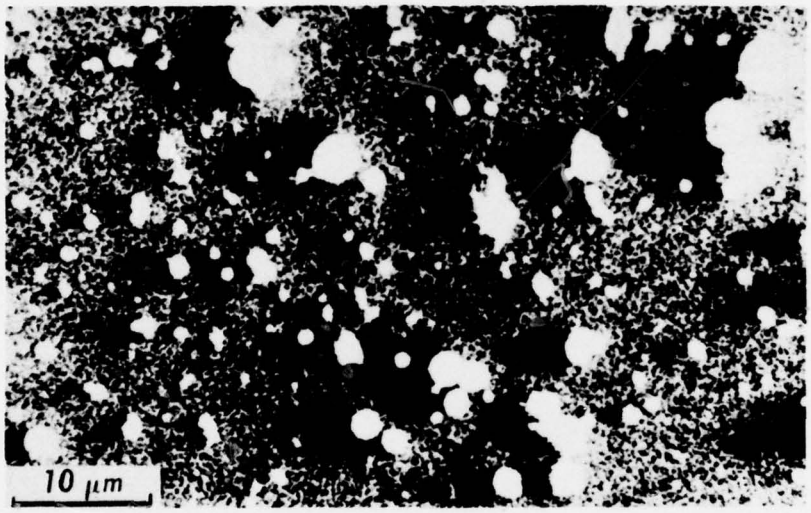

Figure 1 Alumina particles collected in a rocket exhaust jet (3).

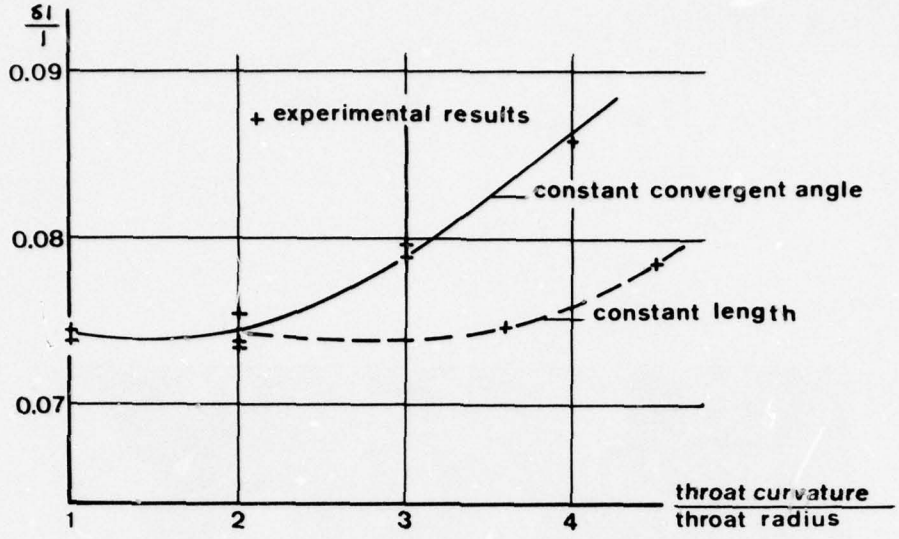

Figure 2 Specific-impulse loss according to the geometrical characteristics of a nozzle (3).

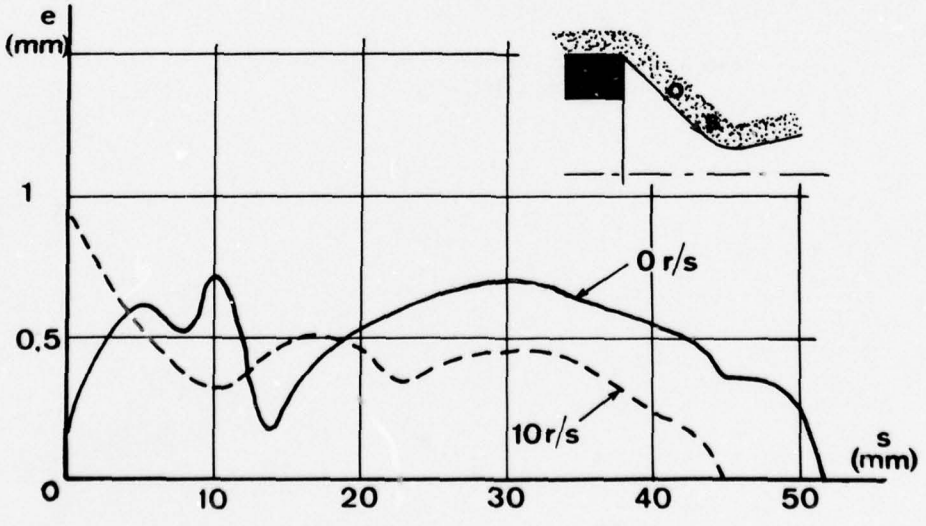

Figure 3 Thickness of the alumina layer deposited on the convergent nozzle of a rotating motor.

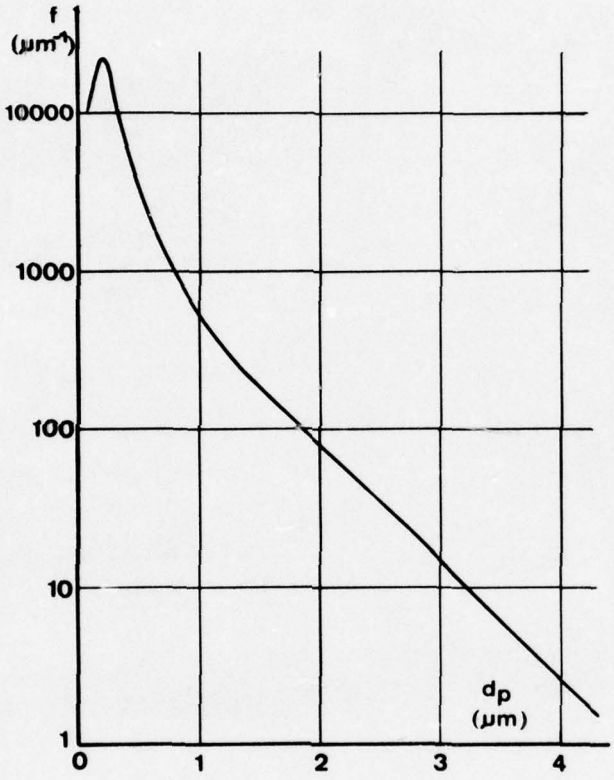

Figure 4 Diameter distribution of alumina particles in a rocket jet.

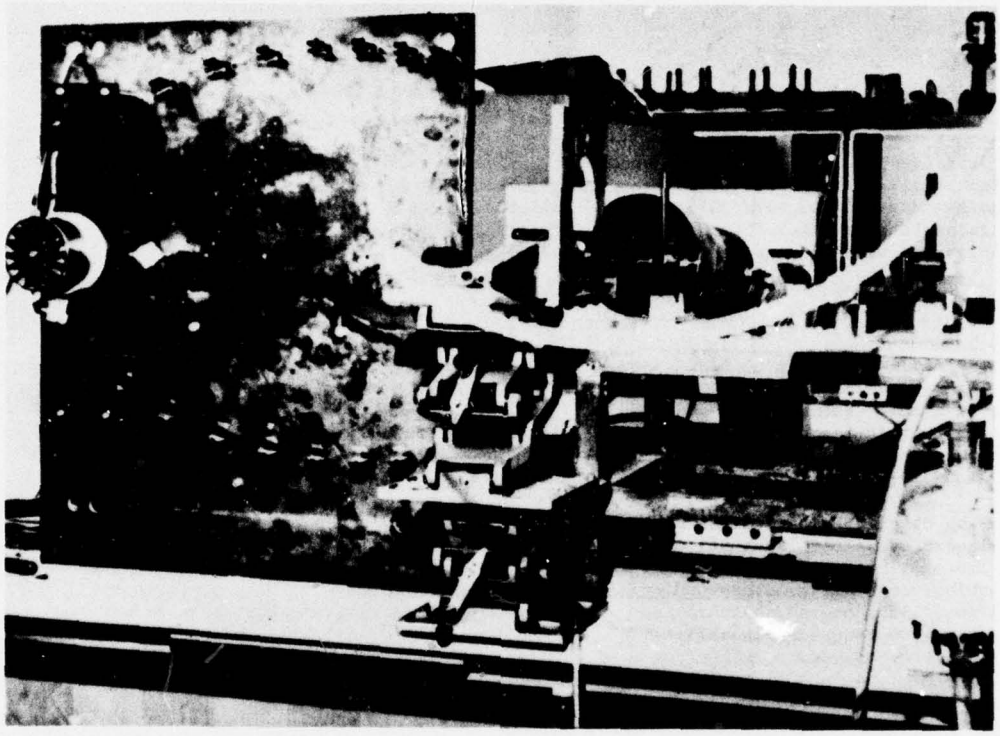

Figure 5 General view of the CERT laser instrumentation.

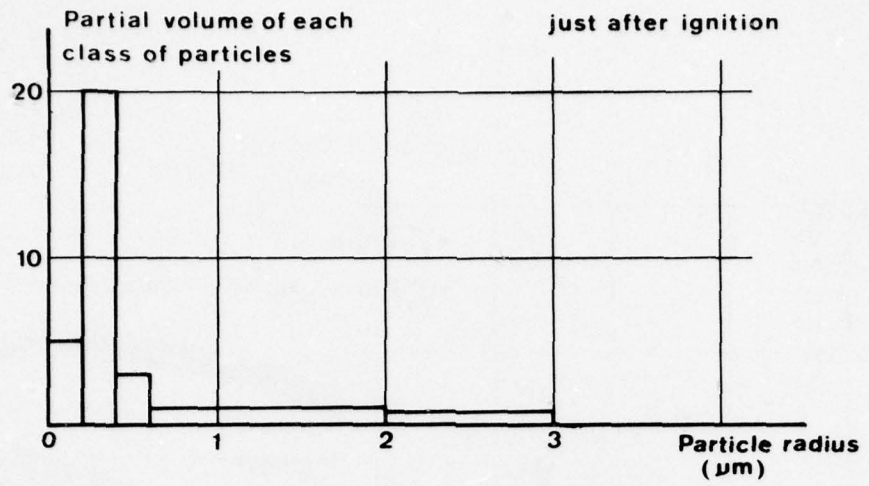

Figure 6 Results obtained at CERT on the laser set-up (4).

- Particles:
  - . distribution *,
  - . interactions *,
  - . drag and thermal exchange laws,
  - . radiation *,
- Gaseous phase:
  - . chemical reactions,
  - . turbulence *,
- Onedimensional or multidimensional treatment.

(* little or none studied)

Figure 7 Assumptions for the computation of flows in rocket motors.

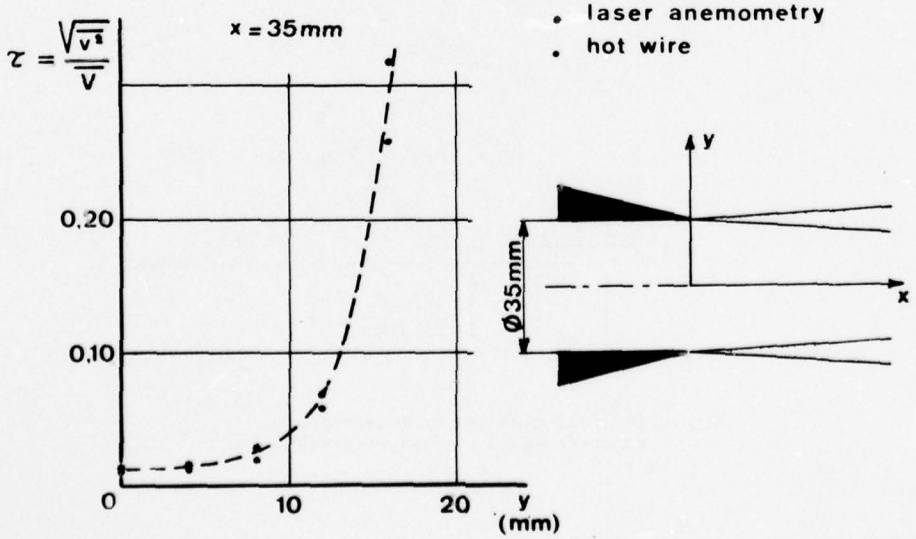

Figure 8 Velocity fluctuation measurement in a free jet (6).

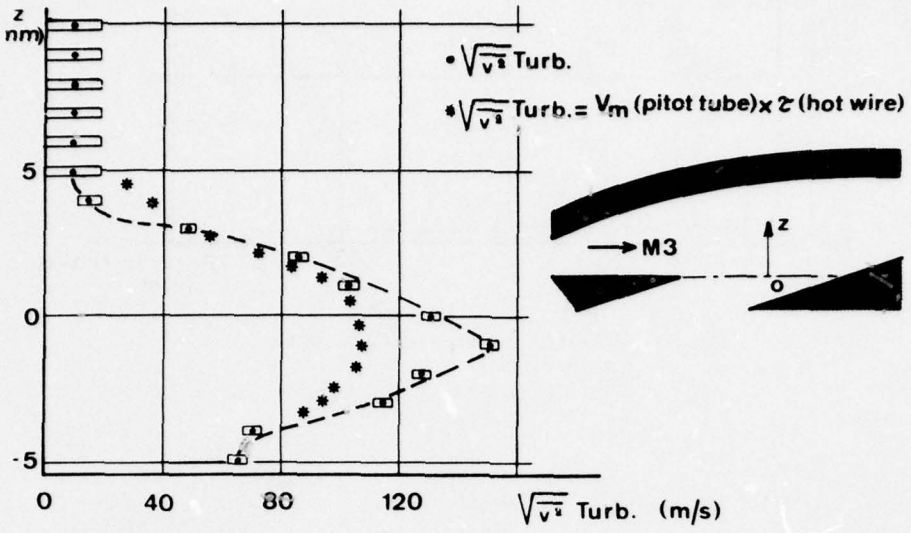

Figure 9 $(\overline{v^2})^{1/2}$ turbulence profile (7).

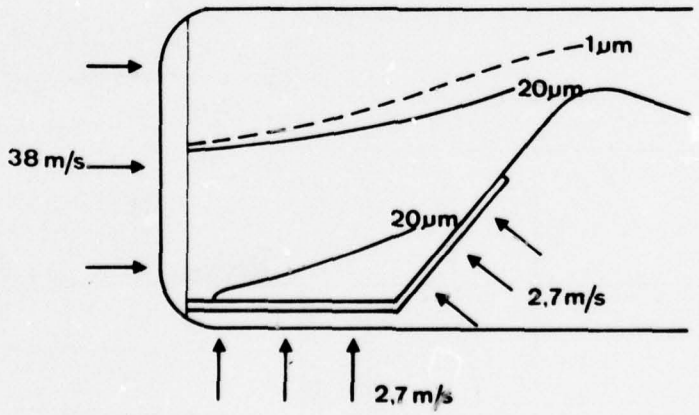

Figure 10 Determination of mean particle trajectories by the photographic method (8).

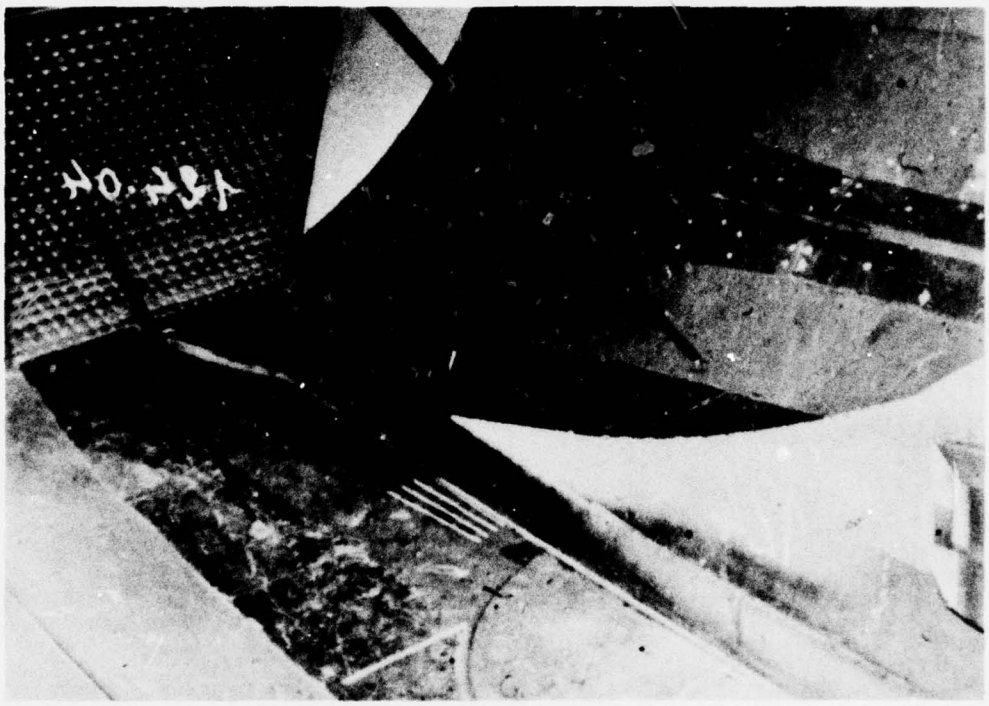

Figure 11 Icing tests of a Concorde 1/6-scale model in the wind tunnel S1-MA(10).

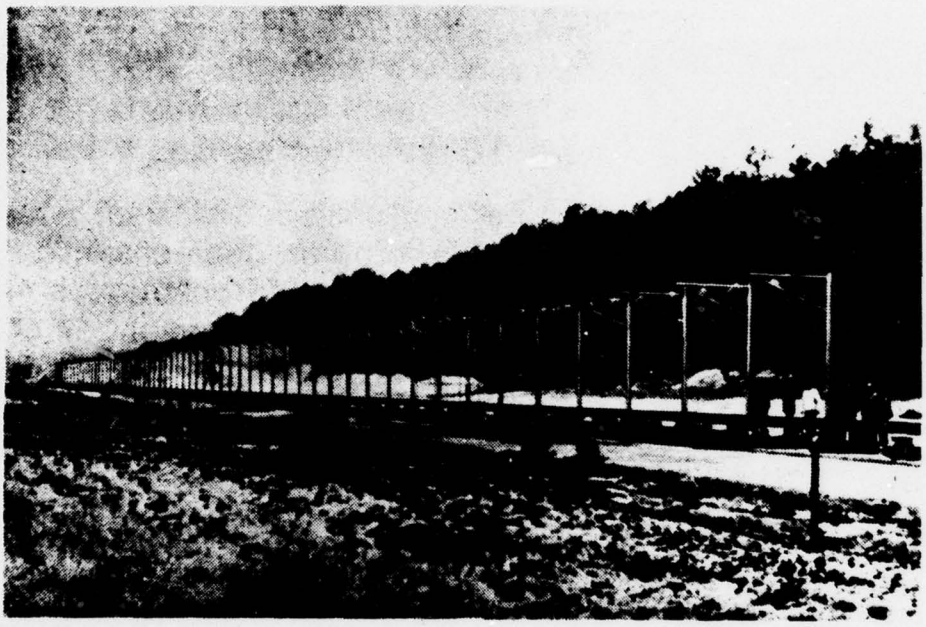

Figure 12 General view of the CEL rain effects plant (11).

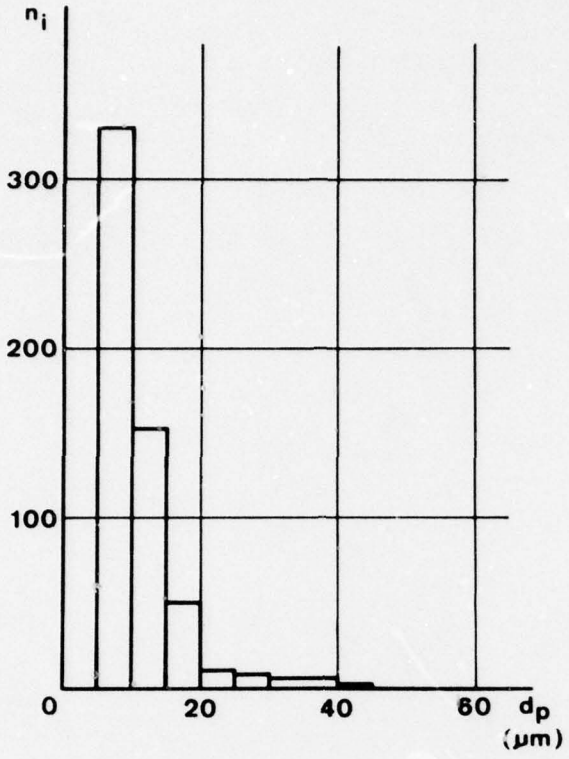

Figure 13 Droplet diameter distribution in an icing cloud (12).

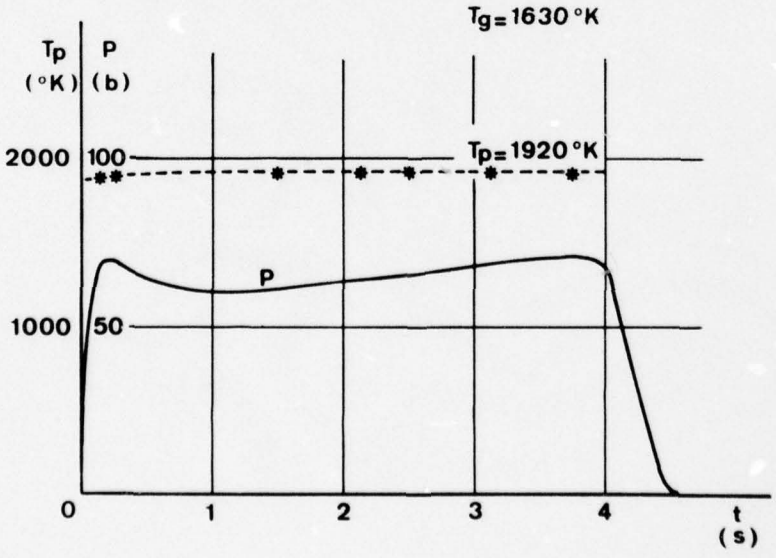

Figure 14 Mean particle temperature measurement in a rocket exhaust jet (14).

B. GAS FLOWS WITH SOLID PARTICLES
Research and Development in Germany

W. Wuest
Professor and Director
Institut für Dynamik Verdünnter Gase
DEUTSCHE FORSCHUNGS- UND VERSUCHSANSTALT
FÜR LUFT- UND RAUMFAHRT E.V.
Aerodynamische Versuchsanstalt Göttingen, Germany

SUMMARY

A general review of German activities in the field of gas flows with solid particles is given. Fundamental research on force and heat-transfer laws and propagation of sound and shock waves is discussed as well as more applied work on generation, conveying, separation and measurement of particles.

1. INTRODUCTION

1.1 Technical Motivation for Research in the Field of Gas Flows with Solid Particles

Two-phase flows are encountered in many engineering problems and in nature. In the following only mixtures of a gas (or a liquid) and solid particles are considered. Such flow problems comprise the conveying of solid particles, dusty gas flow, separation of solid particles, measurement techniques, and the sampling of micrometeorites. For the understanding of such processes, the particle paths in a field of viscous forces, the conductive and radiative heat exchange, the attenuation of sound and shock waves must be known. Fundamental research tends to clear up these problems on single particles and on particle clusters, including interaction effects. In the following, activities in the mentioned fields are reviewed, which have been developed in Germany during recent years.

2. FUNDAMENTAL RESEARCH

2.1 Forces Acting Upon Microscopic Particles

The drag of small particles depends on Reynolds number, Mach number, and heat-transfer rate. It is rather accurately known only for limiting cases as discussed by Wuest (1). For high Mach numbers, the Newtonian drag law with a quadratic dependence on velocity is valid, for high Reynolds numbers, too, a quadratic law describes the turbulent regime. For low Reynolds numbers, however, the drag is inversely proportional to Reynolds number in the Stokes regime, but inversely proportional to the Mach number in the subsonic Knudsen regime. The limit between both regimes is roughly given by the condition that the particle diameter is less than 5 mean free paths. Under atmospheric conditions this corresponds to a particle size of 0.3 μm. Of course, there are smooth transitions between the different regimes. For the transitional regime between free-molecular flow and continuum flow, measurements on uncooled spherical particles were undertaken by Legge and Koppenwallner (2) (Fig. 1). In the Knudsen flow regime there is a smooth transition from the linear to the quadratic law with increasing molecular Mach number S (Fig. 2). The molecular Mach number is defined as the ratio S of the mass velocity to the most probable velocity $\sqrt{2RT}$, so that $S = \sqrt{\gamma/2}\, M$, where R is the gas constant, T the temperature, γ the ratio of the specific heats and M the Mach number. A characteristic feature of this regime is the dependence of the drag of spherical particles on surface temperature. New measurements on cone drag in free-molecular flow by H. Legge (3), which are still in progress (1974), have quantitatively confirmed the theoretical predictions of the dependence of free-molecular drag on surface temperature. No experimental or theoretical data are as yet available for the combined effects of velocity and surface temperature in the transitional regime (see also E.3.1).

2.2 Particle Paths in a Field of Viscous and Centrifugal Forces

The density of solid particles is generally much larger than the density of the ambient gas. Because of inertial effects, particles cannot follow immediately the motion of the gas but show relaxation. The same is true also for temperature changes. As was mentioned, in the free molecular regime drag and surface temperature are coupled, and therefore velocity and temperature relaxation must be comsidered together.

The same problem was treated by Schmitt-v. Schubert (4) using a Laplace transformation. In the physical plane the shape of the frozen shock was given analytically. For small mass fraction of the particles, analytical solutions were obtained for all flow variables on the surface of a wedge. For small ratios of solid mass to gaseous mass, the particle path was considered by Wuest (1) for linear and quadratic drag laws in supersonic wedge and stagnation point flow.

The total changes of particle velocity v_p and temperature T_p are given by the following formulas, where v_G and T_G are the gas velocity and temperature, and ρ_p is the density of the particle material, p the pressure, d the particle diameter, μ and k the viscosity and thermal conductivity of the gas, c_D the drag coefficient, Re and Nu the particle Reynolds number and Nusselt number, and c_p the specific heat of the particles.

$$\frac{Dv_p}{Dt} = \frac{v_G - v_p}{\tau_1} - \frac{1}{\rho_p} \operatorname{grad} p$$

$$\frac{DT_P}{Dt} = \frac{T_G - T_P}{\tau_2}$$

where

$$\tau_1 = \frac{4d^2\rho_P}{3\mu c_D Re}$$

$$\tau_2 = \frac{d_P^2 \rho_P c_P}{6k\ Nu}$$

are the relaxation times for velocity and temperature, and all velocities must be interpreted as vectors. For low particle Reynolds number, the action of pressure may be neglected. This is valid even for the passage of a particle through a shock wave, as was shown by Wuest (1) (see also C.2.1 and E.3).

Perturbed two-phase cylindrical-type flows and two-phase convex-type corner flows were calculated by Healy (5,6) (see also E.9). The particle paths in rotating flows with additional axial flow were investigated by Mühle (7).

2.3 Particle Clusters

The motion of particle clusters has been described by Brauer and Thiele (8). If a cluster is composed of one species only, it is called a monocluster; in the case of several species, it is called a polycluster. In the thesis by Kaskas (Technical University Berlin 1970) a formula for the velocity of one fraction of a polycluster was derived. The formulae have been applied especially to sedimentation processes under the influence of gravity, and it was observed that the sinking of larger particles may produce a rising of smaller particles caused by the reverse flow.

2.4 Thermal Exchanges

For very small particles a complete description of heat transfer is possible for arbitrary velocities. For this case the relaxation time for temperature was derived by Wuest (1). In the hypersonic flow regime, the total heat transfer to spheres is known for a rather extended range of Reynolds numbers as is shown by Fig. 3, where measurements in the hypersonic low-density tunnel at Göttingen are plotted and compared with other data. The heat transfer in gas flows with dust particle has been investigated in the thesis by Hein (9).

Radiant interchange among suspended particles and its effect on thermal relaxation in gas-particle mixtures was studied by Schneider (10) (see also E.3.3). Apart from the total radiative transfer due to the contributions of all particles, there can also be a radiant interchange among particles of different sizes within the same local region. The smaller particles follow the gas temperature more closely than the larger ones and this provides the possibility of radiative heat transfer between different particles. From the basic equations describing this process a linear integro-differential equation was obtained for small temperature disturbances from an equilibrium state. The relative importance of radiation and conduction is characterized by the parameter

$$N_{RC} = \frac{\tau_C(r_n)}{\tau_R(r_n)} = \frac{4\sigma T^{*3}\sigma_{an}}{\pi k\ r_n}$$

with the conductive relaxation time given by

$$\tau_C = \frac{mc_s}{4\pi r_n k}$$

and the radiative relaxation time given by

$$\tau_R = \frac{mc_s}{16\sigma T^{*3}\sigma_{an}}$$

where r_n is the reference radius (most probable particle radius), σ the Stefan-Boltzmann constant, T^* the particle temperature at equilibrium, σ_{an} the nominal absorption cross section of a reference particle, m the mass of an individual particle, and c_s the specific heat of the solid particle material. To get an idea of the magnitude of this parameter we obtain $N_{RC} \approx 1$, if $T^* = 2000$ K and $r_n = 30$ µm.

From a practical point of view, this temperature is of a realistic order of magnitude. The analysis was based on the assumption that the particles are large in comparison to the wave lengths. Wien's law yields a wave length of $\lambda_{max} = 1.5$ µm for maximal intensity at 2000K, so that a particle radius of 30 µm complies well with the assumption.

In Fig. 4 the disturbances of the mean particle-cloud temperature and of the gas temperature are plotted as functions of dimensionless time. With increasing radiation-conduction parameter N_{RC} ($N_{RC} = 0$

no radiation; $N_{RC} = 10$ strong radiation) the temperature range of individual particles becomes narrower. For strong radiation, the temperatures of particles of different sizes tend to equalize. For the numerical calculation, a distribution function was used which contained a free parameter D to characterize the dispersion which was symmetrical about the most probable particle radius.

The heat transfer by radiation in suspensions of solid particles in a gas flow was also considered from a more technical view point by Hein and Lowes (11).

2.5 Propagation of Sound Waves

A survey article on wave propagation in suspensions of solid particles in gas flow was given by Rudinger (12), who considered also German contributions to this problem (see also E.6.2). A thorough investigation of propagation of sound waves and formation on shocks is given by Becker (13) and Schmitt-v. Schubert (14-18). The lag between the velocities and temperatures of gas and particles gives rise to a special class of relaxation phenomena, and the particle flow may serve as model fluid for studying more complex real-gas relaxation problems. For finite values of the products $\omega\tau_1$ and $\omega\tau_2$ of the relaxation times and the angular frequency, Schmitt-v. Schubert (18) obtains complex equations for the frequency-dependent sound velocity and damping. Simple formulas are obtained for small deviations from equilibrium and for the limiting cases of the frequency-independent sound velocity b in frozen flow ($\omega\tau_1 \to \infty$, $\omega\tau_2 \to \infty$), in semifrozen flow (c_1 if $\omega\tau_1 \to 0$, $\omega\tau_2 \to \infty$, c_2 if $\omega\tau_1 \to \infty$, $\omega\tau_2 \to 0$) and in full equilibrium (c with $\omega\tau_1 = \omega\tau_2 = 0$) and the relation $c < (c_1 \gtrless c_2) < b$ holds, that is, the sound velocity for abritrary relaxation parameters lies between the equilibrium sound velocity c and the frozen sound velocity b. The sound velocity in gas flows with solid particles was also investigated by Rumpf and Gregor (19) and Weber (20), who found also a decrease with diminishing particle diameter and frequency and increasing mass rate and velocity difference between particle and gas. The conveying capacity is limited by the critical velocity, which is equal to the local equilibrium sound velocity and, therefore, the mass-flow rate of solid particles cannot be increased beyond a maximum value.

2.6 Formation of Shock Waves

The influence contributed by the particles contained in the gas flow is qualitatively shown in Fig. 5 for different conditions. If we introduce the relaxation lengths λ_1 for velocity, λ_2 for temperature and a characteristic length λ_c, the relative value of these lengths is determining the formation of a shock wave, a fully dispersed wave, or a combination of a frozen shock wave with a dispersed relaxation zone. The relaxation lengths λ_1 and λ_2 are given by

$$\lambda_{1,2} = a_o \tau_{1,2}$$

where a_o is the sound velocity at a reference state of the gas, and $\tau_{1,2}$ are given in 2.2. Let u_o be the gas velocity at a large distance before and u_E, u_F the equilibrium and the frozen velocity behind the shock wave; c_o is the equilibrium sound velocity and b_o the frozen sound velocity of the mixture of gas and particles at large distance before the shock. The results show that a gas with solid particles behaves like a pure gas with two inherent relaxation processes (see also E.6.1).

3. APPLIED RESEARCH

3.1 Generation of Solid Particles

For laboratory investigations, the generation of a dusty flow is of interest. Fuchs and Murashkevich describe a laboratory powder disperser (21). The efficiency of such a device may be checked by short-time micro-holography (22).

3.2 Conveying of Solid Particles

There is no activity in Germany on two-phase effects in rocket propulsion. However, internal flows with solid particles are widely investigated, and survey articles on pneumatic conveying in horizontal straight or curved tubes are given by Brauer and Schmidt-Traub (23) and Vollheim (24,25). The similarity laws, valid for these phenomena were checked by Siegel (26).

Experiments of Krötzsch (27) on the gas flow with solid particles in vertical tubes brought the interesting result that below a limiting concentration, the particle velocity is determined only by collisions with the wall, whereas collisions between particles are negligible. The behavior is very similar to that of rarefied gas flow, and a mean free path $d/6c\sqrt{2}$ should be introduced, where d is the mean particle diameter and c the volume concentration of the solid phase. The limiting concentration of the solid phase then is reached when the mean free path is equal to the tube diameter D; this yields

$$c = \frac{d}{6D\sqrt{2}}$$

(see also C.6). Another aspect of the transport of solid particles is the structure of turbulence, which was investigated by Kazanskij (28) for water flow through pipes and the conveying noise, which was investigated by Flatow (29). Noise increases with increasing gas velocity and with increasing mass rate of solid particles; the noise level is lower with smaller diameter of the particles.

3.3 Separation of Solid Particles

Although industrial dust separators are outside the scope of this review, some results on cyclone separators are also of aerodynamic interest. Since the early work of Prandtl on cyclone separators, their

flow behavior has often been investigated. For the cleaning of chimney gas, the cyclones are now replaced by electrostatic or other filters. However, they are further used in chemical engineering for separation of high particle loads at relatively low Reynolds numbers. Separation takes place in the inlet bend and in the swirl flow of the immersion tube. Calculation of optimal cyclones leads to extremely long tubes if the wall shear stress is not taken into account (30) and according to Gloger and Lukas (31) the efficiency may, therefore, be improved by applying boundary-layer suction.

3.4 Measurement Techniques for Gas Flows With Solid Particles

3.4.1 Analysis of Particle Size

A survey on methods for the measurement of particle sizes is given by Leschonski (32). In the sedimentation analysis, the settling velocity in a suitable liquid is compared with that of an equivalent sphere. With particle sizes below 1 μm, Brownian motion influences the motion in the gravitation field and, therefore, sedimentation in a centrifugal field is preferred. The precision of the sedimentation analysis in a centrifugal field was investigated by Alex (33). Other methods are sifting, optical measurement, and specific surface measurement. The application of Laser light sources allows not only to measure the size of particles but also their concentration (34).

3.4.2 Measurement of Mass Rate of Solid Particles in a Gas Flow

For the measurement of mass flow rate of solid particles in a gas flow numerous methods are used, which range from photoelectric dust-density meters to instruments which measure absorption of radioactive radiation (35) or scattering of light (36). In nearly all cases, the measuring system is in a bypass of the main flow and according to Fig. 6, the particle concentration is measured too high if the suction velocity W_A in the probe is lower than the freestream velocity W_∞ or too low in the opposite case. The probe diameter D_A and the diameter of the limiting stream tubes of the gas D_ρ and of the particles D_s are indicated in the figure. The possible errors are calculated by Bohnet (37). Zenker (38) has verified the calculations by comprehensive measurements (see also C.8.2).

3.5 Sampling of Micrometeorites

In some satellite or high-altitude rocket experiments, cosmic dust was collected and analyzed. Extremely small particles do not hit the collecting surface but follow the streamline, whereas larger particles are less deviated due to inertial forces. An analysis was given by Wuest (1) for some two-dimensional flow configurations such as supersonic wedge flow and viscous hypersonic stagnation flow around a sampling plate. A representative result is given in Fig. 7, where T_w is the wall temperature and T_r the recovery temperature of the heat-insulated plate, ρ_∞ and ρ_P are the undisturbed densities of the gas and of the particles at a large distance from the plate, d_P is the particle diameter, and c_D the particle drag coefficient. The ratio of the width of the particle stream tube which impacts on the plate is plotted as function of the parameter α defined in the figure. These results show that the deviation function is greatly influenced by the temperature of the plate if the flow is free-molecular or near free-molecular.

4. CONCLUSIONS

Main Fundamental Problems to be Solved in the Future

1. Drag force and heat transfer on spheres are known in different regimes. Additional measurements are needed in transitional low density regime for varying surface temperatures.

2. In the low-Reynolds number regime (near free molecular flow) the heat transfer is dependent on surface temperature. No experimental data are available on this behavior.

3. Only scarce measurements on nonspherical particles are available.

4. The behavior of small particles in turbulent flow may depend on the ratio of particle diameter and turbulence length scale. No measured data on these phenomena are available.

5. Gas flow with solid particles may be largely influenced by the ratio of particle mean free path to a characteristic length. Only few measurements are known where this influence has been recognized. Fundamental experiments are needed to get a clear insight. Theoretical approximations should follow the lines of the BKG-model in kinetic theory (39). This may give an adequate description of interaction problems in dense particle flow.

6. An experimental investigation of relaxation phenomena is needed. This may comprise sound and shock propagation measurement or a direct measurement of the velocity and temperature lag of the particles.

7. In high-altitude micrometeorite problems, the particles flow in an ionized gas. In view of such problems, particle flow should also be studied in an ionized gas.

5. REFERENCES

(1) Wuest, W., "Hyperschallströmung staubhaltiger Gase bei geringer Dichte," Z. Flugwiss, Vol. 18, 6, pp. 185-194, 1970.

(2) Legge, H. and Koppenwallner, G., "Sphere Drag Measurements in a Free Jet and a Hypersonic Low Density Tunnel," AVA Göttingen, Report 70 A 37, 1970.

(3) Legge, H., "Widerstandsmessungen an parallel angeströmten Platten und senkrecht angeströmten Scheiben in Überschallfreistrahlen grober Verdünnung," Diss. Univ. Göttingen, 1972 and DLR-FB 73-17, 1973.

(4) Schmitt-v. Schubert, B., "Überschallströmung eines Gases mit festen Partikeln um einen Keil," ZAMP, Vol. 23, 5, 765-779, 1972.

(5) Healy, J.V., "Perturbed Two-Phase Cylindrical Type Flow," The Physics of Fluids, Vol. 13, 3, pp. 551-557, 1970.

(6) Healy, J.V., "Two-Phase Convex-Type Corner Flows," J. Fluid Mechanics, Vol. 41, pp. 759-768, 1970.

(7) Mühle, J., "Untersuchung von Partikelbahnen in Drehströmungen. Part 1. Über den Einfluss der wichtigsten Kennzahlen," Chemie Ing. Techn., Vol. 43, 21, pp. 1158-1168, 1971.

(8) Brauer, H. and Thiele, H., "Bewegung von Partikelschwärmen," Chemie Ing. Techn., Vol. 45, 13, pp. 909-912, 1973.

(9) Hein, K., "Beitrag zum Wärmeübergang in feststoffbeladenen Gasströmen technischer Staubfeuerungen," Thesis, University of Stuttgart, 1972. Extract: Z. VDI Vol. 115, 12, p. 1000, 1973.

(10) Schneider, W., "Radiant Interchange among Suspended Particles and its Effect on Thermal Relaxation in Gas-Particle Mixtures," Proc. Heat Transfer and Fluid Mechanics Inst., Leland Stanford Junior Univ., pp. 353-370, 1972. DFVLR-Sonderdruck 210.

(11) Hein, K. and Lowes, T., "Beitrag zum Strahlungswärmeübergang in feststoffbeladenen Gasströmen," Brennstoff, Wärme, Kraft, Vol. 24, 1, pp. 1-6, 1972.

(12) Rudinger, G., "Wave Propagation in Suspensions of Solid Particles in Gas Flow," Appl. Mech. Rev., Vol. 26, 3, pp. 273-279, 1973.

(13) Becker, E., "Relaxation Effects in Gas Dynamics," Aero. J. Roy. Aero. Soc., Vol. 74, 717, pp. 736-748, 1970.

(14) Schmitt-v. Schubert, B., "Zur eindimensionalen stationären Verdichtungsströmung in einem staubigen Gas," ZAMM, Vol. 47, pp. T168-169, 1967.

(15) Schmitt-v. Schubert, B., "Strömungen von Gasen mit festen Teilchen," Thesis, Technical University Darmstadt, 1968.

(16) Schmitt-v. Schubert, B., "Existence and Uniqueness of Normal Shock Waves in Gas Particle Mixtures," J. Fluid Mech., Vol. 38, pp. 633-655, 1969.

(17) Schmitt-v. Schubert, B., "Struktur stationärer Verdichtungsstösse in Gasen mit festen Teilchen," ZAMM, Vol. 50, pp. 671-682, 1970.

(18) Schmitt-v. Schubert, B., "Schallwellen in Gasen mit festen Teilchen," ZAMP, Vol. 20, pp. 922-935, 1969.

(19) Rumpf, H. and Gregor, W., "Die Schallgeschwindigkeit in Gas-Feststoff-Mischungen," Chemie Ing. Techn., Vol. 45, 14, pp. 924-928, 1973.

(20) Weber, M., "Schallgeschwindigkeit und kritischer Strömungszustand in Gas-Feststoff-Gemischen," Habilitationsschrift, Universität Karlsruhe, 1973.

(21) Fuchs, N.A. and Murashkevich, F.I., "Laboratory Powder Disperser (Dust Generator)," Staub-Reinhalt. d.Luft, Vol. 30, 11, pp. 1-3, 1970.

(22) Seger, G. and Sinsel, F., "Untersuchung einer Zerstäubungsvorrichtung mit Hilfe der Kurzzeit-Mikroholographie," Staub-Reinhalt.d.Luft, Vol. 30, 11, pp. 471-475, 1970.

(23) Brauer, H. and Schmidt-Traub, H., "Pneumatischer Transport körniger Feststoffe durch Rohrleitungen," Chem. Ing. Tech., Vol. 44, 17, pp. 1041-1044, 1972.

(24) Vollheim, R., "Beitrag zur Theorie des pneumatischen Transports," Maschinenbautechnik, Vol. 21, 5, pp. 219-223, 1972.

(25) Voliheim, R., "Pneumatischer Transport," VEB Deutscher Verlag fur Grundstoffindustrie, Leipzig 1971.

(26) Siegel, W., "Experimentlle Untersuchungen zur pneumatischen Förderung körniger Stoffe in waagerechten Rohren mit Überprüfung der Ähnlichkeitsgesetze," VDI Forsch, Heft No. 538, 1970.

(27) Krötzsch, P., "Druckverlust und mittlere Partikelgeschwindigkeit bei stationärer Gas-Feststoff-Strömung im senkrechten Rohr," Chem. Ing. Techn., Vol. 44, 6, pp. 393 and 24, pp. 1354-1360, 1972.

(28) Kazanskij, I., "Zur Turbulenzstruktur von Feststoff-Wasser-Strömungen in Rohrleitungen," Thesis, Technical University Hannover, 1971.

(29) Flatow, J., "Untersuchungen über die pneumatische Flugförderung in lotrechten Rohrleitungen," VDI Forsch. Heft No. 555, 1973.

(30) Muschelknautz, E., "Die Berechnung von Zyklonabscheidern für Gase," Chem. Ing. Techn., Vol. 44, pp. 63-71, 1972.

(31) Gloger, J. and Lukas, W., "Untersuchung des Abscheidegrades von Fliehkraftabscheidern bei Verwendung einer Grenzschichtabsaugung." Luft- und Kältetechnik, Vol. 8, 6, pp. 291-295, 1972.

(32) Leschonski, K., "Kennzeichnung disperser Systeme, Teilchengrössenanalyse," Chem. Ing. Tech., Vol. 45 1, pp. 8-18, 1973.

(33) Alex, W., "Zur Genauigkeit der Teilchengrössenanalyse durch Sedimentation im Zentrifugalfeld," Thesis Universität Karlsruhe, 1972.

(34) Seger, G., "Die Anwendung von Laserlichtquellen zur Kontrolle der Luft auf partikelförmige Verunreinigungen," Messtechn., Vol. 81, pp. 142-148, 1973.

(35) Bosch, J., "Gerät zum kontinuierlichen Bestimmen des Staubstroms in Gasströmen," Staub-Reinhaltung der Luft, Vol. 32, 11, pp. 436-440, 1972.

(36) Borho, K., "A Scattered-Light Measuring Instrument for High Dust Concentration," Staub-Reinhaltung der Luft, Vol. 30, 11, pp. 45-49, 1970.

(37) Bohnet, M., "Staubgehaltsbestimmung in strömenden Gasen," Chemie Ing. Techn., Vol. 45, 1, pp. 18-24, 1973.

(38) Zenker, P., "Untersuchungen über die Staubverteilung von strömenden Staub-Luft-Gemischen in Rohrleitungen," Thesis, Technical University,1970, Extract Z. VDI 114, 2, p. 168, 1972.

(39) Bathnagar, P.L., Gross, E.P. and Krook, M., "A Model for Collision Processes in Gases, I. Small Amplitude Processes in Charged and Neutral One-Component Systems," Phys. Rev., Vol. 94, pp. 511-525, 1954.

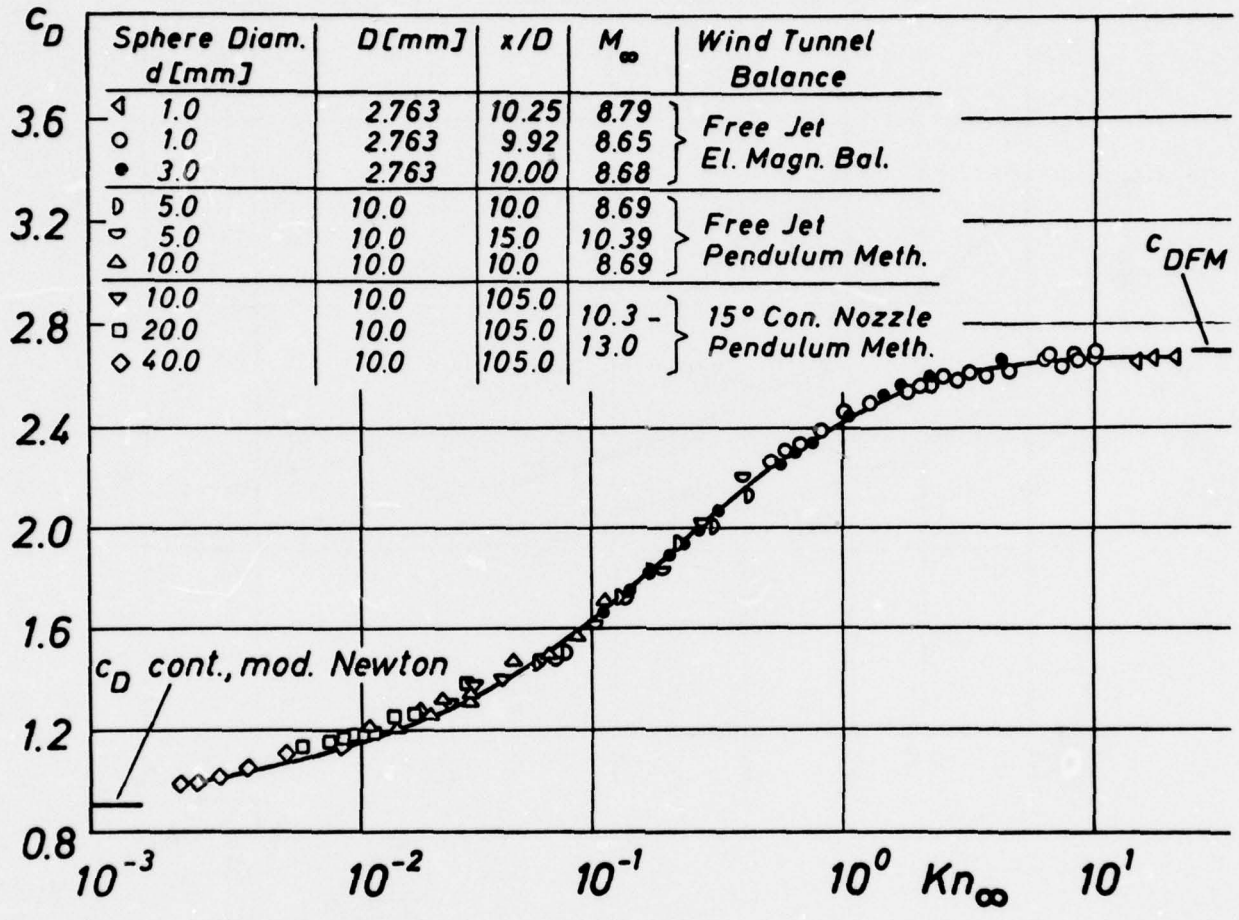

Figure 1 Hypersonic sphere drag in transitional regime, according to measurements by H. Legge and G. Koppenwallner (2).

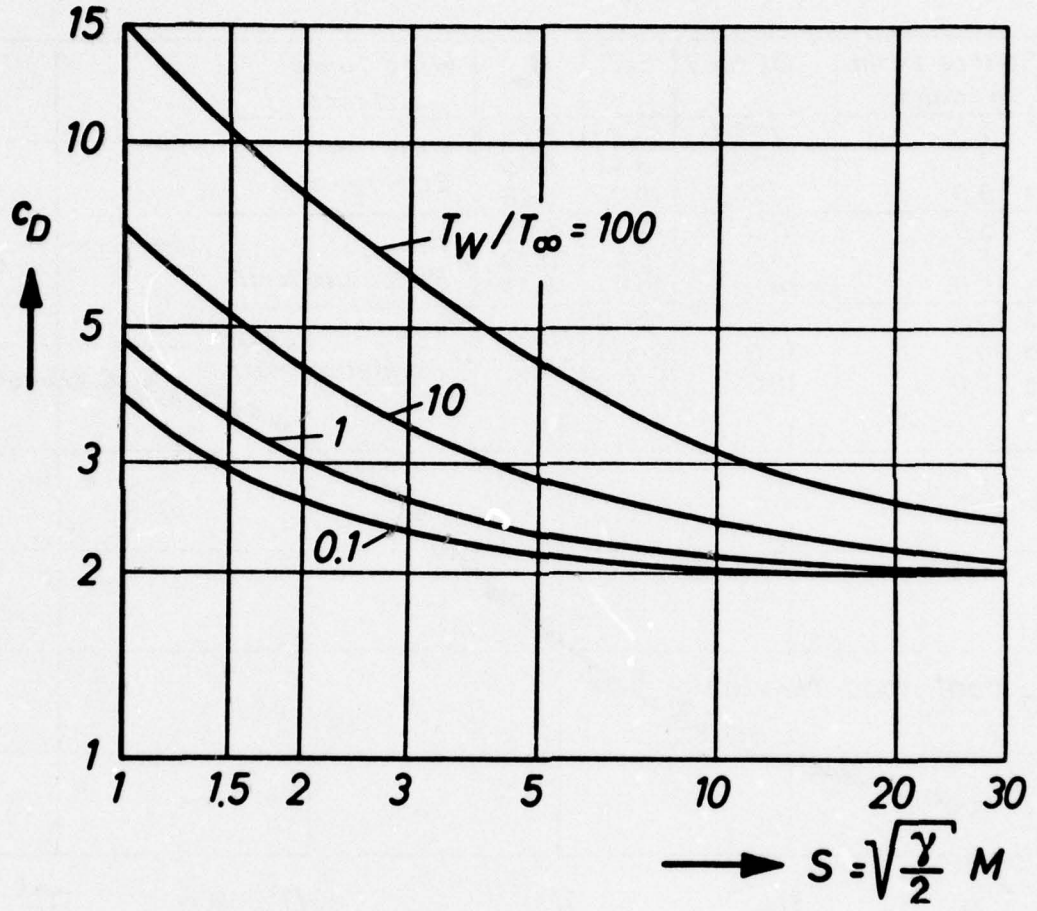

Figure 2 Sphere drag for free molecular flow in dependence of molecular Mach number and surface temperature.

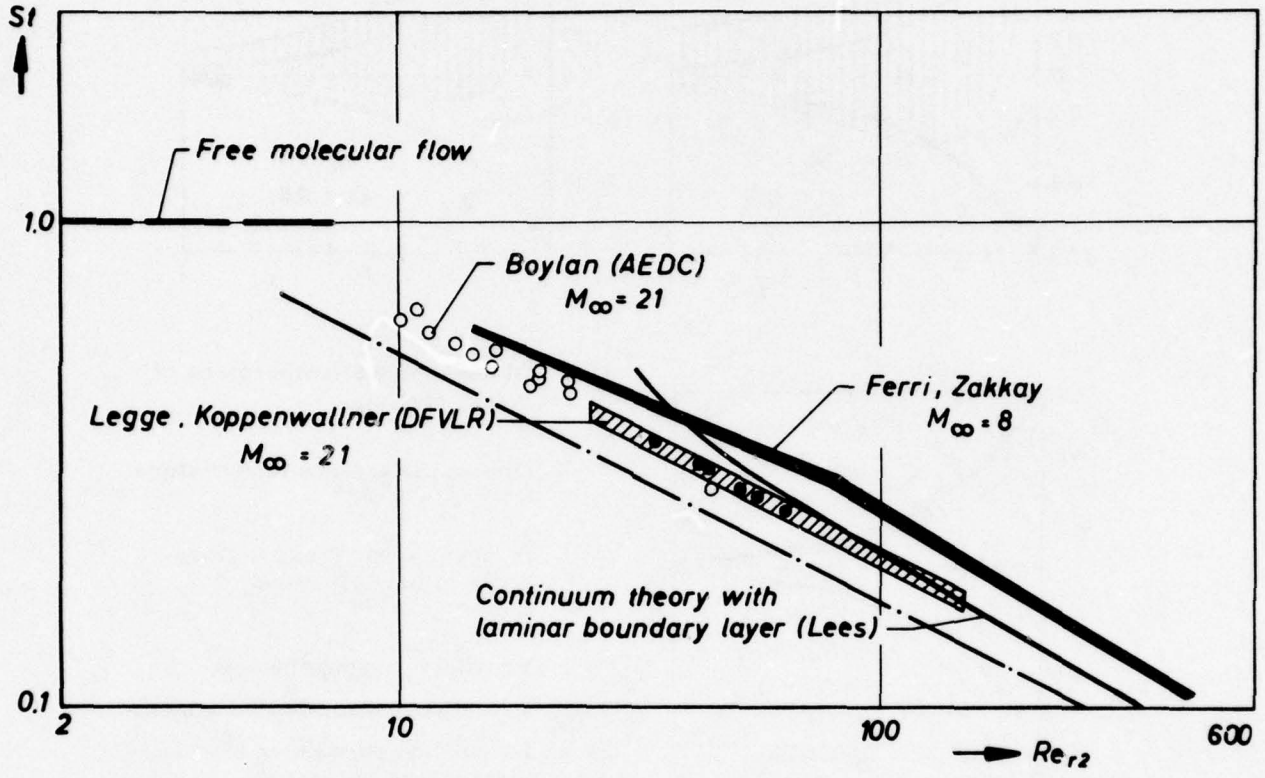

Figure 3 Total heat transfer on a sphere in rarefied hypersonic flow.

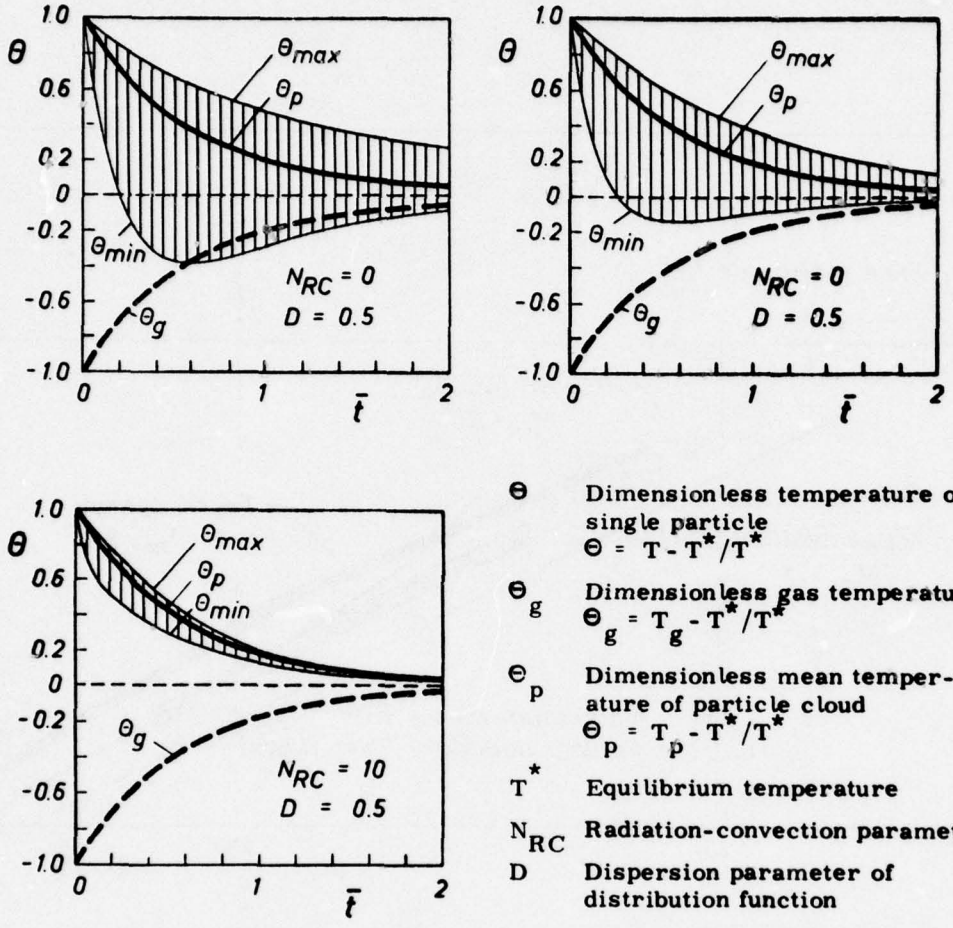

Θ	Dimensionless temperature of single particle $\Theta = T - T^*/T^*$
Θ_g	Dimensionless gas temperature $\Theta_g = T_g - T^*/T^*$
Θ_p	Dimensionless mean temperature of particle cloud $\Theta_p = T_p - T^*/T^*$
T^*	Equilibrium temperature
N_{RC}	Radiation-convection parameter
D	Dispersion parameter of distribution function
t_c	Conductive relaxation time
$\bar{t}$	Dimensionless time; $\bar{t} = t/t_c$
	Temperature range of individual particles indicated by vertically hatching

Figure 4 Radiant interchange among suspended particles, according to W. Schneider (10).

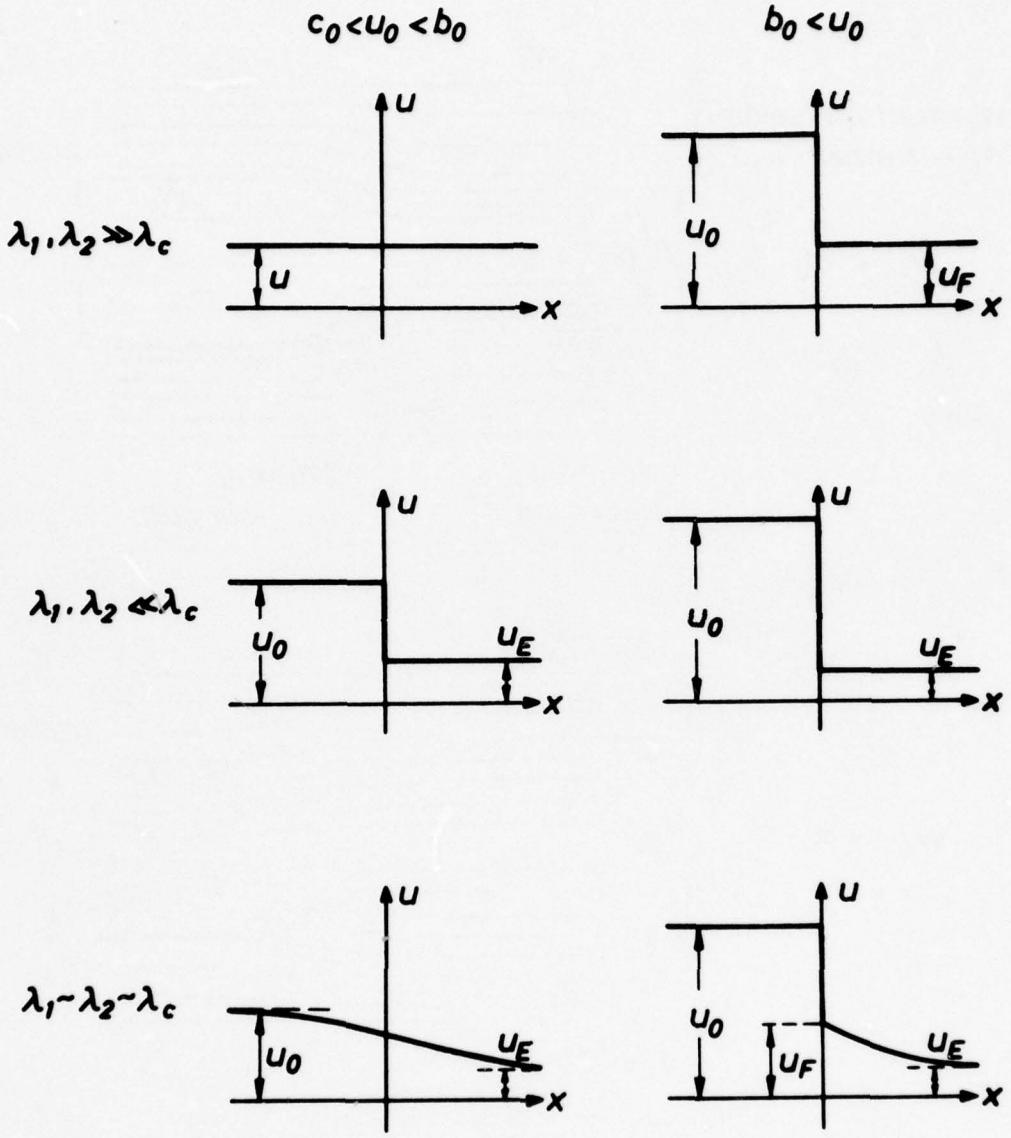

Figure 5 Shock waves in gas flows with solid particles for different relaxation processes, according to B. Schmitt-v. Schubert (15).

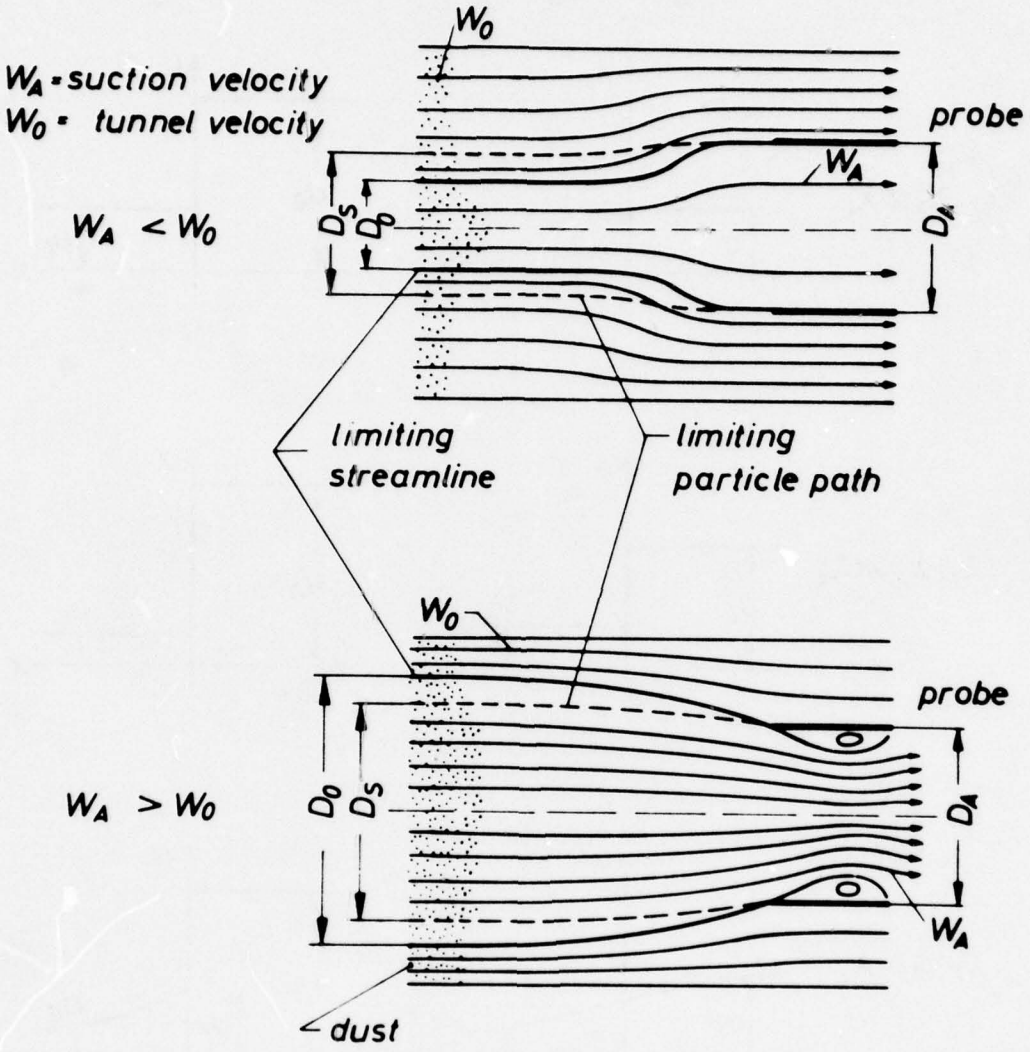

Figure 6 Sampling of gas flow with solid particles for different ratio of suction and free stream velocity, according to M. Bohnet (37).

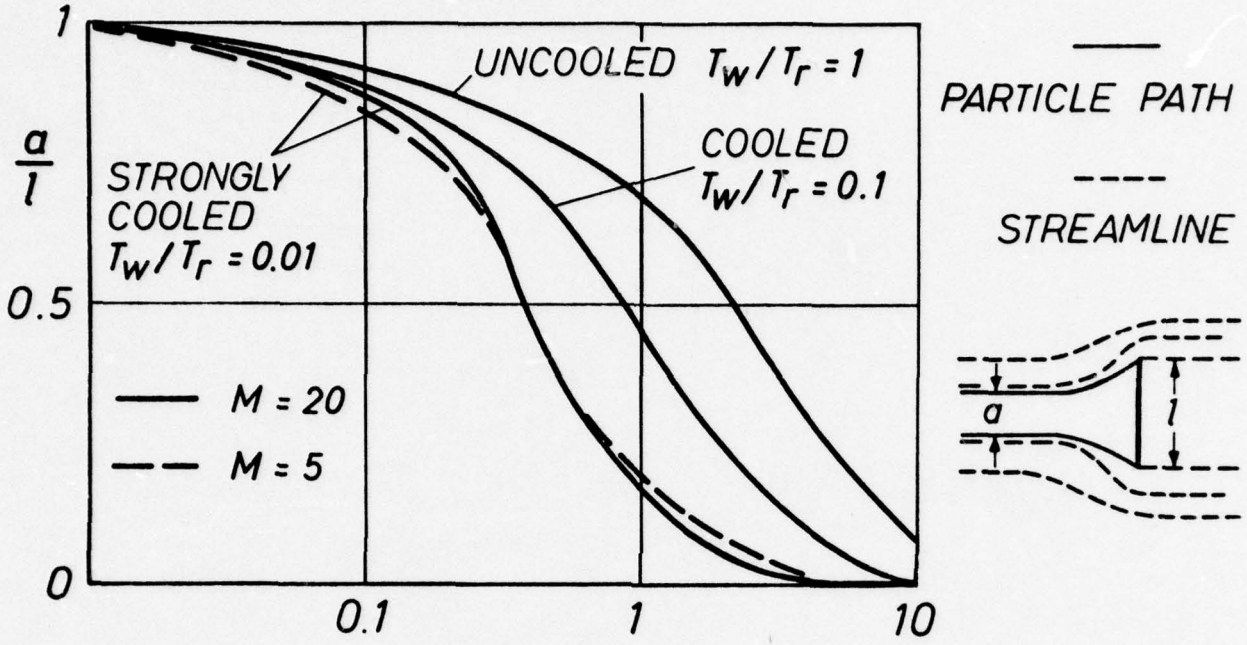

$$\alpha = \frac{l}{d} \frac{\rho_\infty}{\rho_P} \frac{3}{4} c_D$$

Figure 7 Sampling of micrometeorites. Deviation function for hypersonic free molecular flow around a plate, according to W. Wuest (1).

C. A REVIEW OF RESEARCH IN THE UNITED KINGDOM IN THE FIELD OF MULTIPLE FLOWS OF SOLIDS AND GASES

R.A. Duckworth
Professor, Mechanical Engineering Department
City University, St. John Street
London, EC1, England

SUMMARY

This paper represents a survy of research currently being carried out in the United Kingdom. Understanding of solid-gaseous flows is much less complete than in the case of fluid flows partly because of the limitations imposed by the available measuring techniques. Several such techniques are disucssed. The complex nature of gas-particle flows has led to an attempt to obtain a generalized empirical solution which is briefly described. Also included are discussions on particle deposition, entrainment, and erosion caused by the impact of airborne particles.

LIST OF SYMBOLS

a	Semidepth of flat plate or radius of cylinder
A	Cross-sectional area of particle
C_D	Drag coefficient
d	Particle diameter
D	Pipe diameter
e	Electrical permittivity of particle material
g	Gravitational acceleration
i	Electric current
i_ℓ	Leakage current
i_w	Wall current
k	Roughness
L	Pipe length
L_A	Acceleration length
m	Mass of particle
M	Mass flow rate
M*	Mass flow ratio, (M_s/M_f)
Δp	Pressure drop over length l of pipe
Δp_{sA}	Pressure drop due to acceleration
R	Electrical resistance per unit length of pipe
Re	Reynolds number
t	Time
u	Velocity component in x direction
U_a	Fluid velocity in undisturbed region
U*	Friction velocity
v	Velocity component in the y direction
V	Nominal fluid velocity, $(M_f/\rho_f \pi D^2/4)$
V_e	Component of deposition velocity due to interparticle electrical repulsion
V_t	Component of deposition velocity due to turbulence
V_∞	Settling velocity
V_c	Minimum transport velocity

x,y	Particle coordinates
y_o	Distance of grazing streamline from axis of undisturbed flow
θ	Time delay
ϵ	Coefficient of restitution
η	Component of deposition velocity due to interaction of turbulence and electrical components
η_c	Collision efficiency
θ	Pipe inclination
λ	Friction factor, $(\tau_o/\rho_f V^2/8)$
μ	Dynamic viscosity
ν	Kinematic viscosity
ρ	Density
ρ_e	Electrical charge density
ρ^*	Density ratio, (ρ_s/ρ_f)
σ	Stokes number (see Eq. 6)
τ_o	Wall shear stress
φ	Electrical potential, Function of ...

Suffixes

f	Fluid
s	Solid
m	Suspension

1. INTRODUCTION

While a considerable volume of research work is currently being carried out in the United Kingdom in the field of solid-gaseous suspension flows, by far the major effort is related to applications in the chemical, food processing and the materials handling industries. However, a number of these researches may be of interest to workers in the aeronautical industry, and in this paper the author has selected a number of researches which could have relevance in the aeronautical field.

Now although the paper is primarily concerned with solid-gaseous flows, the author also discusses solid-liquid suspension flows where there appears to be a similarity between gaseous and liquid flows and where the use of a liquid in lieu of a gas may be helpful in model studies.

It will be appreciated that our understanding of the mechanism of solid-gaseous flows is much less complete than in the case of fluid flows, and this stems partly from the limitations imposed by the available measuring techniques. However, the relatively new technique of laser-Doppler anemometry appears to offer the prospect of measuring both the particle and fluid velocity distributions and the particle concentration distribution, and such information is likely to lead to a greater physical understanding of suspension flows. This technique and its application in this field will also be discussed in the paper. Where bulk flow behavior is to be examined, the technique of cross correlation has been used very successfully following recent research and development work carried out in the U.K.

While many investigators have formulated mathematical models for the turbulent flow of a suspension of solids under conditions of dilute concentration and including compressiblity and heat transfer effects, the complex nature of such flows has led the writer to attempt to obtain a generalized empirical solution using the technique of dimensional analysis, for the friction factor and other flow parameters.

The problems of particle deposition and entrainment and the erosion caused by the impact of airborne particles such as sand would appear to be of some interest to aeronautical engineers, and these too are discussed.

Inevitably, in a review paper of this nature, the writer has to be selective and it is hoped that the selection of items for disucssion will prove to be of interest to those working in the field of aeronautics.

2. PARTICLE DEPOSITION

2.1 Collision Prediction

In the design of impingement and inertia filters for the removal of particles from an air stream, it is necessary to be able to predict the trajectories of the particles in the region of an obstruction placed

in the path of the suspension flow. On the other hand, there are a number of practically important flow situations in which it is undesirable for the particles to collide with an obstruction. For example, in turbomachinery applications the collision of airborne particles could lead to the deposition of particles on the blade surface with the possibility of impairing the aerodynamic performance, or the collision, in the case of sand or other abrasive particles, could lead to serious erosion (see also E.9).

In an attempt to be able to predict the conditions for collision, Morsi and Alexander (1-4) have studied the trajectories of fine airborne particles, $1 < d < 100$ μm, in a uniform flow field around various body shapes placed in a suspension flow. They determined the trajectories analytically, using the velocity field for a potential flow around various body shapes for the description of the fluid velocities, and combining these velocities with the equations of motion for the particles given by

$$m(du_s/dt) = C_D \rho_f (u_f - u_s)^2 A/2 \tag{1}$$

$$m(dv_s/dt) = C_D \rho_f (v_f - v_s)^2 A/2 \tag{2}$$

where

$$u_s = dx/dt \tag{3}$$

$$v_s = dy/dt \tag{4}$$

and

$$C_D = K_1/Re + K_2/Re^2 + K_3 \tag{5}$$

In Eq. (5), the Reynolds number is defined in terms of the x-component of the relative velocity, thus $Re = (u_f - u_s)d/\nu$, or in terms of the y-component of the relative velocity, $Re = (v_f - v_s)d/\nu$. The constants K_1, K_2, K_3 are selected to give a good fit over the range of Re. This analysis represents an approximation, because it is based on different Reynolds numbers for the x- and y-directions. It should not introduce large errors as long as the component of the relative-velocity vector is much smaller in one coordinate direction than in the other. This assumption apparently was implied by Alexander and Morsi but not explicitly stated. It decouples Eqs. (1) and (2) and thus makes them more tractable. A rigorous treatment would have to compute the drag force in the direction of the relative-velocity vector and then use the x- and y-components of this force in Eqs. (1) and (2) (see also E.3.1). Numerical solution of the equations made it possible to determine the grazing trajectories and hence the collision efficiency η; the latter is defined by y_o/a for a flat plate or a circulat cylinder, where a is the semi-depth of the flat plate or the radius of the cylinder, and y_o is the perpendicular distance from the grazing trajectory in the undisturbed region to the axis of symmetry. Typical trajectories for a flat plate and for a cylinder are shown in Figs. 1 and 2 for different Stokes numbers, where the Stokes number is defined by

$$\sigma = (2/9)\ (Ua/\nu)\ (\rho^*)\ (d/a)^2 \tag{6}$$

with

$$\rho^* = \rho_s/\rho_f.$$

It should be noted that in the case of the flow over an inclined flat plate or an aerofoil, the distortion of the trajectories and the asymmetry of the flow means that the collision efficiency has to be defined in terms of the ratio of the vertical area of the powder flow which collides with the flat plate or aerofoil and the vertical projected area of the flat plate or aerofoil.

In the work described, it will be apparent that the gravitational force on the particle has been neglected, and while no great error is introduced in the case of particles having low settling velocities, this is unlikely to be so for larger or more dense particles, and a term (mg) should be included in Eq. (2). Alexander and Morsi have in fact included the latter and have shown that gravitational effects cause a vertical displacement of the trajectories.

The work would appear to provide a useful basis for further studies into the deposition of particles on aerofoils and other body shapes and for erosion and impact studies (see also A.4, B.3.5, E.3 and 9).

2.2 Deposition Velocity of Charged Particles

Work in the field of Electro-Gas Dynamics (EGD) is currently being studied by Musgrove (5,6), and one of the interesting problems examined is concerned with the drift velocity of the charged particles towards the walls of the EGD generator duct. This study arose because it was thought that the low efficiency obtained when an EGD generator was operated at atmospheric pressure was largely due to parasitic fields caused by the deposition of charge on the walls of the duct.

In this study, silicon carbide particles having a mean diameter of 4.5 μm were transported through a high-soda glass duct of 50 mm in diameter (Fig. 3a) at a velocity of 54 m/s; the particle concentration was 0.30 kg/m^3, corresponding to a number density of 10^{12}/m^3. The resistivity was maintained constant by temperature control at a value of 304 GΩ/m. Under these conditions, Musgrove showed that the deposition velocity, V_D, could be determined from measurements of the electrical potential distribution along the duct; he obtained a value of 0.22 m/s.

In his analysis, he assumed that the deposition velocity is made up of three components: a component arising from the fluid turbulence, V_t, a component due to inter-particle electrical repulsion, V_e, and a component $\eta V_t V_e$ due to the interaction between the turbulence and electrical components. The value of η must be determined experimentally. He further assumed that the radial field is proportional to the charge density, and thus $V_e = (i/i_o)V_{eo}$, where the suffix (o) refers to conditions at x = 0, at the upstream end of the conducting duct section. Now it will be clear from Fig. 3b that the sum of the current i through the duct due to the flow of the charged particles and the wall current i_w due to the transfer of the charge to the duct wall by the deposited particles will be equal to the leakage current i_ℓ, where

$$di_w = -(di/dx)dx = 2\pi r \rho_e V_D dx \tag{7}$$

and

$$i = \pi r^2 \rho_e V_f \tag{8}$$

thus

$$-di/dx = 2(i/r)\ (V_D/F_f) \tag{9}$$

Now from the above assumptions we have

$$V_D = V_t \left[1 + (i/i_o)V_{eo}(1/V_t + \eta)\right] \tag{10}$$

and substituting for V_D from Eq. (9), we obtain

$$-(1/i)\ (di/dx) = (2/r)\ (V_t/V_f) \left[1 + (i/i_o)V_{eo}(1/V_t + \eta)\right] \tag{11}$$

In this equation, the current i may be determined from the potential gradient and the current i_ℓ using the equation

$$i = i_\ell - (1/R)\ (d\varphi/dx) \tag{12}$$

where $d\varphi/dx$ is obtained by numerical or graphical differentiation. Musgrove thus solved Eq. (11) by plotting $-(1/i)\ di/dx)$ against i/i_o, obtaining $2V_t/rV_f$ from the intercept corresponding to $i/i_o = 0$, and $2V_t V_{eo}(1/V_t + \eta)/rV_f$, from the slope of the straight line. If η is assumed to be zero then V_t and V_{eo} are determined directly, and hence V_D. However, if the experiment is repeated at a different fluid velocity while maintaining the current i_o and hence V_{eo} constant at the same value for each velocity, then η may be determined and the assumption $\eta = 0$ is unnecessary.

In cases where the current flow is small, the turbulent component of the deposition velocity dominates and in this case Musgrove showed that

$$\varphi = (Ri_o/KL)\left[(1 - e^{-Kx})/x - (1 - e^{-KL})/L\right] \tag{13}$$

where $K = 2V_D/rV_f$ and L is the length of the conducting tube. Clearly, a single measurement of the potential φ, corresponding to a given value of x suffices to determine V_D. He also showed that when $V_D \ll rV_f$, the potential distribution is parabolic, and that in this case,

$$V_D = 4\varphi_{max} V_f / i_o R L^2 \tag{14}$$

The determination of V_D using Eqs. (13) or (14) is preferable to that based on Eq. (11), since the latter requires that the electrical potential should be differentiated twice and this introduces serious computational errors.

While this technique of determining the deposition velocity was developed in respect of EGD, it is likely to find application in a number of other fields and could be used for a wide range of experimental conditions.

3. PARTICLE REMOVAL

Having discussed at some length the work concerned with the deposition of particles, we now turn our attention to some recent work carried out by Cleaver and Yates at Liverpool University (7) on the problem of particle detachment of submicron-sized particles. In this work, they develop a criterion for the removal of small particles which is based on the non-steady behavior of the viscous sub-layer of a turbulent boundary layer. They suggest that the turbulent bursts which continually disrupt the viscous layer, which are not unlike miniature tornadoes, may be sufficient to cause instantaneous lift forces sufficient to detach a particle.

In arriving at their criterion for particle removal, they assume that the force responsible for the removal is the hydrodynamic lift force and use the equation due to Saffman (8), which shows that the lift is proportional to $\rho_f \nu^2 (dU^*/\nu)^3$, where U^* is the friction velocity. Since previous work has shown that the adhesive force is proportional to the particle diameter, and since the particles will only be removed if the ratio of the lift force to the adhesive force is greater than unity, they arrive at the relationship,

$$(\rho_f \nu^2/d)\ (dU^*/\nu)^3 > \text{Const.} \tag{15}$$

Since $U^* = (\tau_o/\rho)^{\frac{1}{2}}$, then for a given fluid the criterion for particle removal reduces to

$$\tau_o d^{4/3} > B \tag{16}$$

where τ_o is the wall shear stress, d is the particle diameter, and B is a constant. It is this criterion that Cleaver proposes for the removal of particles, and although he does not give values of B for particles of different shape or for different types of adhesive force, he uses the experimental data of Visser (9) for carbon black on a cellophane substrate to show that $\tau_o d^{4/3}$ has the same order of magnitude for different-sized particles, a value of 337×10^{-6} g-cm$^{1/3}$/s^2 for particles of 0.21 μm in diameter. The consistent units to be used in Eq. (16) are therefore g.cm/s^2 for τ_o and cm for d.

To assess the rate at which particles are removed, he assumes that only one burst of turbulence occurs at any one time over an area equal to $630(\nu/U^*) \times 135(\nu/U^*)$, and that the bursts repeat over a time interval of $75\ \nu/U^{*2}$, the location of the bursts being random. He also assumes that the area of the burst is equal to $(\pi/4)(20\ \nu/U^*)^2$, and that a proportion α of this area is cleaned. By dividing the control area into a number of sites, m, where

$$m = (630\ \nu/U^*) \times (135\ \nu/U^*)/0.7854(20\ \nu/U^*)^2 \tag{17}$$

he points out that after n bursts, where

$$n = t(U^{*2}/75\nu) \tag{18}$$

the probable percentage of cleaned surface is given by

$$S(t) = 1 - (1 - \alpha/270)(U^{*2}/75\nu)t \tag{19}$$

where α is assumed to be of the order of 1/100.

4. EROSION STUDIES

During the transport of abrasive materials, such as sand and carborundum in shot blasting operations, wear at pipe bends and in the pipelines presents a serious problem. Arundel (10) and his co-workers at Liverpool Polytechnic have been carrying out experimental studies to assess the relative importance of solids loading, air velocity and the angle of impact. The results of this work indicate that, for velocities less than 100 m/s, Linatex rubber appears to have a high resistance to wear, though at higher velocities mild steel and tool steel are significantly better. The wear rate for mild steel is given by the equation

$$q = 40 \times 10^{-6} (M^*)^{0.5}\ V^{3.3}\ \text{mm}^3/\text{minute} \tag{20}$$

where the impact angle is in the range from 20^o to 30^o, the mass flow ratio M* lies between 0 and 8, and the air velocity V is 155 m/s.

In their future work they intend to study the wear rate in bends in pipes having diameters in the range $20 < D < 40$ mm where the bend radius will be varied up to a maximum of 6D. The particle velocities, trajectories and concentration in the bend will also be studied by laser-Doppler anemometry. Ultrasonic techniques will be used to locate the regions of maximum wear (see also A.4, B.3.5, and E.9).

5. INGRESS OF FOREIGN BODIES INTO AIRCRAFT ENGINE INTAKES

The problem of the ingress of foreign bodies, such as birds, hailstones, ice, etc. in the atmosphere, or of stones, grass, sand, etc. on the ground, or manufacturing debris left in the aircraft following manufacture or maintenance, is a problem that is being given serious consideration in the U.K. (11).

A number of actions may be taken to avoid the problem, by avoiding areas of high bird concentration, good housekeeping in respect of manufacture and maintenance, and by avoiding in-line ahead take off. Although such actions are helpful, further research and development is required. Studies of the flow conditions required for the pick-up of particles and of the trajectories of particles in the vicinity of the aircraft in general and the engine intakes in particular should be undertaken in order that the conditions for the ingress of foreign bodies may be avoided or that preventive action may be taken by careful design and location of the engine intakes. A considerable amount of work has already been carried out in relation to pick-up velocities, particularly in the case of small particles of sand. This was studied extensively some two decades ago by Bagnold (12). More recently Bagnold (13) has been studying the nature of saltation of particles in water, and this too could be helpful even though the flow conditions are not directly comparable. During the commissioning of power stations the pipework has to be purged to remove debris introduced during erection which could be carried into the turbines. A recent study of this problem by Cranfield and Lawrence (14) gives some useful information on pick-up velocities, and the analysis provides a basis for the further study of the pick-up of large particles close to aero-engine intakes.

Design studies should be undertaken in parallel with the research work, to examine the feasibility of modifying the design and location of the engine intakes, and of providing guards, separators, and filters upstream of the intake (see also A.4, B.3.5, and E.9).

6. EMPIRICAL CORRELATIONS FOR SUSPENSION FLOWS

Though many workers have developed empirical correlations for the various flow characteristics of suspensions, with few exceptions these workers have confined their studies to a limited range of the variables involved. It thus appeared to the author, that there would be merit in attempting to generalize the equations for suspension flows, using for this purpose the technique of dimensional analysis. A detailed account of this treatment is given by Rose and Duckworth (15) who deal with the flow of suspensions of particles in liquids and gases in pipelines at various inclinations from the horizontal to the vertical position. Equations are obtained for the length of pipe required for the particles to accelerate from rest to the velocity corresponding to the conditions of established flow, for the pressure drop required to accelerate the particles to this velocity, for the pressure gradient required to maintain the flow of as suspension under established flow conditions and for the minimum fluid velocity required for the transport of the particles in the form of a suspension. They show that, to an acceptable degree of accuracy, the pressure drop for established flow may be computed from the pressure drop in the pipe when conveying the fluid phase only plus a pressure drop which depends upon the characteristics of the solid phase. Data relating to pipe lines varying in diameter from 30 to 400 mm, conveying solids of specific gravities of 1.5 to 11.1 in liquids and gases, are satisfactorily correlated by means of the equations developed. These equations, some of which have been subsequently modified by the author, are summarized below (see also B.3.2).

$$L_A/D = 6\left[(M_s/\rho_f g^{\frac{1}{2}} D^{5/2}) \times (D/d)^{\frac{1}{2}} \times (\rho^*)^{\frac{1}{2}}\right] \tag{21}$$

$$\Delta p_{sA}/(\rho_f V^2/2) = M^* \times {}_A\varphi_1\,(V^2/gd\rho^{*2}) \times {}_A\varphi_2(\theta) \tag{22}$$

$$\Delta p_m(\rho_f V^2/2)(L/D) = \varphi\left[\rho_f VD/\mu, k/D\right] + \left[{}_F\varphi_1(M^*) \times {}_F\varphi_2(d/D) \times {}_F\varphi_3(\epsilon) \times {}_F\varphi_4(\rho^*) \times {}_F\varphi_5(\theta) \times {}_F\varphi_6(V^2/gD)\right] + 2(gD/V^2)\sin\theta\left[1 + M^*(V/V_s)(1 - \rho_f/\rho_s)\right] \tag{23}$$

$$V_s/V_f = 0.5 \times {}_A\varphi_1(V^2/gd\rho^{*2}) \times {}_A\varphi_2(\theta) \tag{24}$$

$$\Delta p = \Delta p_m + \Delta p_{sA} + \rho_f V^2/2 \tag{25}$$

$$V_c/V_\infty = {}_V\varphi_1(d/D) \times {}_V\varphi_2(\theta) \times M^{*0.3} \tag{26}$$

The function ${}_A\varphi$, ${}_F\varphi$, and ${}_V\varphi$ in these equations refer to correlations for acceleration, friction and velocity and can be found in Ref. 15. As an example, the relationship between the solids friction factor function ${}_F\varphi_6(V^2/gD)$ and the Froude number V^2/gD is shown in Fig. 4. It should be noted that, although Eq. (26) is of the same form as that used in Ref. 15, the equation is based on subsequent experimental work carried out by the author for the transport of particles in air. The equation covers the transport of uniformly sized particles of glass, sand, flyash, sodium bicarbonate, aluminum silicate, polyester and seeds, in the size range $0.006 < d/D < 0.1$ and for pipe inclinations in the range $0 < \theta < 90^\circ$.

It should also be noted that the above equations are restricted to particles of sensibly spherical shape having a narrow size distribution. Current work is concerned with the study of the influence of the particle shape factor, the spread of particle sizes, particle cohesiveness, and the influence of electrostatic effects. In a recent series of experiments (16) by the author, in connection with the influence of electrostatic charge level, on the pressure gradient, it was found that the solids friction factor λ_s showed a significant increase as the dimensionless parameter $i^2/eM_s v^3$ was increased, though further work is required before definitive conclusions can be made in respect of the correlation.

7. APPLICATION OF LASER-DOPPLER ANEMOMETRY TO SOLID-GASEOUS FLOWS

The laser-Doppler technique is particularly appropriate for the measurement of two component flows, in that it does not interfere with the flow and makes the measurement of local velocities and concentrations possible (see also A.3, D.5, and E.9). Up to the present time only a limited number of preliminary investigations have been carried out in the U.K., using single and two-mode particle-size distributions flowing in vertical ducts (17,18). This work has indicated that it is not necessary to use mono-sized particles, since a signal is obtained from each particle. It is intended to extend the present work to include the measurement of the particle sizes, velocity and concentration distribution. Future work will examine the radial distribution of the axial and radial velocities of the particles and the fluid carrier, and the particle and fluid Reynolds stresses, in an attempt to refine the models for the prediction of the shear stress and pressure gradients in suspension flows. However, the technique appears to be limited to the study of relatively dilute concentrations of the order of 1.5% by volume and 15:1 by mass.

At Southampton University (17) flow fields in flames as well as in cold flows have been seeded with either solid particles or aerosols, in order to make velocity measurements. Instruments have been developed which make simultaneous measurements of all three components of velocity, in real time, in hot and cold turbulent flows. Intensities , spectra, scales and Reynolds stresses of the turbulence have been deduced. Preliminary studies of the effects of particle loading on the turbulent flow have been made, but the main interest has been in conditions where the particles do not significantly influence the flow.

Crossed-beam correlation studies have also been carried out at Southampton, in which measurements of the covariance of the signals from two crossed laser beams in a two-phase turbulent flow have yielded statistical information about the turbulence in the vicinity of the point of intersection of the two beams.

8. MEASURING TECHNIQUES FOR VELOCITY, VOLUME FLOW AND MASS FLOW

8.1 Velocity and Volume Flow Measurement

In industrial applications, particularly in the chemical and food processing industries, we frequently require to monitor the mean velocity and the volume flux of the suspension, and it is clearly desirable to avoid interference between the instruments used and the suspension flow. For this purpose, cross-correlation techniques of measurement have been studied extensively in the U.K. by Beck and his colleagues at Bradford University (19).

In these studies, two capacitance transducers, which consist of an electrode fitting flush with the internal surface of the duct and insulated from it, are located at stations A and B separated by a distance L along the length of the duct (see Fig. 5). During the passage of the suspension, the capacitance varies and produces a signal m(t) at the upstream transducer, and a signal n(t) at the downstream transducer. The time delay τ between the random signals produced by the transducers is related to the volume flux through the duct. To determine it, and hence the volume flux, an adjustable time delay β is inserted into the output from the upstream transducer; the product of the delayed upstream signal and the downstream signal, $m(t - \beta) \cdot n(t)$, is integrated over a time to yield a cross-correlation function for a range of values of β, as shown in Fig. 5. To determine τ, use is made of the fact that the cross-correlation function will be a maximum when the delay of the upstream signal β is equal to the time delay τ of the random signals over the distance L between the two transducers. Once τ is determined, it is a simple matter to determine either the suspension velocity or the volume flux since,

$$\text{Suspension Velocity} = L/\tau$$

$$\text{Volume Flux} = (\text{Volume of Pipe Over Length } L)/\tau$$

This technique has been used successfully for the on-line control of chemical process plants and for the metering of dust-laden gas streams (see also A.5.2).

8.2 Mass Flow Measurement

Since the mass flux of solids carried in suspension in a carrier fluid affects the turbulence level of the flow, and since the turbulence level can be monitored by a capacitance transducer, it follows that the mass flow of the solids can be measured by means of A/C voltmeter connected to the transducer (20). Although this method of mass flow measurement requires calibration, it has been used quite satisfactorily for the flow of a wide range of powders and granular materials, including cement, flour, wheat and barley (see also B.3.4.2).

The techniques can be used for the measurement of nongravimetric quantities, such as electrostatic charge, and it has been suggested by the Bradford workers, that they could be used for measuring the amount of charge being carried in an aircraft refueling pipe. In the latter application, abnormally high charge conditions exist, and these can lead to explosions which could be avoided if the above techniques were used for detection.

9. CONCLUSION

In this paper a number of researches in the field of multiple flows of solids in gases which have relevance to aeronautical applications have been briefly outlined, though with few exceptions the motivation for the research has not come from the aircraft industry. A number of other researches have been discussed which are primarily of fundamental interest and where the techniques used are likely to find general applications.

The work on particle deposition and collision has application to the build-up of particulate matter on compressor and turbine blading, particularly when this is considered in conjunction with the interesting work on aerodynamic removal by Cleaver.

While the prime objective of aircraft designers must be to avoid the ingress of foreign bodies such as sand into the engine, and the work of Bagnold and others should be helpful in this respect, nevertheless, it is useful to know something of the factors effecting erosion due to particle impact, and the work of Arundel, et al. is likely to be helpful.

Laser-Doppler and cross-correlation techniques are widely used in the aeronautical field, and it will be interesting to see how these are applied to the field of two-component flows. The suggestion by Beck that a simple capacitance transducer may be used to monitor electrostatic charge levels in aircraft fuel lines is of particular interest.

In conclusion, it is hoped that this brief survey of work in the U.K. proves to be useful in stimulating discussion and further work in the field of multiple flows of solids in gases.

10. REFERENCES

(1) Morsi, S.A. and Alexander, A.J., "Collision Efficiency of a Particle with a Sphere and a Cylinder," Paper B2, International Conference on the Pneumatic Transport of Solids in Pipes, British Hydromechanics Research Association, Cranfield, Cambridge University, September 1971.

(2) Morsi, S.A. and Alexander, A.J., "Theoretical Low-Speed Particles Collision with Symmetrical and Cambered Aerofoils," Paper 72-WA/FE-35, ASME Winter Annual Meeting, New York, New York, November 1972.

(3) Morsi, S.A. and Alexander, A.J., "An Investigation of Particle Trajectories in Two-Phase Flow Systems," J. Fluid Mechanics, Vol. 55, 2, pp. 193-208, 1972.

(4) Morsi, S.A. and Alexander, A.J., "Impingement Separators," Paper C4, International Conference on the Pneumatic Transport of Solids in Pipes, British Hydromechanics Research Association, University of Surrey, September 1973.

(5) Musgrove, P.J. and Lovett, C.D., "An Electrical Method for Measuring the Particle Deposition Velocity from a Turbulent Gas Flow," International Conference on the Pneumatic Transport of Solids in Pipes, British Hydromechanics Research Association, University of Surrey, September 1973.

(6) Musgrove, P.J., "Energy from Electro-Gas-Dynamics," Electronics and Power, Vol. 19, pp. 327-330, 1973.

(7) Cleaver, J.W. and Yates, B., "Mechanism of Detachment of Colloidal Particles from a Flat Substrate in a Turbulent Flow," J. Coll. and Interface Sci., Vol. 44, 3, September 1973.

(8) Saffman, P.G., "The Lift on a Small Sphere in a Slow Shear Flow," J. Fluid Mechanics, Vol. 22, pp. 385-400, 1965.

(9) Visser, J., "Measurement of the Force of Adhesion Between Submicron Carbon Black Particles and a Cellulose Film in Aqueous Solution," J. Coll. and Interface Sci., Vol. 34, pp. 26-31, 1970.

(10) Arundel, P.A., Taylor, I.A., Dean, W., Mason, J.S., and Doran, T.E., "The Rapid Erosion of Various Pipe-Wall Materials by a Stream of Abrasive Alumina Particles," International Conference on the Pneumatic Transport of Solids in Pipes, Paper E1, British Hydromechanics Research Association, Cranfield, University of Surrey, September 1973.

(11) Bore, C., Private Communication from Hawker Siddeley Aviation, Ltd., Kingston-Upon Thames, Surrey.

(12) Bagnold, R.A., "The Physics of Wind Blown Sands and Desert Dunes," Methuen, London, 1941.

(13) Bagnold, R.A., "The Nature of Saltation and of 'Bed Load', Transport in Water," Royal Society London, A332, pp. 473-504, 1973.

(14) Cranfield, R.R. and Lawrence, J., "Pipework Purging by Water Flushing," Proc. Institute Mechanical Engineering, Vol. 187, 63/73, pp. 801-808.

(15) Rose, H.E. and Duckworth, R.A., "Transport of Solid Particles in Liquids and Gases," The Engineer, Vol. 227, pp. 478-483, March 1969.

(16) Duckworth, R.A. and Chan, V.K., "The Influence of Electrostatic Charges on the Pressure Gradient During Pneumatic Transport," Paper A5, International Conference on the Pneumatic Transport of Solids in Pipes, British Hydromechanics Research Association, University of Surrey, September 1973.

(17) Bray, K.N.C., Southampton University, Private Communication.

(18) Arundel, P.A., Liverpool Polytechnic, Private Communication.

(19) Beck, M.S., Hobson, J.H., and Mendies, P.J., "Mass Flow and Solids Velocity Measurement in Pneumatic Conveyors," Paper D3, International Conference on the Pneumatic Transport of Solids in Pipes, British Hydromechanics Research Association, Cambridge University, September 1971.

(20) King, P.W., "Mass Flow Measurement of Conveyed Solids, by Monitoring of Intrinsic Electrostatic Noise Levels," Paper D2, 2nd International Conference on the Pneumatic Transport of Solids in Pipes, British Hydromechanics Research Association, Cranfield, University of Surrey, September 1973.

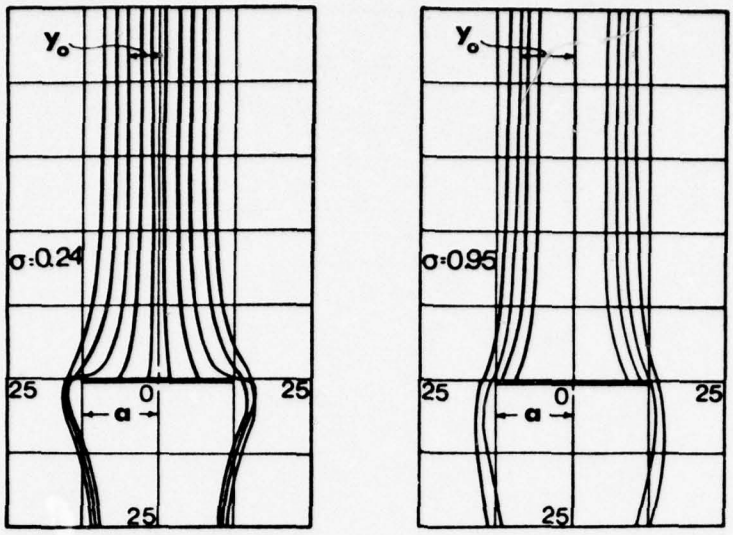

Figure 1 Particle trajectories in the vicinity of a flat plate perpendicular to the direction of flow for two values of the Stokes number (4). (Dimensions are in mm).

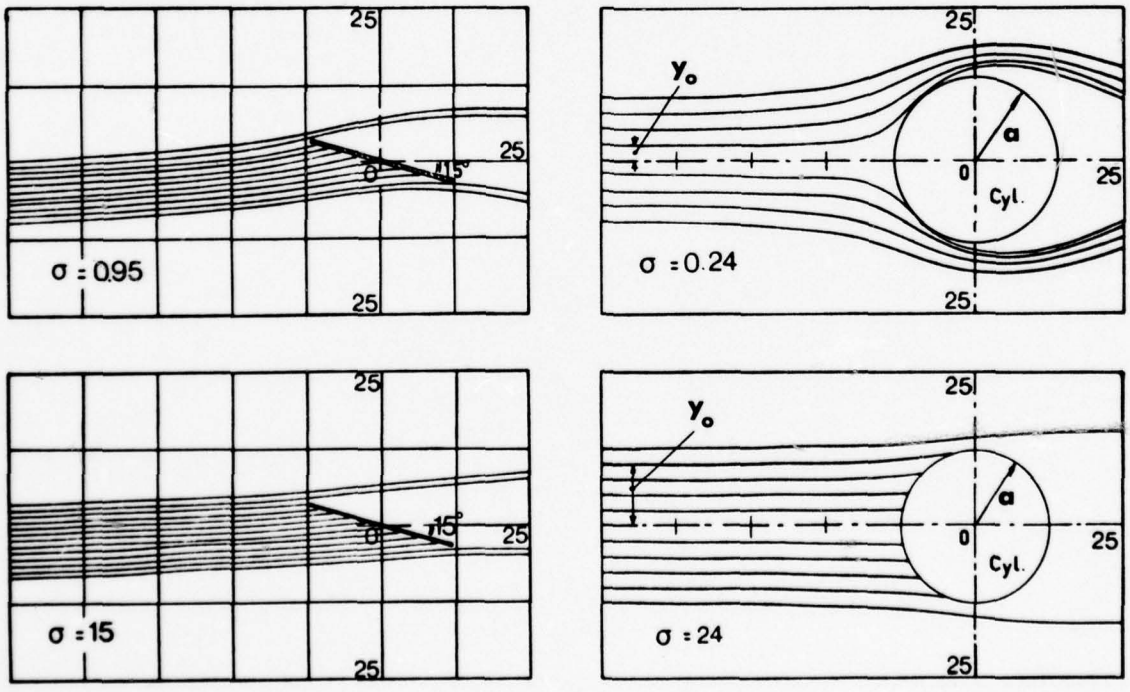

Figure 2 Particle trajectories in the vicinity of an inclined flat plate (15°) and of a circular cylinder for two values of the Stokes number. (Dimensions are in mm)

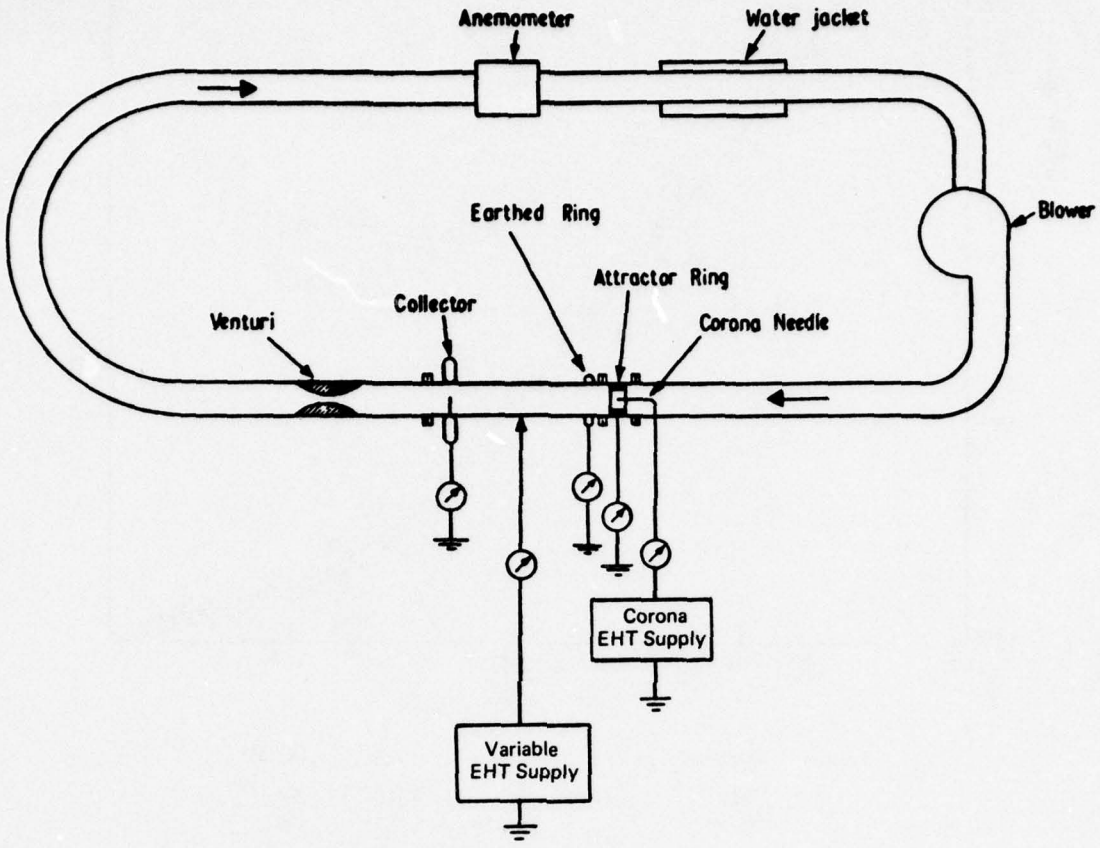

Figure 3a Apparatus used by Musgrove for measurement of deposition velocities.

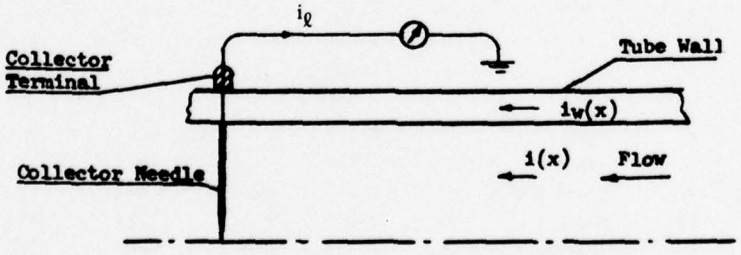

Figure 3b Diagram showing wall and duct current flows (5).

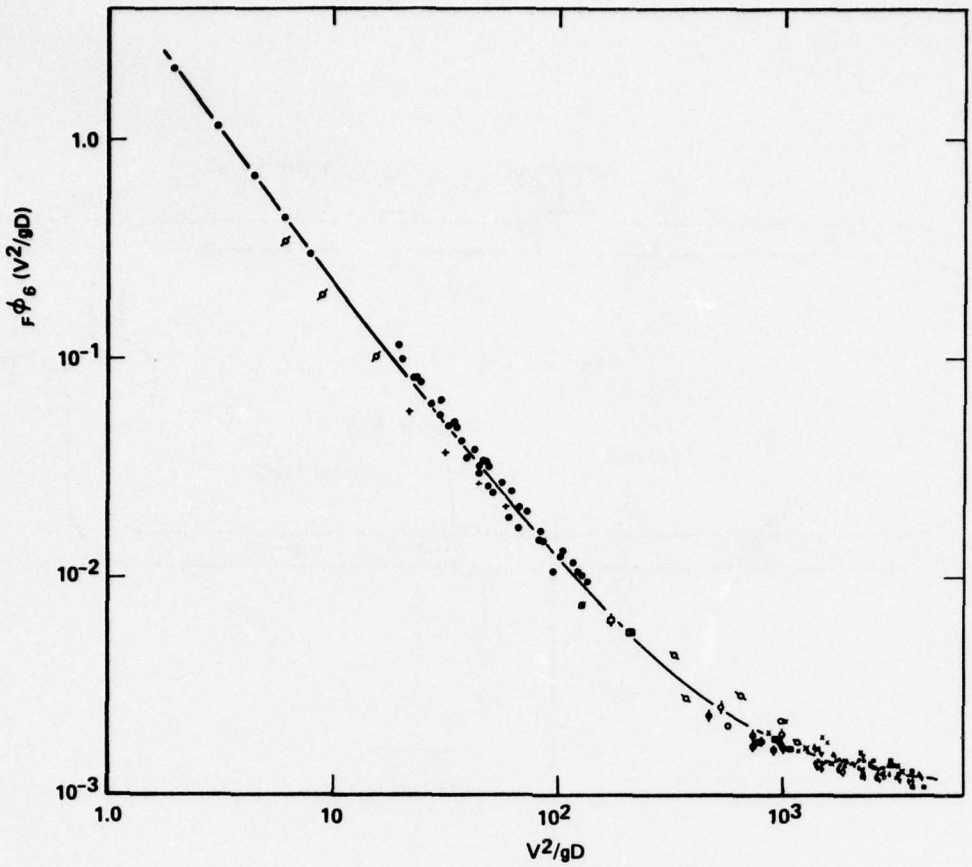

Symbol	Material	Fluid	d (in.)	D (in.)	ρ_s (lb/ft^3)
•	Coal	Water	0·5	3·0	94
⁄	Sand	"	0·118	5·0	165
+	Steel	"	0·125	1·265	460
•	Lead	"	0·095	"	695
◊	Blaud's pills	Air	0·28	2·0	114
◊	"	"	"	3·0	"
◆	Mustard	"	0·08	1·265	126
⁄	Lead	"	0·128	"	695
✕	"	"	0·08	"	"
▲	"	"	0·06	"	"
⁄	"	"	0·043	"	"
▼	"	"	0·022	"	"
⁄	"	"	0·015	"	"
■	Steel	"	0·125	"	450
×	Glass	"	0.118	"	187
◆	Limestone	"	1·25	6·0	89
•	Coke	"	1·0	6·0	32
■	Iron ore	"	0·125	6·0	200
■	Wheat	"	0·20	16·0	
◊	"	"		12·0	
■	"	"		10·0	

Figure 4 Graph relating $_F\varphi_6$ (V^2/gD) *and* V^2/gD (15).

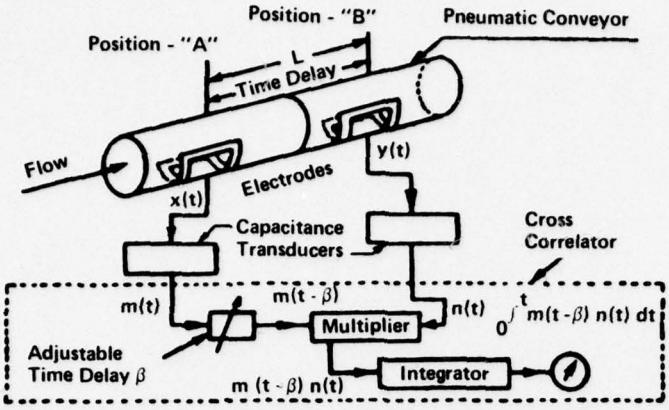

Cross correlation flowmeter

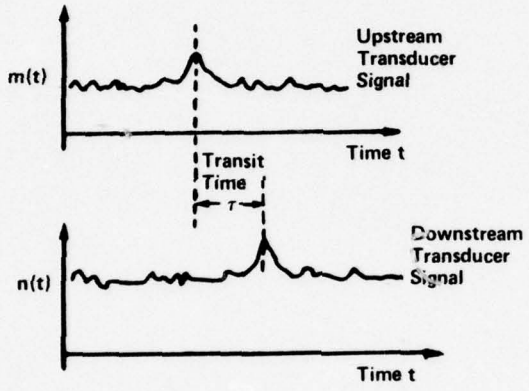

Transducer output signals

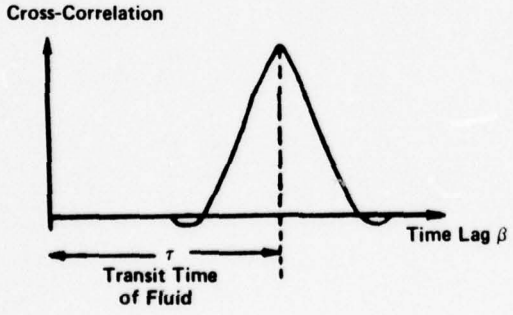

Typical cross-correlation

Figure 5 Cross-correlation technique used for metering of suspension flows (19).

D. FLOW OF SOLID PARTICLES IN GASES - ACTIVITIES AT THE VON KARMAN INSTITUTE FOR FLUID DYNAMICS

Jean J. Ginoux
Associate Director
and
Michel Riethmuller
Assistant Professor
Von Karman Institute for Fluid Dynamics
1640 Rhode-St.-Genèse
Belgium

SUMMARY

Research done at the VKI is briefly reviewed. The topics discussed include low-speed and high-speed gas-particle flow. Theoretical and experimental aspects are discussed as well as some work on instrumentation. In addition, observations in a fluidized bed are briefly described, and development of a laser-Doppler velocimeter is outlined.

LIST OF SYMBOLS

d	particle diameter
P	static pressure
P_o	total pressure
Q_p	particle mass flow
Q_g	gas mass flow
u_p	particle velocity
V_g	gas velocity
x	longitudinal position
y	transversal position
ΔP_m	pressure differential measured in a mixture
ΔP_g	pressure differential due to gas only
η	loading ratio = Q_p/Q_g
ρ_p	density of particle phase in the mixture

1. INTRODUCTION

This paper is a survey of the basic work done at the VKI on gas-particle flows since 1970. It deals successively with low-speed flows, high-speed flows, fluidization and the development of a laser-Doppler velocimeter.

2. LOW-SPEED GAS-PARTICLE FLOWS

In a flowing suspension, the loading ratio, or ratio of the mass flow of solids to that of the gas, is a very important parameter. Buchlin and Riethmuller (1) improved an existing technique of instantaneous measurements of the loading ratio in a venturi tube. They analyzed the theoretical conditions for an optimum geometry and developed an analog data-processing system which allows a direct reading of the loading ratio. It was experimentally and theoretically demonstrated that the ratio of particle and gas velocities, upstream of the venturi tube, had a strong effect on its calibration factor. The latter can be reasonably well predicted as demonstrated by the good agreement found between experimental and theoretical results. Typical venturi-tube calibration curves for two inlet velocity ratios are presented in Fig. 1, where curves a and b refer to particle-to-gas velocity ratios of 0.6 and 0.4. Riethmuller and Ginoux (2) demonstrated that a detailed analysis of gas-particle flows was possible by using a laser-Doppler velocimeter (see instrumentation section). Nouvellon and Riethmuller (3) showed experimentally that the behavior of particles entrained by a gas flow was strongly dependent on particle-wall and particle-particle interactions. The analysis of velocity and concentration measurements, performed in a horizontal pipe, led to the conclusion that a bulk-flow approach was not sufficient to describe a flowing suspension. A study of the kinetics of the particles was thus started by Bouton and Riethmuller (4). Particle trajectories and velocity distribution functions were determined with a laser-Doppler velocimeter in a suspension flowing in a complex geometry. Particle velocity and concentration profiles measured in a horizontal converging duct are represented in Fig. 2. The particle diameter for these experiments is $d = 480 \pm 30$ μm, and the loading ratio is $\eta = 1.98$. Axial distance x is measured from an arbitrary origin with $x = 100$ cm being located at the inlet of the test section (see inset of upper part of the figure). For the conditions of

Fig. 2, the probability density function of the particle velocity, measured at one location in the converging duct, is plotted in Fig. 3. From the analysis of these results, a physical interpretation of the flow of a suspension in a complex geometry was proposed. Particle-particle interactions were shown to be of small importance compared to the wall-particle interaction. A computer program, based on a "semi-kinetic" model of the flow has been written. The results of the calculation were in good agreement with the experimental data.

3. HIGH SPEED GAS-PARTICLE FLOWS

Theoretical and experimental investigations of gas-particle nozzle flows have been performed at the von Karman Institute since 1970. Emphasis was given to the effects of high loading ratios. A one-dimensional analysis has been programmed for an IBM 1130 which was used by Dumortier and Ginoux (5) to perform a dimensionless parametric study of gas-particle nozzle flows in which velocity, temperature, and pressure variations were computed. Transonic solutions for large loading ratios have also been examined. They provided the initial conditions for the analysis of the gas-particle flow in an axisymmetric nozzle which was performed by Johnson (6). His program yielded a numerical solution for the supersonic part of the nozzle in which the partial differential equations were solved by the method of characteristics.

Riethmuller and Thiry (7) measured mass flows and static pressure distributions in nozzles for high loading ratios. The flow was fed to the nozzle from a constant-pressure reservoir, and the diameter of the particles was 250 μm. The converging part of the nozzle was ellipsoidal and the diverging part conical (1.5° half-angle). Typical results are shown in Fig. 4, where the mass flow of the gas has been plotted against the mass flow of the particles. Only data for the last part of the nozzle are shown, since no measurements were made upstream of this portion.

The analysis was based on simultaneous integration of the continuity, momentum, and energy equations for both the gas and the particles (see also E.5 and 7). Newtonian drag of isolated spheres was assumed. The drag coefficient depends on both Reynolds number and Mach number but, effectively, varied only between 0.4 and 0.6. Each particle was assumed to have uniform internal temperature, and the heat-transfer equation was written for isolated spheres with forced convection only. The calculations were started at the inlet section of the nozzle for a prescribed initial particle velocity, but it was found that the results are quite insensitive to this assumption. A comparison of the measured static pressure distributions with theoretical results is presented in Fig. 5. The predicted effect of the particles on the pressure distribution is in good agreement with the experimental results.

After a facility, especially designed for high-speed gas-particle flows with high loading ratios, was completed, an investigation of a gas-particle flow over an obstacle was performed by Bouffinier and Riethmuller (8). Impact forces of a gas-particle jet on a target as well as localized impacts on a small probe were determined. These experimental results have been helpful in providing an insight into the behavior of a high-speed gas-particle jet over an obstacle.

4. FLUIDIZATION

An investigation of the hydrodynamic behavior of a two-dimensional bed in the presence of a cylindrical obstacle was performed by Ginoux, De Geyter, and Kilkis (9).

At superficial velocities below minimum fluidization conditions, local fluidization was photographically observed near the obstacle. Information on the dynamics of the bubble were deduced from the pressure variations measured on the surface of the cylinder.

At minimum fluidization velocity, a study was made of the interaction of a single bubble with the obstacle. These results lead to a better understanding of the heat-transfer mechanism in a fluidized bed.

5. LASER-DOPPLER VELOCIMETER

The development of a laser-Doppler velocimeter was started at the von Karman Institute in 1972. Barker, Riethmuller and Ginoux (10) set up a "fringe" system for the measurement of the velocity of large solid particles (up to 500 μm) in a two-phase flow. The analysis of the special requirements for large-particle measurements was further improved by Riethmuller (11) who proposed a new model of the quality-factor distribution curve for large particles. The Doppler signal obtained from the photodetector is characterized by its quality factor which is the ratio of the amplitude of the Doppler frequency and the overall amplitude of the signal. This quality factor greatly depends on the ratio between particle diameter and fringe spacing. It was generally accepted that it decreased rapidly for large values of the ratio, but a certain number of experiments led to the conclusion that for very large ratios of particle diameter-to-fringe spacing, the quality factor should rise again and then decrease further. This departure from the previously accepted curves should be dependent on the ratio of the particle diameter to the laser light wavelength. An anticipated quality-factor distribution curve was thus proposed, which explained why it was possible to measure the velocity of large particles with a particle diameter to fringe spacing ratio larger than 30. Durst and Eliasson (12) have confirmed this hypothesis.

In the meantime, an electronic Doppler processor was developed by the electronics laboratory of the von Karman Institute. This enabled many investigations to be undertaken with the laser-Doppler velocimeter. Riethmuller and Olivari (13) have performed velocity measurements in wet-steam turbine cascades. Measurements in centrifugal pumps and in two-phase flows have also been made with this equipment. A more recent analysis of the application of the laser-Doppler velocimeter to unsteady flow measurements has been performed by Riethmuller (14). Figure 6 shows a view of the VKI laser velocimeter set up for measurements in a free jet (see also A.3, C.7 and E.9).

6. CONCLUSION

Work on gas-particle flow has been in progress at the VKI only since 1970. The preceding sections describe the status of this program at the present time, and work in this area is continuing.

7. REFERENCES

(VKI TN and TM are available free of charge. VKI PR can be obtained in the form of Xerox Copies which can be purchased. VKI TR are not available.)

(1) Buchlin, J.M. and Riethmuller, M.L. "Mesure de Débit Instantané de Particules Solides dans un Écoulement Biphasique Gaz-Solide," VKI PR 72-309, 1972.

(2) Riethmuller, M.L. and Ginoux, J.J., "The Application of a Laser-Doppler Velocimeter to the Velocity Measurement of Solid Particles Pneumatically Transported," Proc. 2nd Int. Conf. on Pneumatic Transport of Solids in Pipes, Proc. British Hydraulic Research Association, Cranfield, Paper D3, pp. D3-21/D3-32, September 1973.

(3) Nouvellon, D. and Riethmuller, M.L., "Étude Expérimentale d'un Écoulement Gaz-Particules dans une Conduite Horizontale," VKI PR 73-04, 1973.

(4) Bouton, F. and Riethmuller, M.L., "Étude de l'Écoulement d'une Suspension dans un Conduit à Géometrie Complexe," VKI PR 74-15, 1974.

(5) Dumortier, J.C. and Ginoux, J.J., "Aspect Théorique de l'Étude Paramétrique des Écoulements Diphasiques Gaz-Particules Solides dans des Tuyères Convergentes-Divergentes," Specialization Project, Brussels University (Institut d'Aéronautique), 1972.

(6) Johnson, J.R., "Supersonic Gas-Solid Particle Flow in an Axisymmetric Nozzle by the Method of Characteristics," VKI TN 78, 1971.

(7) Riethmuller, M.L. and Thiry, F., "Étude Experimentale de l'Écoulement d'un Mélange Gaz-Particules Solides dans une Tuyère Convergente-Divergente," VKI TR 51, 1971.

(8) Bouffinier, C. and Riethmuller, M.L., "Étude d'un Écoulement Supersonique Gaz-Particules sur un Obstacle," VKI PR 74-19, 1974.

(9) Ginoux, J.J., De Geyter, F., and Kilkis, B., "Hydrodynamics of a Two-Dimensional Fluidized Bed in the Vicinity of a Cylinder with Horizontal Axis," Proc. International Symposium "Fluidization and Its Applications," (La Fluidisation et ses Applications), Toulouse (France) 1-5 October 1973, Cepadues Editions, Toulouse, France.

(10) Barker, Jr., R.H., Riethmuller, M.L., and Ginoux, J.J., "The Development of a Laser-Doppler Velocity Meter for the Measurement of Solid Particle Velocity in a Two-Phase Flow," VKI TN-81, 1972.

(11) Riethmuller, M.L., "Optical Measurement of Velocity in Particulate Flows," VKI Lecture Series 54 "Measurement of Velocities in Single and Two-Phase Flows," February 19-23, 1973.

(12) Durst, F. and Eliasson, B., "Properties of Laser-Doppler Signals and their Exploitation for Particle Size Measurements," Proc. Laser-Doppler Anemometer Symposium Copenhagen 1975, P.O. Box 70, DK-2740, Srovlunde, Denmark, 1976, pp. 457-477.

(13) Riethmuller, M.L. and Olivari, D., "Le Vélocimètre Laser-Principes et Applications," VKI TM 25, 1974.

(14) Riethmuller, M.L., "Laser-Doppler Velocimetry," VKI Lecture Series 73 "Measurement of Unsteady Fluid Dynamic Phenomena," January 27-31, 1975.

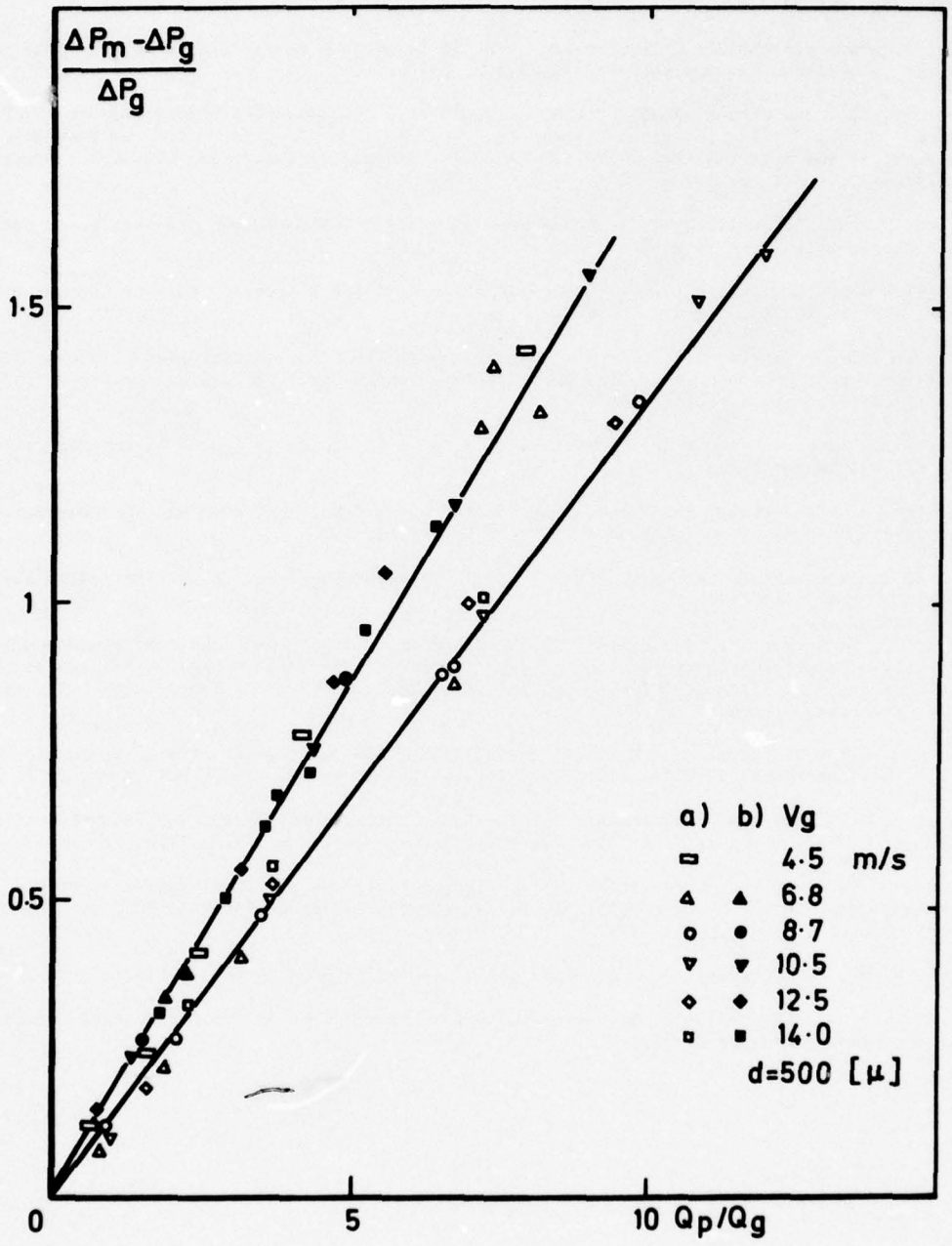

Figure 1 Calibration curve of solid mass flow meter.

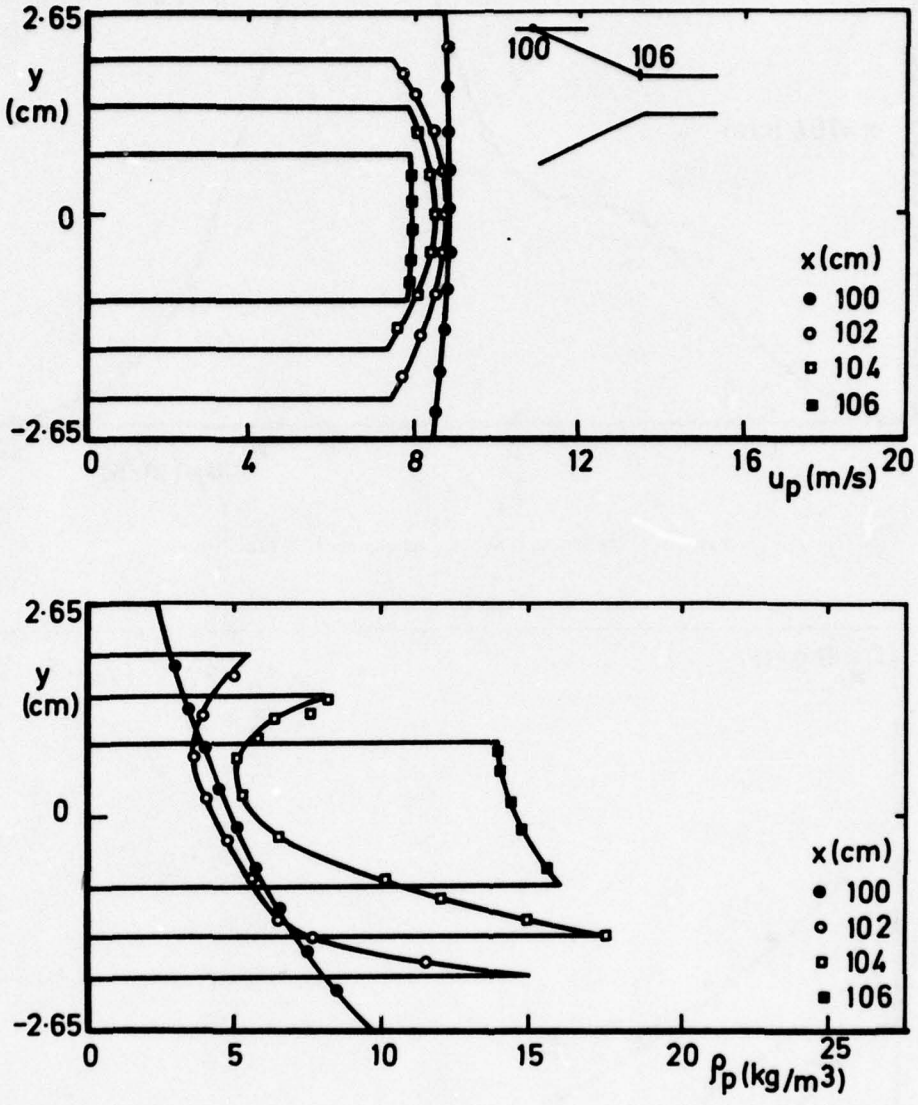

Figure 2 Particle velocity and concentration profiles.

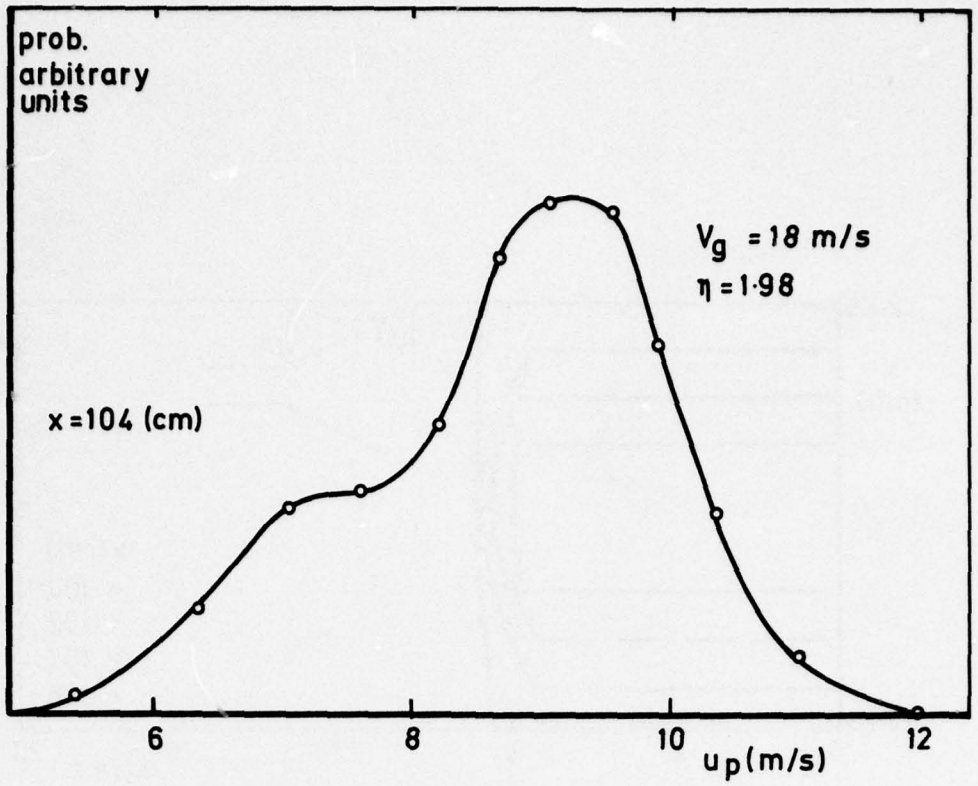

Figure 3 Density function of particle velocity.

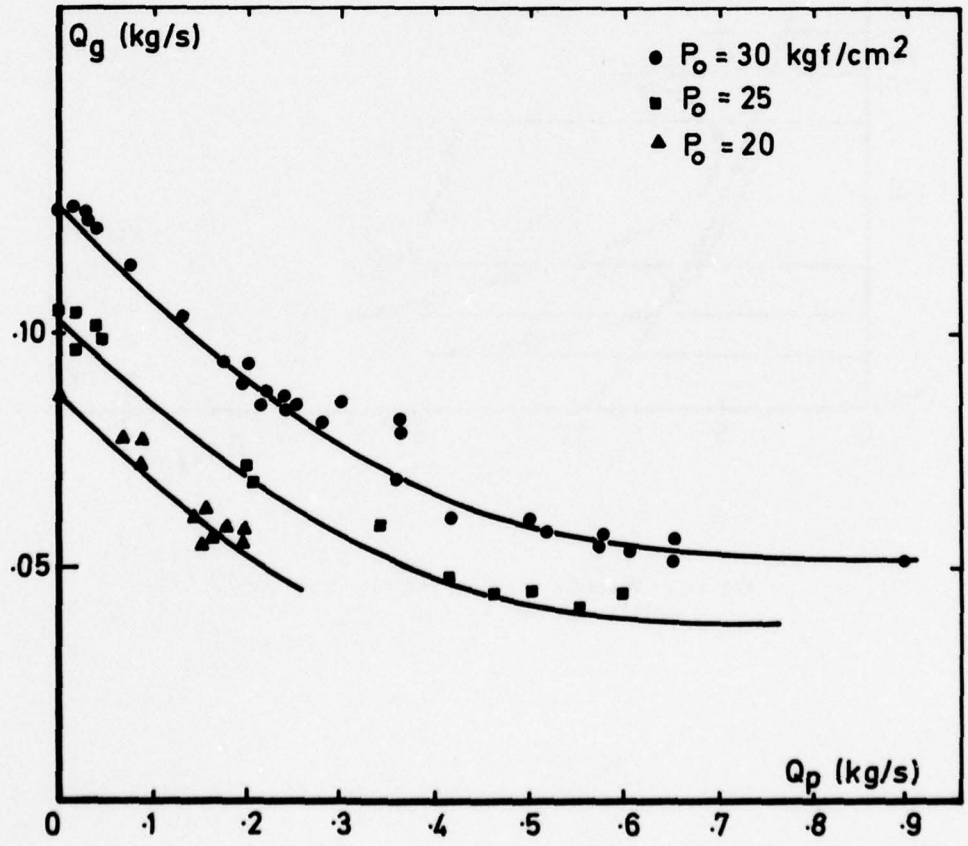

Figure 4 Gas mass flow in a nozzle.

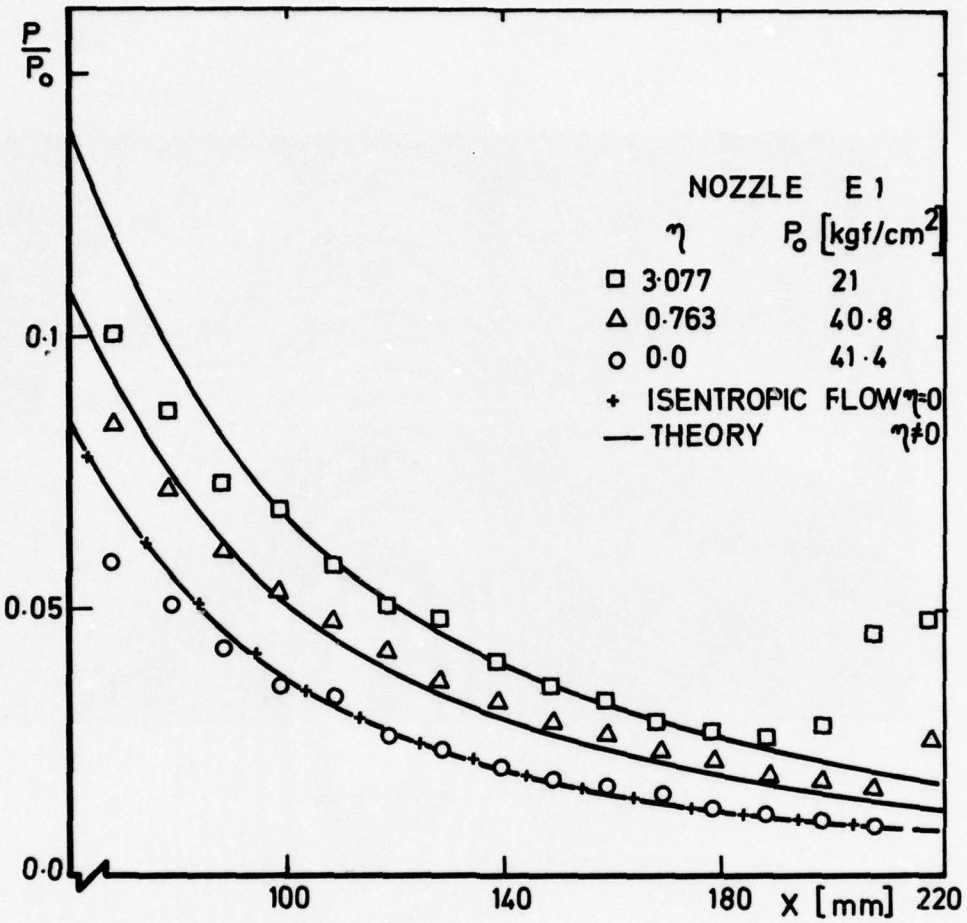

Figure 5 Effect of particle loading on pressure distribution.

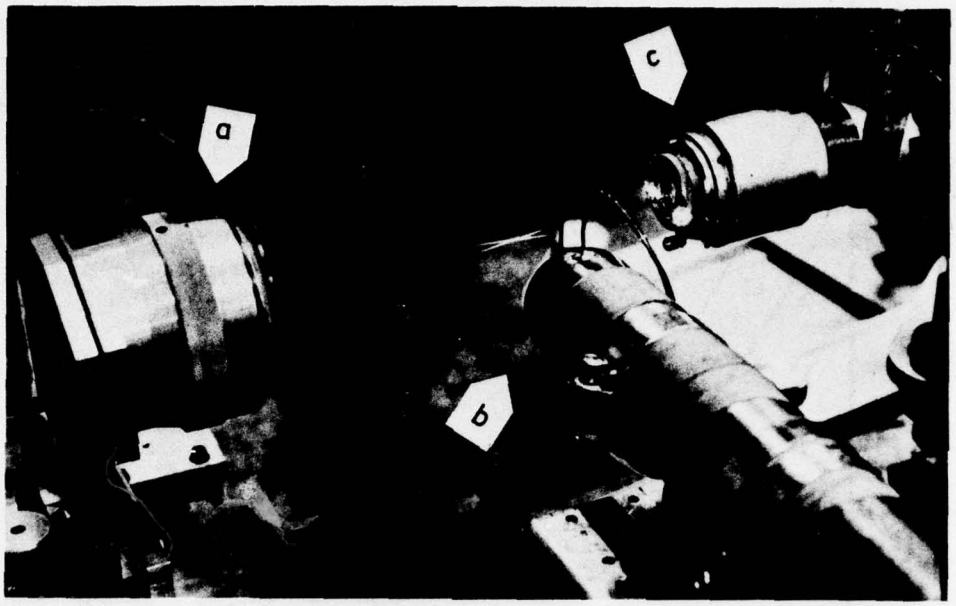

Figure 6 VKI laser Doppler velocimeter
a) illuminating optical unit
b) nozzle
c) receiving optical unit

E. FUNDAMENTALS AND APPLICATIONS OF GAS-PARTICLE FLOW

George Rudinger*
Principal Scientist
Textron's Bell Aerospace Division
Buffalo, New York

SUMMARY

This survey deals with flows of a gas in which small, rigid, and permanent particles are suspended. Particle concentrations range from so low that the particles do not affect the gas flow and can be treated as single particles to so high that the particles occupy an appreciable volume fraction of the mixture. However, dense-phase transport and fluidized beds are not discussed. A number of important applications are outlined. The discussion covers the dynamics of single particles in continuum and low-density flow, the thermodynamics of gas-particle mixtures, and the basic flow equations for one-dimensional flow. Wave propagation, nozzle flow and gas-particle jets are discussed in some detail. Additional examples of analytical and experimental results are given to illustrate important situations. Finally, a brief discussion is given on problems for which satisfactory solutions have not yet been obtained. Emphasis is placed on work performed in the United States.

LIST OF SYMBOLS

A	cross-sectional area of duct
a	speed of sound in the gas phase
a_f, a_e	frozen and equilibrium speed of sound in the gas-particle mixture
C_D	drag coefficient, Eq. (4)
C_f	friction coefficient for a flat plate
$C_f^* = C_f U(t\rho/\mu)^{\frac{1}{2}}$	transformed friction coefficient
c	specific heat of particle material
c_p, c_v	specific heat of gas at constant pressure and constant volume
D	particle diameter
d	duct diameter
E, E_p, E_M	internal energy of the gas, the particles and the mixture
F	effective force between two particle clouds, Eq. (37)
f	correction to the Stokes drag
f_g, f_s	friction factor for a pipe for flow of pure gas and of gas with solid particles
G	Cunningham correction for the drag coefficient
H, H_p, H_M	enthalpy of the gas, the particles, and the mixture
h	heat-transfer coefficient, Eq. (15)
J	momentum-flux ratio, Eq. (47)
$Kn = \lambda/D$	Knudsen number
$K = u_p/u$	velocity ratio
$K = k_1 + ik_2$	complex wave-propagation parameter
k	thermal conductivity of gas phase
L	length of nozzle
ℓ	characteristic length for the interaction between two particle clouds, Eq. (38)
M	Mach number of the gas flow

* Now Adjunct Professor of Mechanical Engineering, State University of New York at Buffalo, Buffalo, New York, 14214.

M_f, M_e	Mach number of the gas-particle mixture, based on the frozen and equilibrium speed of sound
$\dot{m}, \dot{m}_p$	mass flow of gas and particle phase
$Nu = hD/k$	Nusselt number
$Pr = \mu c_p/k$	Prandtl number
p	pressure
p_r	reservoir pressure
R, R_M	gas constant for gas phase and equilibrium mixture
Re	Reynolds number, defined by Eq. (5) unless otherwise noted
$Re_g = \rho du/\mu$	Reynolds number of gas flow in a pipe
T, T_p	gas and particle temperature
T_r	reservoir temperature
t	time
U	velocity of flat plate
u, u_p	gas and particle velocity components in direction x
v, v_p	gas and particle velocity components in direction y
x	coordinate in the main flow direction
Y	maximum lateral penetration
y	coordinate in the lateral direction to the main flow
y_v	thickness of particle-free layer near flat plate
β	equivalence parameter for gas-particle jets, Eq. (45)
γ, γ_M	ratio of the specific heats for gas-phase and equilibrium gas-particle mixture
$\delta = c/c_p$	relative specific heat
ε	particle volume fraction
$\eta = \dot{m}/\dot{m}_p$	loading ratio
λ	molecular mean free path
μ	gas viscosity
ρ	gas density
ρ_p	density of particle material
ρ_M	average density of gas-particle mixture
σ, σ_p	concentration of the gas and particle phases
τ_v	velocity relaxation time, Eq. (9)
τ_T	temperature relaxation time, Eq. (17)
φ	particle mass fraction, Eq. (19)
Ψ	correction factor for C_D to allow for finite particle volume fraction, Eq. (14)
ω	circular frequency of sound waves

Subscripts 0, 1, and 2, and asterisks (*) are defined as needed

1. INTRODUCTION

Gas-particle flows represent one segment of the general class of two-phase flows, that is, flows of mixtures of solid and liquid, solid and gaseous, or liquid and gaseous constituents. Depending on the phases involved and their distribution within the flow, a large variety of flow patterns can be observed. The present discussion deals only with flows in which small particles are suspended in a gas. This more

limited topic still covers an area that is far too extensive for a survey such as this, and further restrictions must be made. Some of the choices were indicated in the initial invitation to prepare this review, and others were influenced by the writer's personal experience.

Viscous interaction and convective heat transfer between a perfect gas and rigid permanent particles will be discussed, while mass transfer by evaporation, condensation or chemical reaction, heat transfer between the flowing mixture and the walls of a duct, as well as breakup of liquid droplets will not be considered. Also excluded are effects of electrostatically charged particles (see C.2.2). The particle concentrations considered vary from extremely low, so that the gas flow is not affected by the presence of the particles, to sufficiently high, that not only modifications of the gas flow become important, but also the volume occupied by the particles must be taken into account. However, the special problems associated with fluidized beds and pipelines for conveying of powdered materials will not be specifically discussed (see also B.3.2 and C.6). Experimental techniques will not be presented as such, but some experimental data are included to illustrate specific flow properties.

Even with these restrictions, there are many flows of practical importance which require sound understanding. An enormous literature is available, as indicated, for example, by the number of references in the frequently cited books by Fuchs (1) and Soo (2), each of which lists some 900 references. The older survey by Torobin and Gauvin (3) also contains nearly 500 references. Thus, the references given here must be considered as representative, and no attempt was made to be all-inclusive. Some basic aspects of the mathematical analysis are briefly outlined in the present review, but reference to the original literature should be made for further details. In accordance with the invitation to prepare this review, emphasis is placed on work performed in the United States.

Since practical applications provide the major motivation for the study of gas-particle flow, the more important applications are indicated in the next section. Subsequent sections deal with the interaction of a gas with individual suspended particles and with particle clouds, the thermodynamic properties of equilibrium gas-particle mixtures, and several specific flows. These are followed by a section in which numerical or experimental examples are given to illustrate the flow properties, and the final section indicates some, as yet unresolved, problems.

2. APPLICATIONS OF GAS-PARTICLE FLOW

This section provides a brief overview of some important applications of gas-particle flow. Illustrative numerical or experimental examples are presented in the subsequent sections.

The particle concentration in flows of practical interest may vary from extremely low, so that the gas flow is not affected by the presence of the particles, to sufficiently high, that not only the gas flow is modified but that the particles occupy a significant fraction of the volume of the mixture.

If the gas flow is not affected by the particles, the latter may be used as tracers to determine local gas motion. An old and well-known technique is to make the particles (smoke) visible by suitable illumination. A more recent development is the laser-Doppler technique, e.g., Stevenson and Thompson (4), in which the particle velocity is inferred from the Doppler frequency shift of scattered laser light. Because of their inertia, the ability of particles to follow rapid changes of the flow velocity may be inadequate, and it becomes important to analyze the accuracy with which particles of a given size can be used as tracers in a specific flow. An example of this application is given in Section 9. Sufficiently small particles can follow even turbulent fluctuations, and the laser-Doppler technique is thus suitable for turbulence studies without interference with the flow. The motion of suspended particles also is of interest for studies of pollution by particulate matter from smoke stacks and other sources, e.g., Stern (5), Soo (6).

A change in the conditions at some point of a flow is "signaled" to other points by waves which produce the necessary flow adjustments. It is thus important to understand how the propagation characteristics of these waves depend on the composition of the medium and the properties of the phases themselves. Energy dissipation associated with particle slip with respect to the gas may be useful for attenuation of blast waves, Kalavsky and Rudin (7), or noise, Temkin and Dobbins (8,9). In his review of pressure waves, Rudinger (10) distinguishes three types: (1) shock waves which produce a transition from one flow condition to another of higher pressure; (2) sound waves which are periodic disturbances of small amplitude and fixed frequency; (3) large-amplitude waves of arbitrary wave form which may produce a net rise or drop of the pressure. The properties of these waves are summarized in Section 6.

As long as the particles do not affect the gas flow, analysis of the gas flow is uncoupled from that of the particle motion. If the particle concentration becomes high enough to affect the gas flow, the analysis becomes much more complicated, because both phases of the flow must be considered at the same time.

Many solid rocket propellants contain a fine metallic powder. These particles provide heat release by combustion, but their main purpose is to suppress pressure oscillations in the combustion chamber, e.g., Horton and McGie (11), Dobbins and Temkin (12). After combustion, such additives may form condensed solid particles (e.g., aluminum oxide) which must be exhausted with the rest of the combustion products. These particles may cause additional erosion in the rocket nozzle by impact on the wall and increased heat transfer. Furthermore, the particles lag during the high flow accelerations in the nozzle, and the resultant viscous drag on the gas flow leads to some degradation of performance. Nozzle flows are discussed at some detail in Section 7.

In a rocket nozzle, the particles may represent 30-40% of the total mass flow. Much higher concentrations, 90% or more, of the total flow may be utilized to transport granulate materials over long distances through conveying pipelines. This application has developed into an important technology of its own, e.g., Spencer, et al., (13), Owen (14), Thornton (15); although conveying will not be specifically discussed, some of the analytical procedures described in the following sections are relevant to it.

For vehicles flying in the atmosphere through dust or rain clouds, it is important to know the impact velocity with which small particles hit the vehicle surface. Studies of particle impact go back to Langmuir and Blodgett (16) who investigated the impact of water droplets on cylinders representing the leading portion of airplane wings. At high altitudes, the air can no longer be treated as a continuum, because the molecular mean-free-path becomes comparable with or even larger than, the particle dimensions. However, at hypersonic speeds, the compression by the leading shock may raise the density sufficiently to allow the flow around the nose of the body to be treated as a continuum. On this basis, Probstein and Fassio (17) computed the collection efficiency of slender wedges, cones, cylinders and spheres.

Erosion by suspended particles is important also for turbomachinery in which particles are deliberately included in the flow for the purpose of pumping, or are present as a result of ingestion from the atmosphere, Spencer, et al. (13), Tabakoff, et al. (18-22), Clevenger and Tabakoff (23), Grant and Tabakoff (24). An illustration of particle trajectories in a turbine cascade is given in Section 9 (see also A.4 and C.4).

The inability of particles to follow rapid flow changes is customarily used to separate particles from a gas flow or to classify particles into different size fractions, Langmuir and Blodgett (16), Levin (25), Golovin and Putnam (26), Lapple (27). Cyclones, multiple-plate impactors, and other devices are commercially available in many forms. Since particles of different sizes respond to flow changes at different rates, collisions between particles may be induced which can modify the flow, Marble (28,29), or may be of interest for their own sake, for instance, coalescence of cloud droplets under the influence of thunder, Temkin (30).

The converse problem arises if particles are to be retained in a vessel through which gas is flowing. In a fluidized bed, gravity provides the force necessary to hold the particles against the drag of an upward directed gas flow. Such beds have become of extreme importance for many chemical processes, e.g., Leva (31), Zenz and Othmer (32). An extension of the gravitational fluidized bed is a rotating bed in which the centrifugal field takes the place of gravity. Such schemes have been proposed to contain the active material of a nuclear reactor and, at the same time, extract the heat energy by the flowing gas, Hatch,et. al. (33), Jackomis and von Ohain (34), Turman and Hasinger (35), Ravets, et al. (36). As pointed out earlier, special problems associated with fluidized beds are not discussed in this review.

A suggestion that gas flows of extremely high total enthalpy might be produced by using gas-particle flows was made by Johnson and von Ohain (37). They proposed to accelerate a stream of solid particles to the high velocity that can be obtained with a heated light gas (hydrogen or helium) and, after separation of the particles from this gas, to use the particles for the acceleration of a working fluid (air) to a high velocity. This technique would produce the final velocity without going through phases of extremely high static pressures or temperatures. The technical feasibility of this scheme has not yet been demonstrated.

The foregoing potential application would involve extensive use of gas-particle jets. Understanding of such jets is important also for atomizing systems, rocket exhausts, injection of powdered fuels into a combustion chamber by means of a carrier gas (or liquid), and water-augmented air cushion vehicles. In the last mentioned application, it was proposed to obtain thrust augmentation by injecting the water spray, produced by the escaping flow from the air cushion, into the propulsive duct, Hope-Gill, et al. (38); in effect, this application would involve injection into a cross flow through a relatively long and narrow longitudinal slot.

Although a great deal is known about gas jets, e.g., Abramovich (39), Margason (40), Skifstad (41), Kamotani and Greber (42), only little information is available on gas-particle jets. Abramovich (39) at first treated a two-phase jet as if it were a gas jet of increased density. Subsequently (43), he reported that two jets of equal average density injected into a quiescent gas develop differently. The gas-particle jet seems narrower and longer ranged. He ascribed this different behavior to the effect of the particles on the turbulence of the flow.

An attempt was made by Soo (2) to analyze particle diffusion for a jet issuing into a stagnant gas. He concluded (on page 359) that "diffusion of particles is completely similar to the diffusion of momentum of the fluid." This finding seems to contradict his statement on page 83 that the particle diffusivity is only 1 to 10% of the eddy diffusivity.

A few experiments on lateral injection of a gas-particle jet into a supersonic cross flow were reported by Edelman, et al. (44). These investigators used low particle flow rates, mostly below 50% of the jet gas flow. Particle trajectories were computed for two extreme cases. In one limit, the particles were assumed to be in equilibrium with the gas; in the other limit, the gas-phase trajectory was assumed unaffected by the particles, and the particle trajectory was computed for various drag coefficients. The results differed remarkedly for different assumptions. Experimentally, they found that the particles remain "locked" with the gas-phase stream, and concluded that "reasonable estimates of jet penetration can be obtained using existing empirical relations." Salzman (45) injected gas-particle jets laterally into an air stream and determined both the centerline of the trajectory and jet spreading in the plane of the trajectory with an isokinetic sampling probe. The turbulence level of the cross stream had little influence on the jet trajectory but had a marked effect on dispersion. He observed some separation of the centerline of the particle stream from that of the carrier gas. Rudinger (46) also studied lateral injection into a flow and observed complete separation of the particles from the carrier gas. These effects are closely related to the size of the injected particles and are further discussed in Section 8.

Almost all flows of technical importance are turbulent. It is therefore of considerable significance that the friction coefficient for gas-particle flow may be considerably lower than that for pure gas flow. The existence of this effect has been known for some years, and has variously been ascribed to electrostatic effects, Richardson and McCleman (47), reduction of the gas viscosity, Sproull (48), thickening of the laminar sublayer, Peskin and Dwyer (49), and general turbulence suppression, Soo (2). These and other related studies were reviewed and extended by Kane and Pfeffer (50) and Pfeffer and Kane (51) who concluded that the thickening of the laminar sublayer is the predominant effect. With particle sizes between 10 and 60 μm and particle flow rates up to four times the gas flow rate, they found a reduction of the friction

pressure drop by about 40% under optimum conditions. A few of their results are discussed in Section 9.

3. GAS-PARTICLE INTERACTION

3.1 Viscous Drag of Single Particles

Particles suspended in a gas flow move under the influence of forces exerted on them by the gas, but if the particle concentration is low enough, the reaction of these forces affects the gas flow only to a negligible extent. Interactions of particles with wakes of other particles then also are of no consequence. This condition is satisfied if the average spacing between particles is about 50 or more particle diameters. The particles then represent not more than about 1% of the mass of the mixture (Section 4).

The equation of motion for a spherical particle in a gas flow, which itself need not be constant, is given, e.g, Hinze (52), Soo (2), Rudinger (53),by

$$\frac{\pi D^3}{6}\rho_p\frac{D_p u_p}{Dt} = \text{Viscous Drag} - \frac{\pi D^3}{6}\frac{\partial p}{\partial x}$$

$$+\frac{1}{2}\frac{\pi D^3}{6}\rho\left(\frac{Du}{Dt}-\frac{D_p u_p}{Dt}\right)+\frac{3}{2}D^2\sqrt{\pi\rho\mu}\int_0^t\frac{\frac{Du}{Dt'}-\frac{D_p u_p}{Dt'}}{\sqrt{t-t'}}dt' \qquad (1)$$

(See Nomenclature for the definition of symbols.)

where the substantial derivatives must be taken along the trajectories of the gas and of the particles, so that

$$\frac{D}{Dt} = \frac{\partial}{\partial t}+u\frac{\partial}{\partial x} \quad \text{and} \quad \frac{D_p}{Dt} = \frac{\partial}{\partial t}+u_p\frac{\partial}{\partial x} \qquad (2)$$

Lateral forces on the particles may develop as a result of particle rotation, slip in the shear flow of a boundary layer, and other effects. Such forces will not be discussed here,but some reference to them is made in Sections 3.2 and 9.

The left-hand side of Eq. (1) represents the product of mass and acceleration, and the right-hand side indicates various forces that act on the particle. The viscous drag is discussed below. The second term shows the effect of the pressure gradient in the gas for which the gas acceleration can be substituted Hinze, (52), because of the momentum equation

$$\rho\frac{Du}{Dt} = -\frac{\partial p}{\partial x} \qquad (3)$$

If the gas flow is affected by the particles, Eq. (3) does not hold (Section 5), and the substitution then is not permissible. The third term indicates the force needed to accelerate the added mass which, for spherical particles, equals one-half of the mass of the displaced fluid. The integral term, also known as Basset force, accounts for deviation of the flow pattern around the particle from that for steady flow; it represents the influence of the history of the motion on the instantaneous force. Under the usual conditions, in which ρ_p is about three orders of magnitude greater than ρ, only the viscous drag needs to be considered, Hinze (52), Fuchs (1), Hjelmfelt and Mockros (54). However, the effect of the history of the motion may affect the particle trajectory under extreme conditions. Lewis and Gauvin (55) injected particles into the flow of an argon plasma torch and determined their motion by streak photography. They measured the residence time between leaving the torch exit and arrival at a distance of 178 mm. These results were compared with calculated residence times based on the best available drag data, Beard and Pruppacher (56)(see Table 1). Under these extreme conditions, the effect of acceleration was to increase the residence time by about 10% for 30-μm particles and 30% for 140-μm particles. Their preliminary recommendation was to use the acceleration terms with correction factors previously determined by Odar and Hamilton (57) for accelerated motion of spheres in a liquid.

Viscous drag is a complicated function of the flow conditions which, in general, can be described only by empirical relationships based on experimental data. The drag force for a spherical particle can be written as

$$\text{Viscous Drag} = C_D\cdot\frac{\pi D^2}{4}\cdot\frac{1}{2}\rho\left|u-u_p\right|(u-u_p) \qquad (4)$$

which defines the force in terms of a drag coefficient, the frontal area of the particle, and the dynamic head of the flow relative to the particle. The square of the relative velocity is written in this form to insure the correct sign of the force. In continuum flow, the drag coefficient is a function only of the particle Reynolds number

$$Re = \frac{\rho D\left|u-u_p\right|}{\mu} \qquad (5)$$

For low Reynolds numbers, the well-known classical Stokes solution

$$C_D = \frac{24}{Re} \qquad (6)$$

applies. The drag then takes the simple form

$$\text{Stokes Drag} = 3\pi D\mu(u - u_p) \tag{7}$$

For higher Reynolds numbers, extensive experimental data are available. The relationship between C_D and Re is shown in Fig. 1, e.g., Schlichting (58), and is usually referred to as "standard drag coefficient." The agreement of data from different sources appears quite good, but note the discussion of Table 1 below. Line 1 in the figure represents Stokes theory of Eq. (6) and line 2 the extension derived by Oseen. Many empirical fits to the standard drag curve have been proposed, e.g, Torobin and Gauvin, Part I (3), Fuchs (1), Soo (2). The equation of motion for a single particle then becomes

$$\frac{du_p}{dt} = u_p \frac{du_p}{dx} = \frac{u - u_p}{\tau_v} f \tag{8}$$

where

$$\tau_v = \frac{D^2 \rho_p}{18\mu} \tag{9}$$

and f is a correction factor to the Stokes drag. Since f is a function of the Reynolds number, Eq. (8) can, in general, be integrated only numerically. For Stokes drag (f = 1) and for a constant gas velocity, Eq. (8) indicates that the velocity difference $u - u_p$ decays exponentially with a relaxation time τ_v given by Eq. (9). For larger Reynolds numbers, τ_v merely becomes a convenient qualitative measure of velocity relaxation (see also B 2.2 and C.2.1).

The present survey deals with small particles, usually smaller than 100 μm. The Reynolds number then rarely exceeds several hundred. For this range, the relationship

$$C_D = \frac{24}{Re}\left(1 + \frac{1}{6} Re^{2/3}\right) \tag{10}$$

represents a good fit to the standard drag curve. It was first proposed by Klyachko in 1934 (1). Apparently independently, it was later suggested by Putnam (59) who pointed out that it may lead to integrable equations. For most applications, these data are sufficiently accurate, but situations may arise when a higher accuracy is needed, for instance, the study by Lewis and Gauvin (55) referred to earlier. Maxworthy (60) pointed out that for very low Reynolds numbers, it is "impossible to be sure of the drag to better than ± 20%, even if one is very generous with data that scatters between the Stokes drag and values above the Oseen drag." He, and subsequently Beard and Pruppacher (56), performed more accurate measurements. The latter are considered by Lewis and Gauvin the most precise ones currently available. A comparison of the standard drag coefficient, as given in a table by Fuchs (1) with Eqs. (4) and (10), and some of the data by Beard and Pruppacher is shown in Table 1.

Table 1

Comparison of Particle Drag Coefficients

Reynolds Number	Drag Coefficient			
	Standard	Eq. (10)	Stokes	B&P*
0.01	2400	2420	2400	
0.1	243	249	240	242.7
1	26.9	28.0	24.0	26.45
10	4.33	4.26	2.40	4.149
100	1.09	1.10	0.24	1.073
500	0.568	0.552	0.048	
1000	0.469	0.424	0.024	
2000-10000	0.40			

* Beard and Pruppacher (56)

This table indicates that Eq. (10) represents the standard drag coefficient to better than 5% for Reynolds Numbers up to about 500 and to better than 10% even at Re = 1000. The agreement with the data by Beard and Pruppacher is not quite so good. In contrast, Stokes drag is a good approximation only for Reynolds numbers less than one. Nevertheless, it is frequently used for qualitative calculations, because it leads to particularly convenient relationships.

Since the viscous drag and the gas and particle velocities are vectors, Eq. (8) represents only one component of a vector equation, and analogous equations could be written for the other components (see also C.2.1). Often, flows are treated as quasi-one-dimensional, and the question of other components does not arise. It should be pointed out, however, that the drag vector has the direction of the vector difference of the gas and particle velocities and that the absolute value of this difference must be used in

calculating the Reynolds number and the drag force. Thus, if u, u_p, v and v_p represent the components of the gas and particle velocities in two dimensions, the absolute value $|u - u_p|$ in Eqs. (4) and (5) must be replaced by $[(u - u_p)^2 + (v - v_p)^2]^{\frac{1}{2}}$. Consequently, the same value of f appears in all component equations and the gas velocity in one direction affects the component of the drag in a direction at right angles to it. Only for a constant value of f, as for Stokes drag, do the component equations become uncoupled and can be solved independently. This coupling of the equations can have significant consequences as demonstrated in Section 3.2 and 9.

Throughout the preceding discussion it is implied that the gas flow can be treated as a continuum. If the particles are extremely small, or the gas density is quite low, the molecular mean free path in the gas, λ, may become comparable with the particle dimensions, and it then becomes necessary to apply a correction to the drag coefficient. This correction, sometimes called "Cunningham correction" can be expressed in terms of the Knudsen number which is defined as $Kn = \lambda/D$. To correct the drag coefficient, the latter is divided by G which is given by, e.g., Fuchs (1),

$$G = 1 + Kn\ (2.492 + 0.84\ e^{-1.74/Kn}) \tag{11a}$$

It follows from kinetic theory that the Knudsen number is a function of the ratio of the Mach number of the flow to the particle Reynolds number, Schaaf and Chambré (61). Experimentally determined drag coefficients therefore can also be presented in terms of Mach number and Reynolds number. Carlson and Hoglund (62), after reviewing available data proposed the relationship

$$G = 1 + (M/Re)(3.82 + 1.28\ e^{-1.25\ Re/M}) \tag{11b}$$

Beckwith and Bushnell (63) also derived correlations to represent the then available data. They suggested relationships with constants that are changed for various ranges of the Mach and Reynolds numbers. Details of this correlation and a table of the required constants may be found in a paper by Yanta (64). The most recent measurements appear to be the ballistic-range data by Bailey and Hiatt (65) which cover the entire range from continuum to near-free-molecular flow, free-stream Mach numbers from 0.1 to 20, and Reynolds numbers from 0.2 to 10^6. A summary of their data is presented in Fig. 2. Korkan, et al. (66) modified the Beckwith and Bushnell correlation to allow for different gas and particle temperatures and to improve the fit of the experimental data. Still further improvements are described in a recent paper by Henderson (67) (see also B.2.1).

3.2 Viscous Drag of Particle Clouds

If the particle concentration is sufficiently high, the reaction of the sum of the drag on all particles becomes large enough to affect the gas flow. Furthermore the force on each particle may be affected by the presence of other particles. Direct collisions between particles of equal size are infrequent, except at the high concentrations of fluidized beds or dense-phase conveying. However, suspensions of uniformly sized particles are rare, and collisions between particles of different size then may result, because they follow different trajectories. Also the volume of a particle wake may be two or three orders of magnitude larger than the volume of the particle itself. Thus, particle-wake interactions may be significant, even if the volume occupied by the particles is negligible. The resultant uncertainty of the drag coefficient was emphasized by Torobin and Gauvin (3) and Hoglund (68).

Since no generally valid methods are available to evaluate deviations from the standard drag coefficient, it becomes necessary to derive effective drag coefficients from experimental observations. The results of several such studies were collected and discussed by Torobin and Gauvin, Part V (3), and by Soo (2). The data collected by Soo are shown in Fig. 3, and the contrast between this figure and Fig. 1 is striking. While some of the scatter of the data may be the result of experimental errors, the major trends are probably real. Torobin and Gauvin stated that "the use of the standard drag curve for drag estimation to the second figure ... outside the Stokesian region is not valid."

Ingebo (69) measured the acceleration of spray droplets injected into a wind tunnel and found

$$C_D = \frac{27}{Re^{0.84}} \quad (6 < Re < 400) \tag{12}$$

shown as line I4 in Fig. 3. He believed that the deviations from the standard drag were caused by the acceleration of the particles.

Crowe, et al. (70) used high-speed movies, and Selberg and Nicholls (71) employed multiple-flash photography, to observe the particle motion in a shock tube. Both investigations yielded higher than standard drag coefficients. The difference was tentatively ascribed to surface roughness of the particles.

Rudinger (72,73) used streak photography and light scattering to determine particle motion in a shock tube. Both techniques led to the same result, shown as line R48 in Fig. 3,

$$C_D = \frac{6000}{Re^{1.7}} \quad (5 < Re < 200) \tag{13}$$

for 29-μm particles and values about 60% higher for 62-μm particles. Other features of the results are that C_D approaches the standard drag curve for higher Reynolds numbers and that it is independent of the particle loading ratio over the range of the experiments (0.05 - 0.36). To explain these results, turbulence, wall effects, electrostatic forces, particle rotation, or asymmetric vortex shedding were considered. With the possible exception of turbulence, none of these effects should be expected to have a large direct effect on the drag coefficient, but all of them tend to produce longitudinal and lateral perturbations of the particle trajectories. Such perturbations are too small to be observed, and the effective drag coefficient is thus derived from the average trajectory. Even if the standard drag coefficient is applicable to the microscopic particle motion, the apparent, or effective, drag coefficient derived from

the average motion is different because of the nonlinearity of the equation of motion outside the range of Stokes drag. On the basis of this consideration, Rudinger (73) could qualitatively explain all features of the shock-tube data.

The effect of particle slip appears in the gas initially only in the particle wakes. Since mixing of these wakes with the rest of the gas is not instantaneous, neighboring particles may not be immediately affected. This mixing delay also may influence the effective drag coefficient, Rudinger (74). The effect of a particle cloud on the drag of individual particles must depend also on the particle volume fraction ϵ. A statistical analysis of Tam (75) for small slip velocities yields a correction factor for Stokes drag given by

$$\Psi = \frac{4 + 3\epsilon + 3(8\epsilon - 3\epsilon^2)^{\frac{1}{2}}}{(2 - 3\epsilon)^2} \tag{14}$$

For the concentrations used in the foregoing shock tube experiments, the particle volume fraction is less than 10^{-3} and this correction factor then yields less than 1.1. Therefore, it cannot explain the observations, but the fact that the derivative $d\Psi/d\epsilon$ approaches infinity as ϵ approaches zero indicates that even small particle concentrations may have a significant effect on the drag coefficient.

All phenomena mentioned in the foregoing may affect the particle motion in a manner that is unknown at this time and also may depend on the particular flow system. They contribute to the uncertainty of the drag coefficient, but their consequences are implied in effective drag coefficients that are derived from experimental observations. This reasoning may help to explain the wide scatter of the experimental data shown in Fig. 3 (see also C.6).

3.3 Gas-Particle Heat Transfer

In compressible flow, any velocity change is accompanied by a temperature change. Thus, both the velocity and the temperature of suspended particles can lag behind the corresponding gas values. The rate at which the particle temperature can follow the gas temperature is described by the equation

$$\frac{\pi D^3}{6} \rho_p c \frac{dT_p}{dt} = h\pi D^2 (T - T_p) \tag{15}$$

where the heat-transfer coefficient h can be conveniently expressed in terms of the Nusselt number $Nu = hD/k$. For pure heat conduction, the value $Nu = 2$ applies, but additional heat transfer by convection takes place if the particle moves with respect to the gas. The Nusselt number then becomes a function of the particle Reynolds number. A frequently used relationship is, e.g., Knudsen and Katz (76)

$$Nu = 2.0 + 0.6\, Pr^{1/3}\, Re^{1/2} \tag{16}$$

where $Pr = \mu c_p/k$ is the Prandtl number. If the particle temperature were high enough for radiative heat transfer to become important, a more elaborate heat-transfer coefficient would be needed, Simmons and Spadaro (77), Soo (2) (see also B.2.4).

If $Nu = 2$ is assumed and T is constant, Eq. (15) indicates that the temperature difference $T - T_p$ decreases exponentially with a time constant

$$\tau_T = \frac{1}{12} \frac{D^2 \rho_p c}{k} = \frac{3}{2} Pr\, \delta\, \tau_v \tag{17}$$

where the last form is obtained by introducing Eq. (9) and the definition of the Prandtl number (see also B.2.2). Since $\delta = c/c_p$ is of order one, and the Prandtl number of many gases is close to 2/3, the time constants for velocity and temperature relaxation often are approximately equal, Marble (78), Rudinger (53).

As in the case of velocity relaxation, τ_T becomes merely a convenient qualitative indication of the rate of temperature relaxation if the particle moves with respect to the gas (see also B.2.2).

The foregoing relationships imply that the temperature is uniform throughout the particle, but heat flux into, or out of, the particle requires internal temperature gradients. Uniform temperature can be assumed if the rate of temperature equalization within the particle is fast compared with the rate of heat transfer between the particle and the gas. Rudinger (53) has shown that this condition is almost always satisfied, except for particles of very low thermal conductivity immersed in a gas of very high thermal conductivity, such as magnesium oxide particles in hydrogen.

So far, only heat exchange with single particles has been considered. In the case of particle clouds, uncertainties arise for the same reasons as for the drag coefficient. The few available experimental data were summarized by Hoglund (68) with the statement that a "line through these data lies about a factor of 5 below the single-particle data at $Re \approx 10$, crosses the single-particle curve at $Re \approx 50$ and rises to about twice the single-particle curve at $Re \approx 100$."

4. THERMODYNAMIC PROPERTIES OF GAS-PARTICLE MIXTURES

Before discussing the analysis of gas-particle flow, it is useful to consider the general thermodynamic properties of such mixtures which enter into all flow calculations. Derivation of these quantities can be found scattered through many publications, e.g., Soo (79), Hoglund (68), Marble (29,78), Kliegel (80), Kriebel (81), Rudinger (53,82), Kraiko and Sternin (83). In deriving these properties, careful distinction must be made between the density of the particle material ρ_p and the amount of particle material in a

unit volume of the mixture - the particle concentration - denoted by σ_p. Similarly, there is a distinction between the gas density ρ and the gas concentration σ. The densities and concentrations are related by

$$\sigma_p = \epsilon\rho_p \text{ and } \sigma = (1 - \epsilon)\rho \tag{18}$$

where ϵ is the volume fraction occupied by the particles. The mass fraction of the particles therefore is given by

$$\varphi = \frac{\sigma_p}{\sigma+\sigma_p} \tag{19}$$

Combination of these equations yields

$$\frac{\epsilon}{1-\epsilon} = \frac{\sigma_p}{\sigma}\frac{\rho}{\rho_p} = \frac{\varphi}{1-\varphi}\frac{\rho}{\rho_p} \tag{20}$$

and

$$\rho_M = \sigma + \sigma_p = \frac{(1-\epsilon)\rho}{1-\varphi} = \frac{\epsilon\rho_p}{\varphi} \tag{21}$$

An alternative form of this equation is

$$\frac{1}{\rho_M} = \frac{1-\varphi}{\rho} + \frac{\varphi}{\rho_p} \tag{22}$$

(Although all publications make or imply the distinction between density and concentration, the terminology and symbols used are not uniform. Care is therefore needed in the interpretation of a particular nomenclature.)

If the mixture is flowing through a duct of cross section A, the local mass flows are given by $\dot{m} = \sigma uA$ and $\dot{m}_p = \sigma_p u_p A$. These flow rates are constant only if the flow is steady. Their ratio, known as the loading ratio, then becomes

$$\eta = \frac{\sigma_p u_p}{\sigma u} = \frac{\epsilon}{1-\epsilon}\frac{\rho_p}{\rho}\frac{u_p}{u} = \frac{\varphi}{1-\varphi}\frac{u_p}{u} \tag{23}$$

It is clear from these equations that η is constant for steady flow, but φ is constant only if u_p/u is also constant. Furthermore, ϵ is constant only if σ_p is constant, because the particles may be considered as incompressible.

Under usual conditions, the density ratio ρ/ρ_p is of the order of 10^{-3}. The particle volume fraction thus becomes significant only for rather high particle loadings and can be neglected for low or moderate loadings. Note that vanishing particle volume implies mathematically that ρ_p goes to infinity and ϵ to zero in such a manner that the product $\epsilon\rho_p$ remains equal to σ_p.

The average distance between neighboring particles is of the order $D/\epsilon^{1/3}$. For particle diameters less than 0.1 mm, mass fractions as low as 0.03, and a density ratio ρ/ρ_p of the order of 10^{-3}, the average particle spacing would be less than about 3mm. Consequently, both the particles and their average separations generally are quite small compared with the dimensions of typical flow fields. Thus, it seems natural to treat the particles as species of heavy molecules with a molecular weight that is several orders of magnitude larger than that of the gas, even for particles as small as 0.01 μm. For any mixture composition of practical interest, the number density of the particles thus is insignificant in comparison with that of the gas molecules, and the contribution of the particles to the pressure of the mixture is negligible. The pressure of a gas-particle mixture therefore is that of the gas phase alone which, for a perfect gas, is given by

$$p = \rho RT \tag{24}$$

To obtain an equation of state for the mixture, the gas density in Eq. (24) must be expressed in terms of the density of the mixture, and one obtains, with the aid of Eq. (21)

$$p = \frac{\rho_M(1-\varphi)}{1-\epsilon} RT = \frac{\rho_M}{1-\varphi\ \rho_M/\rho_p} R_M T \tag{25}$$

where $R_M = (1-\varphi)R$ is the gas constant of the mixture. Clearly, Eq. (25) is not the equation of state of a perfect gas because of the density term in the denominator which is directly related to the particle volume fraction. A mixture of solid particles with a perfect gas may be treated as a perfect gas with modified thermodynamic properties only if the particle volume can be neglected. This result is a direct consequence of the fact that the particle volume does not change during compression of the mixture.

The internal energy is given by the properly weighted average of the internal energy of the constituents as

$$E_M = (1-\varphi)E + \varphi E_p = (1-\varphi)c_v T + \varphi c T_p \tag{26}$$

The enthalpy then follows from its definition and Eq. (22) as

$$H_M = E_M + \frac{p}{\rho_M} = (1-\varphi)\left(c_v T + \frac{p}{\rho}\right) + \varphi\left(cT_p + \frac{p}{\rho_p}\right)$$

$$= (1-\varphi)c_p T + \varphi\left(cT_p + \frac{p}{\rho_p}\right) = (1-\varphi)H + \varphi H_p \tag{27}$$

Thus, the enthalpy of the particle phase depends on the gas pressure. Since φ/ρ_p is of order ϵ, according to Eq. (21), this contribution is omitted if the particle volume is neglected.

The ratio of the specific heats of an equilibrium mixture ($u = u_p$) is obtained as the ratio of the properly weighted specific heats at constant pressure and constant volume. It is most conveniently expressed in terms of the loading ratio which, for equilibrium flow, is related to the particle mass fraction by $\eta = \varphi/(1-\varphi)$, and one obtains

$$\gamma_M = \gamma \frac{1+\eta\delta}{1+\gamma\eta\delta} \tag{28}$$

This result shows that the specific heat ratio of a mixture is always smaller than that of the gas phase and approaches one as the loading ratio is increased. A specific-heat ratio of one implies isothermal flow. In this case, the heat capacity of the particles is so large compared with that of the gas that temperature changes in the gas during compression or expansion can be compensated by heat transfer to or from the particles without significantly changing their temperature. Some analyses of heavily loaded gas-particle flow can be considerably simplified by assuming isothermal flow (Section 7).

The last property to be discussed here is the speed of sound. As in the case of relaxing gas flows, one must distinguish between the frozen speed of sound a_f and the equilibrium speed a_e. In frozen flow, no viscous interaction or heat transfer between the gas and the particles takes place, and a_f thus becomes equal to the speed of sound in the gas phase

$$a_f^2 = a^2 = \gamma RT \tag{29}$$

The equilibrium speed of sound has been derived in different ways by various investigators with or without taking the particle volume into account, but all results can be reduced to

$$\left(\frac{a_e}{a}\right)^2 = \frac{(1-\varphi)[1 + \delta\varphi/(1-\varphi)]}{(1-\epsilon)^2[1 + \gamma\delta\varphi/(1-\varphi)]} \tag{30}$$

If ϵ is neglected, a_e approaches zero monotonically as φ is increased, but at sufficiently high particle concentrations the influence of ϵ becomes significant, and a_e reaches a minimum value. Still higher concentrations lead to a rapid increase of a_e which reaches infinity at $\varphi = 1$, the speed of sound in the incompressible solid. This behavior is demonstrated in Fig. 4 for $\gamma = 1.4$, a density ratio $\rho/\rho_p = 0.01$ and the typical value $\delta = 1$. Parts of the curves are shown also for the rather extreme values $\delta = 0.05$ and $\delta = 10$. This figure demonstrates the large effect of the particle loading on a_e which is only slightly modified by the particle volume in the range of moderate particle loadings considered here.

5. GENERAL FLOW EQUATIONS

The motion of isolated particles, which do not affect the gas flow, is discussed in Section 3. To describe flows with higher particle concentrations requires that the velocity, concentration and temperature of the gas and of the particles be determined as functions of the position and time coordinates. The required six equations are represented by the continuity, momentum, and energy equations for each phase. For three-dimensional flows, these equations can be written in tensor notation, Marble (29,78), or in vector form, Kraiko and Sternin (83), Soo (2). Numerical solutions for general three-dimensional flows would require major computing efforts, and investigations usually are limited to cases of one-dimensional flow.

Several assumptions must be made to derive the basic flow equations, some of which already have been mentioned earlier:

1. The gas obeys the perfect - gas low, and the specific heats are constant;

2. The particles are spherical, of uniform size (unless specially noted), and incompressible; their specific heat is constant, and the temperature is uniform within each particle;

3. The particles are uniformly distributed over the cross-section of a duct, and their size and average spacing are small compared with the cross-sectional dimensions of the duct;

4. Duct flows are treated as one-dimensional, so that changes of the cross-sectional area must be sufficiently gradual. Boundary-layer effects and heat exchange with the walls are not considered (unless specially noted). However, viscosity and thermal conductivity of the gas enter into the calculation of particle drag and heat transfer between the particles and the gas;

5. Both the drag coefficient and the Nusselt number must be prescribed as functions of the Reynolds number and, if necessary, also of the Mach number or Knudsen number;

6. The particles do not contribute to the pressure and do not collide with each other (unless

specially noted);

7. In the flows discussed here, no external forces (such as gravity or electrostatic fields) or mass transfer between the gas and the particles are considered.

Derivation of the flow equations follows the same general approach as for a pure gas. Numerous references can be found for one-dimensional steady flow with or without taking the particle volume into account, e.g., Soo (2,79), Bailey et al. (84), Kliegel (80), Marble (29,78), Hassan (85), Rudinger (86). These equations can be extended to nonsteady flow, Rudinger and Chang (87), Migdal and Agosta (88), Rudinger (53), Wallis (89).

The continuity equations for the gas and for the particles are

$$A \frac{\partial \sigma}{\partial t} = - \frac{\partial (\sigma u A)}{\partial x} \tag{31}$$

and

$$A \frac{\partial \sigma_p}{\partial t} = - \frac{\partial (\sigma_p u_p A)}{\partial x} \tag{32}$$

The momentum and energy equations for the gas and for the particles contain gas-particle interaction terms with opposite signs. It is therefore convenient to eliminate these terms once by adding the corresponding equations. The momentum equation for the entire mixture thus becomes

$$\sigma \frac{Du}{Dt} + \sigma_p \frac{D_p u_p}{Dt} = - \frac{\partial p}{\partial x} \tag{33}$$

where the substantial derivatives have the meaning previously indicated by Eqs. (2). The effect of the particles is not directly "felt" over the entire cross-section of the duct but appears initially only in the particle wakes. Soo (2,90) suggested that the momentum term for the particles in Eq. (33) therefore should be multiplied by an "effectiveness correction" with a value between zero and one. Rudinger (74) pointed out that a violation of Newton's laws would result if this factor were assumed constant, because it implies that the viscous drag acts on the particles while its reaction would not affect the entire gas; he suggested that the delay in the mixing of the particle wakes with the rest of the gas might be taken into account by letting Soo's effectiveness correction go to one as the particles approach equilibrium with the gas. Because of the uncertainty of the mixing rate of the wakes, the consequences of this delay are not known, but they are implied in any experimentally determined drag coefficient (section 3.2).

The energy equation of the mixture is given by

$$A \frac{\partial}{\partial t} \left[\sigma \left(\frac{1}{2} u^2 + c_v T \right) + \sigma_p \left(\frac{1}{2} u_p^2 + c T_p \right) \right]$$

$$= - \frac{\partial}{\partial x} \left[(\sigma u A \left(\frac{1}{2} u^2 + c_p T \right) + \sigma_p u_p A \left(\frac{1}{2} u_p^2 + c T_p + \epsilon \frac{p}{\sigma_p} \right) \right] \tag{34}$$

The remaining two equations represent the gas-particle interaction. Particle motion is described by Eq. (1). Omitting the history integral and terms of order ρ/ρ_p, and substituting Eq. (33) for the pressure gradient, yields an equation analogous to Eq. (8) for a single particle

$$(1-\epsilon) \frac{D_p u_p}{Dt} = \frac{u - u_p}{\tau_v} f \tag{35}$$

The ϵ-term in this equation appears, because the pressure gradient now depends on the acceleration of both phases.

The relationship of gas-particle heat transfer, after substitution of Eq. (17) and the definition of the Nusselt number into Eq. (15), becomes

$$\frac{D_p T_p}{Dt} = \frac{T - T_p}{\tau_T} \cdot \frac{Nu}{2} \tag{36}$$

The system of equations to be solved is thus given by Eqs. (31)-(36) and appropriate assumption for C_D and Nu. Since the gas pressure and the particle volume fraction appear as additional variables in these equations, the equation of state, Eq. (24), and Eqs. (18) are needed to complete the system. In general, solution of these equations requires a considerable computational effort. Fortunately, simplifications often are possible: the flow may be steady, the particle volume fraction may be negligible, or deviations from equilibrium flow may be so small that linearization in terms of such deviations becomes permissible. For steady flow through a duct of constant cross section Eqs. (31)-(34) can be integrated to yield algebraic relationships, and only Eqs. (35) and (36) remain differential equations. Even then, analytical solutions are rarely obtainable. The analysis of several special flows is indicated in the following sections.

Occasionally, it may be of interest to assess the consequences if not all particles are of the same size. The particulate phase then is divided into groups each of which contains only particles of one size having its own relaxation times τ_v and τ_T. Equations corresponding to Eqs. (32), (35) and (36) then must

be written for each group, and the particle terms in Eqs. (33) and (34) must be replaced by sums of the corresponding terms for each particle size. The resultant extended system of equations can be solved in the same manner as the original system at an increased computational effort, Kliegel (80), Kriebel (81), Soo (2).

Since particles of different sizes approach equilibrium with the gas as different rates, collisions between particles may become important. A technique to take such collisions into account was suggested by Marble (28,29). He assumed $\epsilon = 0$ and $f = 1$ and derived the force acting between two clouds of particles having diameters D_1 and D_2 as

$$F = \frac{\sigma_{p_1} \sigma_{p_2}}{\sigma} \left| u_{p_1} - u_{p_2} \right| (u^*_{p_2} - u^*_{p_1})/\ell \tag{37}$$

In this equation, the asterisks indicate the velocities which the particles would have in the absence of collisions, and ℓ represents a characteristic length

$$\ell = \frac{2}{3} \frac{\rho_p (D^3_1 + D^3_2)}{\rho (D_1 + D_2)^2} \tag{38}$$

Thus, the particle acceleration, given by Eq. (35), must be written for each particle size and contains the additional collision term F/σ_{p1} for the particles of size D_1 and $-F/\sigma_{p2}$ for the particles of size D_2. Two more equations of the form of Eq. (35), but without the collision terms, must be written for u^*_{p1} and u^*_{p2} to account for these new variables. An example of this approach is shown in section 6.1.

6. PRESSURE WAVES

6.1 Shock Waves

An analysis of shock waves in gas-particle mixtures was first performed by Carrier (91), and a number of analyses were published subsequently, e.g., Soo (2,79), Kliegel (80), Marble, (29,78), Rudinger (53,92), Kriebel (81) (see also B.2.6). If the shock propagates through a duct of constant cross section, the flow is steady in a coordinate system fixed in the shock wave, and Eqs. (31)-(34) can be integrated to yield algebraic relationships. The gas-particle mixture, generally assumed to be in equilibrium, enters the wave with a velocity that must be greater than the equilibrium speed of sound a_{eo} given by Eq. (30), where subscript zero indicates the conditions ahead of the shock. The equilibrium shock Mach number is thus defined as $M_e = u_o/a_{eo}$. The shock front is traversed by the particles in such a short time that their velocity and temperature has not changed. Accordingly, the change of the gas across the shock front is determined by the frozen Mach number $M_f = u_o/a_o$ and is given by the well-known Rankine-Hugoniot shock relationships for a pure gas. Immediately behind the shock front, both the velocity and temperature of the particles thus are different from the corresponding gas values.

A great distance behind the shock, equilibrium between the phases is reestablished ($u_e = u_{pe}$ and $T_e = T_{pe}$). The basic equations then simplify sufficiently that analytical relationships can be obtained between the upstream and the equilibrium conditions even for a finite particle volume, Rudinger (82). If $\epsilon = 0$, the equations become the same as for a pure gas for a Mach number M_e and a specific-heat ratio γ_M given by Eq. (28). Relaxation from the frozen to the equilibrium conditions must be obtained by numerical integration of the equations for assumed correlations for C_D and Nu. A typical relaxation zone is shown in Fig. 5 for the conditions given in the caption. The final equilibrium conditions are indicated, and the large extent of the relaxation zone should be noted.

It is instructive to explore the consequences of making different assumptions for C_D and Nu. Results for the gas pressure and the particle velocity are shown in Fig. 6 for all combinations of three drag coefficients and two heat transfer coefficients. The drag coefficient has a marked effect, while the influence of the heat-transfer coefficient is quite small. Corresponding results for the gas and particle temperatures are shown in Fig. 7 which illustrates that variations in the relaxation zone need not be monotonic and that heat transfer is more important than drag, as one should expect (see also A.5.3).

If the particle volume cannot be neglected, the equilibrium velocity is increased. This effect becomes significant for $\epsilon_o = 0.01$ and is quite large for ϵ_o greater than 0.05. In contrast, the equilibrium pressure is decreased but the change is almost insignificant, Rudinger, (53,82).

Oblique shocks may be analyzed by considering the normal and tangential components as in the case of a pure gas, Morgenthaler (93), Okauchi (94). Note that the equations for the two components are not uncoupled unless the factor f in Eq. (35) is assumed constant, as pointed out in Section 3.1.

If different particle sizes are considered, Kliegel (80), Kriebel (81), Soo (2), the velocity relaxation for each particle size appears similar to the one in Fig. 5 with the smaller particles approaching equilibrium with the gas faster than the larger ones. Zung, see Marble (29), performed calculations for two particle sizes with allowance for collisions between the particles. This example is shown in Fig. 8 and demonstrates that such collisions tend to draw the two particle velocities together (see also A.5.4).

Shock transition requires $M_e > 1$, but the existence of a discontinuous shock front implies $M_f > 1$. Since the equilibrium speed of sound is smaller than the frozen speed of sound, a velocity range $a_e < u_o < a_f = a_o$ exists for which shock transition is possible but a discontinuous shock front is not. The limiting value of M_e for which $M_f = 1$ is shown in Fig. 9 as a function of the particle mass fraction for three values of δ and for $\gamma = 1.4$. Within this range, only a gradual transition from the initial to the final equilibrium conditions is possible in the form of a dispersed shock wave. A special starting procedure for the numerical integration is needed to obtain initial deviations from equilibrium. Kriebel (81) assumed

initial perturbations that would be produced by a weak compression wave, and Rudinger (95) linearized the equations to obtain starting conditions in terms of a small perturbation of the gas velocity. Results for dispersed shocks were presented also by Kliegel (80). An example of a dispersed shock is shown in Fig. 10 and comparison with Fig. 5 indicates a much longer relaxation zone.

It is evident from Fig. 9 that dispersed shocks can have appreciable strength. Dispersed oblique shocks should be expected to occur also in supersonic flow around sufficiently slender bodies. Because of the absence of a discontinuous shock front, dispersed shocks may not be readily visible in schlieren photographs, and no observations of such waves, apparently, have been reported so far.

6.2 Sound Waves

The rate at which particles can respond to fluctuations in a flow is indicated by the relaxation times τ_v and τ_T of Eqs. (9) and (17). Interaction of sound waves with a cloud of particles therefore becomes most important if their period is not too different from the relaxation times.

Flow changes in a sound field are small, and linearization of the basic flow equations then becomes possible. Temkin and Dobbins (8) used this approach to derive periodic solutions of the form $\exp[i(Kx-\omega t)]$ where $K = k_1 + ik_2$ is a complex propagation parameter. The real part $k_1 = \omega a$ represents the dispersion and the imaginary part k_2 the attenuation of the wave. Some of their results are shown in Figs. 11 and 12 where these parameters, in dimensionless form, are plotted as functions of $\omega\tau$ for several values of the loading ratio. Maximum attentuation occurs near $\omega\tau = 1$ and is shifted toward higher frequencies with increasing loading ratio. The sound velocity, which has a value a_o for $\eta = 0$, approaches the equilibrium value a_e, given by Eq. (30), for low frequencies, and the frozen value $a_f = a_o$ at high frequencies; it varies most rapidly near $\omega\tau = 1$. Marble (29) performed a similar analysis. He compared this theory with an earlier, more detailed, analysis by Epstein and Carhart (96), which considered the flow field around individual particles, and concluded that it is completely adequate for wavelengths which are long compared with the size of the particles (see also B.2.5).

6.3 Large-Amplitude Waves

The general flow equations, Eqs. (31)-(36) are hyperbolic and therefore can be solved by the method of characteristics for pressure waves of arbitrary shape and magnitude. Rudinger and Chang (87) treated the unknown gas and particle conditions as one set of unknowns, while Migdal and Agosta (88) considered the particle terms as sources or sinks of drag and heat in a gas flow. There is little practical difference between these points of view. Both studies assumed a negligible particle volume.

The six simultaneous partial differential equations have six characteristics in the position-time plane which everywhere have the local velocities $u \pm a$, u and u_p, where u_p is counted threefold. This degeneracy of the u_p-characteristics was explained by Sauerwein and Fendell (97) as a consequence of neglecting the partial pressure of the particles. Flow changes along the characteristics are given by equations which contain all the terms of a pure-gas flow, e.g., Rudinger (98), with additional terms that are proportional to the local particle concentration. The most distinguishing feature of large-amplitude waves is their continually changing wave form with the possibility that compression waves coalesce to form shock waves at initially unknown times and locations. Numerical solutions therefore may involve substantial computational efforts.

A different approach was taken by Johnson, et al. (99) who explored the "particle-in-cell" method, e.g., Amsden (100). Their example of shock propagation and reflection yielded good agreement with results obtained by the method of characteristics. They concluded that the method could be applied with confidence to problems in two and three dimensions, as had been done for problems of pure-gas flow.

7. NOZZLE FLOW

For a steady flow through a nozzle, Eqs. (31), (32), and (34) can be integrated to yield algebraic relationships which must be solved together with the remaining Eqs. (33), (35), and (36). This system of equations can readily be written in a form that is suitable for numerical integration for a prescribed flow at the nozzle inlet and a selected nozzle shape $A(x)$, e.g., Bailey, et al. (84), Hultberg and Soo (101), Soo (2). In general, the prescribed inlet flow may not be able to pass through the nozzle throat (choking) or may recompress, instead of expand, after passing through the throat. This behavior is a general property of nonequilibrium nozzle flows, since the flow rate compatible with a throat area depends on the relaxation processes in the nozzle. It is then necessary to use some iteration scheme by changing either the throat or the inlet flow until compatible conditions are found.

Because of the lateral flow accelerations in the nozzle, the particles tend to move toward the nozzle wall in the convergent section and stay near the axis in the divergent section (see also A.2.1). A schlieren photograph of a two-dimensional nozzle flow with 14.4-μm particles by Gilbert et al. (102) is shown in Fig. 13. These authors state that the result with 2.7-μm particles is "remarkably similar." It can be seen that the particle distribution is only moderately nonuniform in the convergent section near the throat but severely so in the divergent section. The size of the nozzle in Fig. 13 was not stated, but one should expect the nonuniformity to become less severe as the size of the nozzle is increased. Calculations based on one-dimensional flow through the divergent section of a nozzle, therefore, may be only qualitatively correct.

To overcome the problem of uneven particle distribution in the divergent section, Bailey, et al. (84) determined the two-dimensional gas flow without particles by the method of characteristics for steady supersonic flow and then computed particle trajectories in this flow. Since the effect of the particles on the flow is neglected, this method is valid only for relatively low particle loading. A computing procedure, based on the method of characteristics, in which gas-particle interaction is taken into account, was developed by Kliegel and Nickerson (103) and used to compute the flow through various nozzles.

The performance of a nozzle is reduced by the losses resulting from particle lag. Bailey, et al. (84) emphasized that once an appreciable lag has been established during the flow accelerations, the loss cannot be recovered by lengthening of the nozzle to let the particles approach equilibrium with the gas. The losses can be minimized by making the area changes as gradual as possible, and within a prescribed overall length, an optimum nozzle shape can be determined. Optimum nozzle contours for gas-particle flow, apparently, were first derived by Marble (104) from the linearized flow equation. Later, Hoffman and Thompson (105) developed a numerical variational technique which was applied by Elsbernd and Hoffman (106) to a study of the influence of various design parameters on thrust and optimum nozzle contour. Their results are summarized in Table 2.

Table 2

Influence of design parameters on optimum thrust and nozzle contours (+ indicates a significant influence, and - denotes relative unimportance).

Parameters	Thrust	Contour
Particle size	+	-
Particle loading	+	+
Particle drag coefficient	+	-
Particle heat-transfer coefficient	-	-
Nozzle inlet angle	+	-
Radius of nozzle throat	-	+
Nozzle size	+	-

If the flow of a gas-particle mixture through a prescribed nozzle is needed, one must integrate the equations by one of the indicated methods. More convenient techniques are available if a general understanding is to be obtained rather than numerical answers to a specific problem.

One method is to assume that deviations from equilibrium are small. If one sets $\epsilon = 0$, $u = u_p$ and $T = T_p$, the basic equations reduce to the well-known equations for one-dimensional nozzle flow with the thermodynamic properties outlined in Section 4. Small deviations from this flow then may be analyzed by linearizing the equations in terms of a suitable small parameter. Rannie (107) and Marble (29,78) derived a number of relationships between the perturbations of the flow variables.

For larger deviations from equilibrium, an inverse method may be used, based on the assumption that $\epsilon = 0$ and that f and Nu are constants. If the particle velocity is prescribed as a function of x, Eq. (34) can be solved for the gas velocity. The remaining variables and the nozzle shape then can be found by successive substitution into the other basic equations. This approach, in which the nozzle shape A(x) is implied in the initial assumption for u(x), is no more arbitrary than if A(x) is assumed and $u_p(x)$ computed. For example, if u_p increases linearly with x, then $u_p/u = K$ is constant, and analytical relationships are obtained for all flow variables in the same form as the nozzle equations for one-dimensional gas flow with modified thermodynamic properties which are functions of K. For $K = 1$, these become equal to those given in Section 4. This method has been used by a number of authors, e.g., Soo (2,79), Bailey et al. (84), Kliegel (80). Nozzles for which the velocity ratio is constant have a shape similar to that of typical nozzles, particularly near the throat; Kliegel called them "constant-fractional-lag nozzles." A similar analysis was performed by Hassan (85) who assumed u_p to be proportional to $x^{\frac{1}{2}}$.

The foregoing analyses apply for particle loadings for which the particle volume can be neglected. If the ϵ-terms are retained in the equations, numerical integration is required. Rudinger (86) performed such calculations for the convergent section of constant-fractional-lag nozzles. The influence of the particle volume becomes noticeable when ϵ approaches 5%. In these flows, the gas and particle temperatures vary only slightly between the flow reservoir and the nozzle throat, consistent with the statement in Section 4 that high loadings tend to produce isothermal flow. If one assumes $T = T_p = \text{const}$, the energy equation and the heat-transfer equation are eliminated, and the remaining equations lead to simple algebraic solutions in terms of the velocity ratio K. A comparison of this approximate method with the "exact" solution, based on numerical integration of the equations, is shown in Fig. 14, where the ratios of the throat conditions, marked by asterisks, are plotted as functions of the loading ratio and the particle volume fraction at the nozzle inlet. Results of the approximate analysis with $\epsilon = 0$ are indicated by the broken lines. Subscripts r and o indicate condition at the reservoir and at the nozzle inlet. It is interesting to note that a range of η exists, roughly between 5 and 50, for which the isothermal flow with $\epsilon = 0$ agrees with the "exact" solution within about 3%. The agreement becomes poorer at lower loading ratios, where the flow should not be treated as isothermal, and at higher loading ratios, where the particle volume should not be neglected. The approximate theory with $\epsilon = 0$ leads to the particularly simple relationships

$$u_*/a_{e,r} = [\gamma(1 + \eta K)]^{-\frac{1}{2}} \tag{39}$$

$$p_*/p_r = e^{-\frac{1}{2}} = 0.6065 \tag{40}$$

$$A_*/A_o = u_o p_o/(u_* p_*) \tag{41}$$

The simplifications that result from the assumption of isothermal flow may have other useful applications. Rudinger (108) used it to analyze the addition of heated particles to a gas flow.

8. GAS-PARTICLE JETS

The limited information available on gas-particle jets is indicated in Section 2. If such jets behaved like equivalent gas jets, the large literature on gas jets would be directly applicable. To be equivalent, a gas jet should have not only the same average density but also the same mass flow and momentum flux.

Particles injected into a gas flow must travel a considerable distance to reach the gas velocity, and they may impact on the walls of the jet tube and thereby loose kinetic energy. In general, one should not assume, therefore, that the gas and particle velocities are equal. Let σ_1 and u_1 be the concentration and velocity of the gas jet which carries particles at a loading ratio η, concentration σ_p and velocity u_p; denote by σ_2 and u_2 the corresponding quantities of a heavier gas without particles. Equal average density then requires

$$\sigma_2 = \rho_2 = \sigma_1 + \sigma_p = \sigma_1 \left(1 + \eta \frac{u_1}{u_p}\right) \tag{42}$$

where Eq. (23) has been used. The flow rates are equal if $\rho_2 u_2 = \sigma_1 u_1 (1 + \eta)$. After substitution for ρ_2/σ_1 from Eq. (42), the ratio of the two gas velocities becomes

$$\left(\frac{u_2}{u_1}\right)_{\text{Eq. Flow}} = \frac{1 + \eta}{1 + \eta(u_1/u_p)} \tag{43}$$

Similarly, equal momentum flux requires $\rho_2 u^2_2 = \sigma_1 u^2_1 + \sigma_p u^2_p$, and it follows that

$$\left(\frac{u_2}{u_1}\right)_{\text{Eq. Mom.}} = \left[\frac{1 + \eta(u_p/u_1)}{1 + \eta(u_1/u_p)}\right]^{\frac{1}{2}} \tag{44}$$

It is always possible, at least in principle, to select a gas which satisfies Eq. (42), but Eqs. (43) and (44) can be satisfied simultaneously only if $u_p/u_1 = 1$ and then yield $u_2 = u_1$. Thus, a gas jet cannot be rigorously equivalent to a nonequilibrium gas-particle jet. Deviation from equivalence can be expressed by the parameter

$$\beta = \frac{(u_2/u_1)_{\text{Eq. Mom.}} - (u_2/u_1)_{\text{Eq. Flow}}}{(u_2/u_1)_{\text{Eq. Flow}}} \tag{45}$$

which is zero for $u_p/u_1 = 1$ and should be as small as possible if equivalence is to be approximated. (The conditions $\eta = 0$ or $\eta = \infty$ which also lead to $\beta = 0$ are trivial.) Substitution for η from Eq. (42) leads to the relationship between β and u_p/u_1 shown in Fig. 15 for several combinations of light and heavy gases and negligible particle volume ($\sigma_1 = \rho_1$). For any value of u_p/u_1, a maximum of β is reached when $\rho_2/\sigma_1 = 1 + (u_1/u_p)$. The locus of these maxima is shown as the broken line. Clearly, the particle velocity must be greater than 40 or 50% of the gas velocity if the equivalence condition is to be satisfied within a few percent. Rudinger (46) injected nitrogen jets carrying glass particles of 33-μm average size into a subsonic cross flow of air at loading ratios between 2.3 and 25. Penetration of the centerline of the jet trajectory, y, was determined from photographs. Separate experiments with a laser-Doppler system indicated that u_p/u_1 ranged from about 0.4 to 0.6 as the velocity of the carrier gas was varied between 20 and 90 m/s. The condition for equivalence thus was approximately satisfied, and the momentum-flux ratio, which alone determines penetration of a gas jet, was computed (with subscript s indicating the cross flow) as

$$J = \frac{\sigma_1 u^2_1 (1 + \eta u_p/u_1)}{\rho_s u^2_s} \tag{46}$$

Some results of these experiments are shown in Fig. 16, where the filled-in symbols indicate that two experimental points were too close together to be shown separately. This figure indicates that particle penetration increases as the loading ratio decreases. However, schlieren photographs of light and heavy pure-gas jets yielded a penetration that is considerably below that of the particles (broken line in Fig. 16). It was suspected that the particles separate from the carrier gas and behave as isolated particles. Indeed, calculations on this basis gave trajectories which could have been brought into agreement with the experimental observations by a small shift of the injection point. Such a shift should be expected as the result of the initial gas-particle interaction before the particles separate from the carrier gas. Confirmation of this behavior was obtained from simultaneous schlieren and regular photographs of jets for which helium was used as carrier gas.

It is interesting to compare these results with those obtained by Salzman (45) and Edelman et al. (44) referred to in Section 2. Salzman used loading ratios between about 11 and 22, and 15-μm particles. These particles probably reached a larger fraction of the gas velocity than the 33-μm particles of the foregoing experiments. He assumed velocity equilibrium and derived several correlations for the penetration, one of which is given by

$$\frac{y}{d} = 2.63J^{0.385}\left(\frac{x}{d}\right)^{0.23} \tag{47}$$

but also noted a displacement of the particle centerline relative to the gas centerline. Edelman et al. used 1 to 5-μm particles at loading ratios below 0.5 and observed that the gas and particle centerlines coincide. Thus, if the particles are sufficiently small, the concept of an equivalent jet may be applied, and existing correlations for gas jets may be used provided the momentum-flux ratio is properly computed. Large particles separate from the carrier gas; their trajectory can be computed as for isolated particles, but a small shift of the injection point may be needed. The magnitude of this shift and its dependence on the various parameters, such as the relaxation time τ_v, loading ratio, and jet diameter, are not known at this time. Intermediate particle sizes lead to intermediate trajectories.

9. EXAMPLES

A few examples are included in the preceding sections. Several more are given in the following to demonstrate other applications of the analysis to specific problems or to illustrate some aspect by experimental observations. A few references to related studies also are given.

Often a flow field is too complicated to be amenable to a mathematical analysis, for example, the particle trajectories in the flow through turbine cascades. Tabakoff et al (18,19,109) injected particles into the flow through a two-dimensional model and obtained high-speed motion pictures. A few trajectories are shown in Fig. 17 which indicates that small displacements can lead to widely different trajectories. Impact velocities derived from such data are useful for erosion studies, as discussed in Section 2 (see also A.4, B.3.5, and C.7 and 7).

Particle motion in a corner expansion of a supersonic flow - Prandtl-Meyer flow - represents another example of a two-dimensional flow. Assuming that the particles do not affect the flow, Marble (78) derived the equation for the particle trajectory and solved it numerically. He showed that the departure of the trajectory from the gas streamlines is due more to lag in the tangential than in the radial direction (see also B.2.2).

The development of chemical lasers requires understanding of the flow in small mixing nozzles where measurements are difficult because of the small dimensions and high flow velocities and temperatures. To assess the suitability of the laser-Doppler technique, calculations were performed for a flow of nitrogen through a typical convergent-divergent laser nozzle in which M = 4 is reached in a distance of about 60 mm. These calculations were based on the drag coefficient given by Eq. (10). Because of the low densities in the expanding gas, the correction factor of Eq. (11) was included and reached several hundred for low reservoir pressures. A few results are shown in Fig. 18, Moon (110), for a reservoir pressure of 10 atm., a reservoir temperature of 1330 K and calcium fluoride particles of various sizes. The velocity ratio u_p/u is plotted as a function of x/L, where x is measured from the throat and L is the total length of the nozzle. Clearly, particles much larger than 0.1 μm are not suitable tracers under such extreme conditions. Continuous operation of the laser-Doppler system requires up to about 10^5 particles/mm^3. The corresponding loading ratio is about 6×10^{-5} for 0.1-μm particles and 6×10^{-2} for 1-μm particles. To check the influence of this loading on the flow, an equilibrium flow was assumed and the velocity at the nozzle exit with and without particles was calculated. The difference was found to be less than 0.5% as long as the loading ratio did not exceed 0.01. Thus, 0.1-μm particles would not affect the flow significantly (see also A.3, C.7 and D.5).

To demonstrate how the nonlinearity of the equation of motion affects two-dimensional trajectories of single particles (Section 3.1), consider a particle injected with the velocity components u_{po} and v_{po} in the direction and at right angles to the direction of a constant gas flow having a velocity u. Using the drag law of Eq. (10), Rudinger (111) derived an analytical solution for the maximum particle penetration, Y. The ratio of this penetration to the penetration without cross flow is shown in Fig. 19 as a function of a Reynolds number, defined here as $Re = \rho D v_{po}/\mu$, for several values of $(u - u_{po})/v_{po}$. Clearly, penetration is significantly reduced unless $u - u_{po}$ is smaller than v_{po}. Numerical solutions for lateral injection of single particles were obtained also by Brandt and Perini (112), who used various drag coefficients and Mach number effects in their calculations. Otterman (113) analyzed the motion of particles injected into the boundary layer flow around the stagnation point of a body; he treated the flow as incompressible but included lateral forces on the particles that result from particle rotation and boundary-layer shear. The effect of four assumptions for the drag coefficient on the particle trajectory in different high-speed flow fields was explored by Korkan et al. (66). These authors found that the results are significantly affected for particles injected at 45° into a supersonic flow and for particle motion in a Prandtl-Meyer expansion. In contrast, particle trajectories behind an oblique shock are insensitive to the assumption for the drag coefficient.

The foregoing examples deal with single particles or particle concentrations low enough not to affect the gas flow. Liu (114) analyzed laminar incompressible gas-particle flow along an infinite flat plate which is impulsively accelerated to a constant velocity U. He assumed negligible particle volume and Stokes drag and derived the variations of the friction coefficient with time. Subsequently, Hamed and Tabakoff (115,116) analyzed the same problem but extended it by allowing for a finite particle volume according to Eq. (14) and by including in the analysis the lateral lift forces caused by particle slip and rotation in the shear layer near the plate. They defined a Reynolds number $Re = U^2\tau_v\rho/\mu$, which is thus a measure of the plate velocity, and introduced a transformed friction coefficient $C_f^* = C_f U(t\rho/\mu)^{\frac{1}{2}}$, where the wall shear stress is given $C_f\rho U^2/2$. Some of their results, for Re = 25 and several values of the density ratio ρ_p/ρ are shown in Fig. 20. The friction coefficient reaches a maximum shortly after the start of the motion and then decreases asymptotically toward its equilibrium value. Liu's limiting values for frozen and equilibrium flow are included in the figure. For frozen flow at t = 0, which is equivalent to the absence of particles, both theories give the same value $C_{f_o}^*$. For equilibrium flow, Liu's theory yields $C_{f_e}^* = (1 + \eta)^{\frac{1}{2}}$ which agrees well with the theory of Hamed and Tabakoff. It also indicates a maximum of the friction coefficient near $t/\tau_v = 1.5$, but the maximum appears to be slightly lower. The good agreement

between these theories indicates that the additional effects included by Hamed and Tabakoff have only a minor effect, at least, at the low velocities considered. The lateral forces produce a particle-free layer of thickness y_v near the wall. The ratio y_v/D is shown in Fig. 21 as a function of the dimensionless time t/τ_v for $\epsilon_o = 0.001$, $\rho_p/\rho = 450$, and several values of a Reynolds number defined as before. The thickness of the particle-free layer is only a few particle diameters, but the largest indicated Reynolds number of 100 corresponds to a plate velocity of only about 3 m/s for 10-μm particles.

The problem of an oscillating infinite flat plate was analyzed by Liu (117), and steady flow over a semi-infinite flat plate was treated by Marble (29,78) and Singleton (118). Boundary-layer flows of gas-particle mixtures were studied also by Soo (2), Otterman and Lee (11) and Tabakoff and Hamed (22).

According to these analyses, the pressure gradient in a laminar flow increases with increasing particle loading. In turbulent flow through pipes the opposite behavior may be observed under some conditions. This effect has been known for some time, and various explanations have been suggested, as indicated in Section 2. Typical results by Kane and Pfeffer (50) are shown in Fig. 22. These data were obtained in a vertical flow of air with 36-μm glass particles. The friction coefficient with and without particles is defined in terms of the gas variables for consistent interpretation of the data. Thus, the pressure gradient for the flow with solids is given by $f_s\rho u^2/2d$ and that for the clean gas flow by $f_g\rho u^2/2d$, where d is the duct diameter. The ratio of the friction factors f_s/f_g is shown in the figure as a function of the loading ratio for several Reynolds numbers, defined here as $Re_g = \rho du/\mu$. A marked reduction of the friction factor can be seen to occur for some conditions. Drag reduction was achieved for all particle sizes (15-55 μm) in vertical tubes but only for the smaller sizes in horizontal tubes indicating a detrimental effect of sedimentation. The effect is only a weak function of Re_g. As pointed out in Section 2 it appears that this phenomenon can be explained by the thickening of the laminar sublayer caused by the particles.

10. UNRESOLVED PROBLEMS

The preceding sections indicate the variety of gas-particle flows that are of practical importance and methods available for their analysis. Unresolved problems still remain, and some of these are discussed in the following.

The choice of an appropriate drag coefficient must be faced for almost every analysis. This problem is discussed at some length in Section 3.2. The customary approach has been either to ignore this problem and use the standard drag coefficient, or even Stokes drag, or to use a drag coefficient derived from experimental observations in a different flow system. Since determination of the drag coefficient for the system of interest is generally not practical, a more detailed analysis of the processes that affect the particle motion would be desirable but extremely difficult. In numerical evaluations of specific flows, at least the sensitivity of the results to various assumptions for the drag coefficient should be assessed (see, for instance, Fig. 6). A similar uncertainty exists with respect to the heat-transfer coefficient. This parameter affects mainly the gas and particle temperatures and has only a small influence on the particle motion, as indicated by Figs. 6 and 7. It should be of concern for calculations that involve mass transfer between the gas and the particles or heat transfer to and from the walls of the duct which were not considered here.

In many flows of practical importance, the gas cannot be considered as perfect. Work is currently in progress at AECD to study particle trajectories in real-gas flow through Prandtl-Meyer expansions, oblique shocks and nozzles, using the latest drag-coefficient data.

Throughout this entire review, the particles are considered to be spherical, a condition that is rarely satisfied in engineering applications. Several measures to indicate the size of irregularly shaped particles can be defined, Fuchs (1), Lapple (27), such as sieve size or the diameter of a sphere having the same volume as the particle. A frequently used measure is the Stokes diameter which is the diameter of a sphere having the same settling velocity and therefore the same drag coefficient. This measure appears to be the most reasonable one to use for calculations of non-equilibrium flows. Some shapes, such as disks or cylinders tend to settle in a preferred orientation and may also perform an oscillatory motion during settling, Marchildon, et al. (120,121) Christiansen and Barker (122); it seems unlikely that this orientation is maintained in the turbulent environment of a flowing suspension with a resultant uncertainty of the drag coefficient. Relationships between drag coefficient and particle shape and concentration remain to be established.

The lack of information on gas-particle jets is emphasized in Sections 2 and 8. If such jets are injected into a cross flow, sufficiently small particles remain substantially immersed in the gas jet, and their penetration does not depend on the particle size. Sufficiently large particles should be expected to separate from the gas jet and move along a trajectory that depends on the relaxation time τ_v; penetration then increases approximately with the square of the particle size. The extent of the different regimes and its dependence on the flow variables is largely unknown at this time, and considerably more work is needed before these flows are fully understood. Injection into a cross flow through a longitudinal slot is mentioned in Section 2 in connection with water-augmented air cushion vehicles. No information on such flows appears to be available even for pure-gas jets.

In Section 9, the different behavior of the friction coefficient for laminar and turbulent flow is discussed, and it is clear that simply replacing the viscosity by a constant eddy viscosity could not account for the observed variations of the friction coefficient in turbulent flow. As in the case of turbulent flow of a pure gas, the basic equations should include terms corresponding to the Reynolds stresses. Such equations were derived by Panton (123), but no models have been developed so far to evaluate these additional terms.

There are many still unresolved problems also in the fields of instrumentation, design of engineering equipment, and analysis of flows that involve processes specifically excluded in the preceding sections. Their discussion would go beyond the scope of the present review.

11. REFERENCES

(1) Fuchs, N. A., "The Mechanics of Aerosols," MacMillan, New York, 1964.

(2) Soo, S. L., "Fluid Dynamics of Multiphase Systems," Blaisdell, Waltham, Mass., 1967.

(3) Torobin, L. B. and Gauvin, W. H., "Fundamental Aspects of Solids-Gas Flow. Part I: Introductory Concepts and Idealized Sphere Motion in Viscous Regime," Canad. J. Chem. Engng., Vol. 37, pp. 129-141, 1959. "Part II: The Sphere Wake in Steady Laminar Fluids," ibid., pp. 167-176, 1959. "Part III: Accelerated Motion of a Particle in a Fluid," ibid., Vol. 38, pp. 224-236, 1959. "Part IV: The Effects of Particle Rotation, Roughness and Shape," ibid., pp. 142-153, 1960. "Part V: The Effects of Fluid Turbulence on the Particle Drag Coefficient," ibid., pp. 189-200, 1960. "The Drag Coefficients of Single Spheres Moving in Steady and Accelerated Motion in a Turbulent Fluid," AIChE J., Vol. 7, pp. 615-623, 1961.

(4) Stevenson, W. H. and Thompson, H. D., Editors, "The Use of the Laser-Doppler Velocimeter for Flow Measurements," Workshop Proceedings, Project SQUID, Purdue University, 1972.

(5) Stern, A. C., Editor, "Air Pollution," Vol. I, Second Ed., Academic Press, New York, 1968.

(6) Soo, S. L., "Diffusion and Fallout of Particulates Emitted by Aircraft Engines," ASME Paper 71-WA/AV-2, 1971.

(7) Kalavsky, P. Z. and Rudin, L., "The Attenuation of Air Blast by Rain, Part 1, The Effect of Water Content in Air on the Peak Shock Overpressures Produced by Small Charges," Nav. Ord. Lab. NAVORD Report 3646; AFSWP Report 1121 (AD-218770), 1959.

(8) Temkin, S. and Dobbins, R. A., "Attenuation and Dispersion of Sound by Particulate-Relaxation Processes," J. Acoust. Soc. Am., Vol. 40, pp. 317-324, 1966.

(9) Temkin, S. and Dobbins, R. A., "Measurements of Attenuation and Dispersion of Sound by an Aerosol," J. Acoust. Soc. Am., Vol. 40, pp. 1016-1024, 1966.

(10) Rudinger, G., "Wave Propagation in Suspensions of Solid Particles in Gas Flow," Appl. Mech. Reviews, Vol. 26, pp. 273-279, 1973.

(11) Horton, M. D. and McGie, M. R., "Particulate Damping of Oscillatory Combustion," AIAA J., Vol. 1, pp. 1319-1326, 1963.

(12) Dobbins, R. A. and Temkin, S., "Propagation of Sound in a Gas-Particle Mixture and Acoustic Combustion Instability," AIAA J., Vol. 5, pp. 2182-2186, 1967.

(13) Spencer, J. D., Joyce, T. J., and Faber, J. H., Editors, "Pneumatic Transportation of Solids," U.S. Dept. of the Interior, Bureau of Mines, Pittsburgh, Pa., IC8314, 1966.

(14) Owen, P. R., "Pneumatic Transport," J. Fluid Mech., Vol. 39, pp. 407-432, 1969.

(15) Thornton, W. A., "The Pneumatic Transport of Solids in Pipes - A Bibliography," British Hydromechanics Research Association, Cranfield, Bedford, 1972.

(16) Langmuir, I. and Blodgett, K., "Mathematical Investigation of Water Droplet Trajectories," Army Air Forces Technical Report No. 5418, Washington, D.C., 1946.

(17) Probstein, R. F. and Fassio, F., "Dusty Hypersonic Flows," AIAA J., Vol. 8, pp. 772-779, 1970.

(18) Tabakoff, W. and Hussein, M. F., "Trajectories of Particles Suspended in Fluid Flow Through Cascades," J. Aircraft, Vol. 8, pp. 60-62, 1971.

(19) Tabakoff, W. and Hussein, M. F., "Measurements of Particulated Gas Flow Pressure on Cascade Nozzles," J. Aircraft, Vol. 8, pp. 121-123, 1971.

(20) Tabakoff, W. and Hussein, M. F., "Pressure Distribution on Blades in Cascade Nozzles for Particulate Flow," J. Aircraft, Vol. 8, pp. 736-738, 1971.

(21) Tabakoff, W. and Hussein, M. F., "Effect of Suspended Solid Particles on the Properties in Cascade Flow," J. Aircraft, Vol. 9, pp. 1514-1519, 1971.

(22) Tabakoff, W. and Hamed, A., "Analysis of Cascade Particle-Gas Boundary Layer Flows with Pressure Gradient," AIAA Paper 72-87, 1972.

(23) Clevenger, W. B., Jr. and Tabakoff, W., "Erosion in Radial Inflow Turbines - Vol. I: Erosive Particle Trajectory Similarity," NASA CR-134589. "Vol. II: Balance of Centrifugal and Radial Drag Forces on Erosive Particles," NASA CR-134616, 1974.

(24) Grant, G. and Tabakoff, W., "Erosion Prediction in Turbo-machinery Due to Environmental Solid Particles," AIAA Paper 74-16, 1974.

(25) Levin, L. M., "Precipitation of Particles from an Aerosol Stream on Obstacles," Dokl. Akad. Nauk SSSR, Vol.. 91, pp. 1329-1332, 1953.

(26) Golovin, M. N. and Putnam, A. A., "Inertial Impaction on Single Elements," I&EC Fundamentals, Vol. I, pp. 264-273, 1962.

(27) Lapple, C. E., "Particle-Size Analysis and Analyzers," Chem. Engng., May 20, pp. 1-8, 1968.

(28) Marble, F. E., "Mechanics of Particle Collision in the One-Dimensional Dynamics of Gas-Particle Mixtures," Phys. Fluids, Vol. 7, pp. 1270-1282, 1964.

(29) Marble, F. E., "Dynamics of Dusty Gases," Annual Review of Fluid Mechanics, Vol. 2, pp. 397-446, 1970.

(30) Temkin, S., "Cloud Droplet Collision Induced by Thunder," J. Atmospheric Sci., Vol. 26, p. 776, 1969.

(31) Leva, M., "Fluidization," McGraw-Hill, New York, 1959.

(32) Zenz, F. A.and Othmer, D. F., "Fluidization and Fluid-Particle Systems," Reinhold, New York, 1960.

(33) Hatch, L. P., Regan, W. H., and Powell, J. R., "Fluidized Solids as a Nuclear Fuel for Rocket Propulsion," ARS Journal, Vol. 31, pp. 547-548, 1961.

(34) Jackomis, W. N. and von Ohain, H. J. P., "Aeromechanical Characteristics of Nuclear Reactor Cavities Using Colloidal Fuels," AIAA Paper No. 70-1222 or U.S. Air Force, Aerospace Research Labs. Wright-Patterson Air Force Base, Report ARL 70-0272, 1970.

(35) Turman, B. N. and Hasinger, S. H., "Experimental Flow Studies of the Colloid Core Reactor Concept," U.S. Air Force, Aerospace Research Labs., Wright-Patterson Air Force Base, Report ARL 71-0281, 1971.

(36) Ravets, J. M., Black, D. L, Faulkner, J. E., et al., "Parametric Study of the Colloid Core Reactor Rocket Engine," U.S. Air Force, Energy Conversion Research Lab./Aerospace Research Labs., Wright-Patterson Air Force Base, Report ARL TR 74-0017, 1974.

(37) Johnson, E. G. and von Ohain, H. J. P., "Generation of Ultra High Total Enthalpy Gases through Multicomponent Flow Techniques," AIAA Paper 72-167. See also Synoptic AIAA J., Vol. 10, pp. 1561-1562, 1972.

(38) Hope-Gill, C. D., Rudinger, G., Zelazny, S. W., and Morgenthaler, J. H., "Bell Aerospace Water-Augmented Vehicle (WAVE) Study," National Technical Information Service Report No. AD-765332, 1973.

(39) Abramovich, G. N., "The Theory of Turbulent Jets," M.I.T. Press, Cambridge, Mass., 1963.

(40) Margason, R. J., "The Path of a Jet Directed at Large Angles to a Subsonic Free Stream," NASA TN D-4919, 1968.

(41) Skifstad, J. G., "Aerodynamics of Jets Pertinent to VTOL Aircraft," J. Aircraft, Vol. 7, pp. 193-204, 1970.

(42) Kamotani, Y. and Greber, I., "Experiments on a Turbulent Jet in a Cross Flow," AIAA J., Vol. 10, pp. 1425-1429, 1972.

(43) Abramovich, G. N., "The Effect of Admixture of Solid Particles, or Droplets, on the Structure of a Turbulent Gas Jet," Soviet Physics - Doklady, Vol. 15, pp. 101-104, 1970.

(44) Edelman, R. B., Fconomos, C. and Boccio, J., "Analytical and Experimental Study of Some Problems in Two-Phase Flows Involving Mixing and Combustion with Application to the B-O-H-N System," AIAA Paper 70-737. See also AIAA J., Vol. 9, pp. 1935-1940, 1971.

(45) Salzman, R. N., "Injection of a Solid-Gas Jet into a Uniform Transverse Stream," Thesis, West Virginia University, Morgantown, W. Va., 1973.

(46) Rudinger, G., "Some Aspects of Gas-Particle Jets in a Cross Flow," ASME Paper 75-WA/HT-5, 1975.

(47) Richardson, J. F. and McCleman, M., "Pneumatic Conveying - Part II: Solids Velocities and Pressure Gradients in a One-Inch Horizontal Pipe," Trans. Instn. Chem. Engrs., Vol. 38, pp. 257-266, 1960.

(48) Sproull, W. T., "Viscosity of Dusty Gases," Nature, Vol. 190, pp. 976-978, 1961.

(49) Peskin, R. L. and Dwyer, H. A., "A Study of the Mean Flow Characteristics of Gas-Solid Suspensions," Rutgers University, New Brunswick, N.J., Technical Report, No. 101-ME-F, 1964.

(50) Kane, R. S. and Pfeffer, R., "Characteristics of Dilute Gas-Solids Suspensions in Drag Reducing Flow," NASA CR-2267, 1973.

(51) Pfeffer, R. and Kane, R. S., "A Review of Drag Reduction in Dilute Gas-Solid Suspension Flow in Tubes," Int. Conf. on Drag Reduction, Cambridge, England, Sept. 4-6, 1974, British Hydromechanics Research Assoc., Cranfield, Bedford. Proc. published 1976.

(52) Hinze, J. O, "Turbulence," McGraw-Hill, New York, 1959.

(53) Rudinger, G., "Relaxation in Gas-Particle Flow," Chapter 3 of Nonequilibrium Flows, Vol. 1, Part 1, P. P. Wegener, Editor, Marcel Dekker, New York, pp. 119-161, 1969.

(54) Hjelmfelt, A. T. and Mockros, L. F., "Motion of Discrete Particles in a Turbulent Fluid," Appl. Science Res., Vol. 16, pp. 149-161, 1966.

(55) Lewis, J. A. and Gauvin, W. H., "Motion of Particles Entrained in a Plasma Jet," AIChE J., Vol. 19, pp. 982-990, 1973.

(56) Beard, K. V. and Pruppacher, H. R., "A Determination of the Terminal Velocity and Drag of Small Water Drops by Means of a Wind Tunnel," J. Atmospheric Sciences, Vol. 26, pp. 1066-1072, 1969.

(57) Odar, F. and Hamilton, W. S., "Forces on a Sphere Accelerating in a Viscous Fluid," J. Fluid Mech., Vol. 18, pp. 302-314, 1964.

(58) Schlichting, H., "Boundary Layer Theory," 4th Edition, McGraw-Hill, New York, 1962.

(59) Putnam, A., "Integrable Form of Droplet Drag Coefficient," ARS J., Vol. 31, pp. 1467-1468, 1961.

(60) Maxworthy, T., "Accurate Measurements of Sphere Drag at Low Reynolds Numbers," J. Fluid Mech., Vol. 23, pp. 369-372, 1965.

(61) Schaaf, S. A. and Chambré, P. L., "Flow of Rarefied Gases." Section H of Fundamentals of Gas Dynamics, H. W. Emmons, Editor. "High Speed Aerodynamics and Jet Propulsion," Vol. III, Princeton University Press, Princeton, N.J., 1958.

(62) Carlson, D. J. and Hoglund, R. F., "Particle Drag and Heat Transfer in Rocket Nozzles," AIAA J. Vol. 2, pp. 1980-1984, 1964.

(63) Beckwith, I. E.and Bushnell, D. M., "Effect of Intermittent Water Injection on Aerodynamic Heating of a Sphere-Cone at Flight Velocities to 18000 Feet per Second," NASA TM X-1128. Constant parameters of the correlations may be found in Yanta (64).

(64) Yanta, W. J., "Measurements of Aerosol Size Distributions with a Laser-Doppler Velocimeter (LDV)," AIAA Paper 73-705, 1973.

(65) Bailey, A. B. and Hiatt, J., "Sphere Drag Coefficients for a Broad Range of Mach and Reynolds Numbers," AIAA J., Vol. 10, pp. 1436-1440, 1971. More extensive data are given in the report by the same authors: Free-Flight Measurements of Sphere Drag at Subsonic, Transonic, Supersonic and Hypersonic Speeds for Continuum, Transition and Near-Free-Molecular Flow Conditions. ARO, Inc., Report No. AEDC-TR-70-291.

(66) Korkan, K. D., Petrie, S. L., and Bodonyi, R. J., "Particle Concentrations in High-Mach Number Two-Phase Flows," AIAA Paper 74-606, 1974.

(67) Henderson, C. B., "Drag Coefficients of Spheres in Continuum and Rarefied Flows,", AIAA J., Vol. 14, pp. 707-708, 1976.

(68) Hoglund, R. F., "Recent Advances in Gas-Particle Nozzle Flows," ARS J., Vol. 32, pp. 662-671, 1962.

(69) Ingebo, R. D., "Drag Coefficients for Droplets and Solid Spheres in Clouds Accelerated in Air Streams," NACA TN 3762, 1956.

(70) Crowe, C. T., Nicholls, J. A. and Morrison, R. B., "Drag Coefficients of Inert and Burning Particles Accelerating in Gas Streams," Ninth Symp. (International) on Combustion, Academic Press, New York, pp. 395-406, 1963.

(71) Selberg, B. P. and Nicholls, J. A., "Drag Coefficient of Small Spherical Particles," AIAA J., Vol. 6, pp. 401-408, 1968.

(72) Rudinger, G., "Experiments on Shock Relaxation in Particle Suspensions in a Gas and Preliminary Determination of Particle Drag Coefficients," Multi-Phase Flow Symposium, N.J. Lipstein, Editor, ASME, New York, pp. 55-61, 1963.

(73) Rudinger, G., "Effective Drag Coefficient for Gas-Particle Flow in Shock Tubes," Trans. ASME, J. Basic Engng., Vol. 92D, pp. 165-172, 1970.

(74) Rudinger, G., "Reply to Comments by S. L. Soo," see ref. (90), Phys. Fluids, Vol. 7, pp.1884-1885, 1964.

(75) Tam, C. K. W., "The Drag on a Cloud of Spherical Particles in Low Reynolds Number Flow," J. Fluid Mech., Vol. 38, pp. 537-546, 1969.

(76) Knudsen, J. G. and Katz, D. L., "Fluid Mechanics and Heat Transfer," McGraw-Hill, New York, 1958.

(77) Simmons, F. S. and Spadaro, F. G., "Thermal Lag of Solid Carbon in Rocket Nozzle Flow," Pyrodynamics, Vol. 2, pp. 177-189, 1965.

(78) Marble, F. E., "Dynamics of a Gas Containing Small Solid Particles," Combustion and Propulsion, 5th AGARD Colloque, Pergamon Press, Oxford, pp. 175-213, 1963.

(79) Soo, S. L., "Gas Dynamic Processes Involving Suspended Solids," AIChE J., Vol. 7, pp. 384-391, 1961.

(80) Kliegel, J., "Gas Particle Nozzle Flows," Ninth Symp. (International) on Combustion, Academic Press, New York, pp. 811-826, 1963.

(81) Kriebel, A. R., "Analysis of Normal Shock Waves in Particle Laden Gas," Trans. ASME, J. Basic Engng., Vol. 86D, pp. 665-665, 1964.

(82) Rudinger, G., "Some Effects of Finite Particle Volume on the Dynamics of Gas-Particle Mixtures," AIAA J., Vol. 3, pp. 1217-1222, 1965.

(83) Kraiko, A. N. and Sternin, L. E., "Theory of Flows of a Two-Velocity Continuous Medium Containing Solid or Liquid Particles," J. Appl. Math and Mech., Vol. 29, pp. 482-496 (Translated from the Russian), 1965.

(84) Bailey, W. S., Nielsen, E. N., Serra, R. A., and Zupnik, T. F., "Gas-Particle Flow in an Axisymmetric Nozzle," ARS J., Vol. 31, pp. 793-798, 1961.

(85) Hassan, H. A., "Exact Solutions of Gas-Particle Nozzle Flows," AIAA J., Vol. 2, pp. 395-396, 1964.

(86) Rudinger, G., "Gas-Particle Flow in Convergent Nozzles at High Loading Ratios," AIAA J., Vol. 8, pp. 1288-1294, 1970.

(87) Rudinger, G. and Chang, A., "Analysis of Nonsteady Two-Phase Flow," Phys. Fluids, Vol. 7, pp. 1747-1754, 1964.

(88) Migdal, D. and Agosta, V. D., "A Source Flow Model for Continuum Gas-Particle Flow," Trans. ASME, J. Appl. Mech., Vol. 34E, pp. 860-865, 1967.

(89) Wallis, G. B., "One-Dimensional Two-Phase Flow," McGraw-Hill, New York, 1969.

(90) Soo, S. L., "Comments on Shock Relaxation in Flows Carrying Particles," Phys. Fluids, Vol. 7, pp. 1883-1884, 1964.

(91) Carrier, G. F., "Shock Waves in a Dusty Gas," J. Fluid Mech., Vol. 4, pp. 376-382, 1958.

(92) Rudinger, G., "Some Properties of Shock Relaxation in Gas Flows Carrying Small Particles," Phys. Fluids, Vol. 7, pp. 658-663, 1964.

(93) Morgenthaler, J. H., "Analysis of Two-Phase Flow in Supersonic Exhausts",Detonation and Two-Phase Flow, S. S. Penner and F. A. Williams, Editors. Academic Press, New York, pp. 145-171, 1961.

(94) Okauchi, K., "Dusty Gas Flow Through an Oblique Shock Wave," J. Aero/Space Sciences,Vol. 29, pp. 230-231, 1962.

(95) Rudinger, G., "Discussion of Kriebel (81)," 1964.

(96) Epstein, P. S. and Carhart, R. R., "The Absorption of Sound in Suspensions and Emulsions," I. Water Fog in Air, J. Acoust. Soc. Am., Vol. 25, pp. 553-565, 1953.

(97) Sauerwein, H. and Fendell, F. E., "Method of Characteristics in Two-Phase Flow," Phys. Fluids, Vol. 8, pp. 1564-1565, 1965.

(98) Rudinger, G., "Nonsteady Duct Flow: Wave Diagram Analysis," Dover Publications, New York, 1969.

(99) Johnson, P. W., Massey, B. S. and Collins, R., "Propagation and Reflection of Plane Shock Waves in Dusty Gases," Brit. J. Appl. Phys., Vol. 17, pp. 1195-1200, 1966.

(100) Amsden, A. A., "The Particle-in-Cell Method for the Calculation of the Dynamics of Compressible Fluids," Los Alamos Scient. Lab. Report LA-3466, 1966.

(101) Hultberg, J. A. and Soo, S. L., "Two-Phase Flow Through a Nozzle," Astronautica Acta, Vol. 11, pp. 207-216, 1965.

(102) Gilbert, M., Allport, J., and Dunlap, R., "Dynamics of Two-Phase Flow in Rocket Nozzles," ARS J., Vol. 32, pp. 1929-1930, 1962.

(103) Kliegel, J. R. and Nickerson, G. R., "Flow of Gas-Particle Mixtures in Axially Symmetric Nozzles," Detonation and Two-Phase Flow, S. S. Penner and F. A. Williams, Editors, Academic Press, New York, pp. 173-194, 1962.

(104) Marble, F. E., "Nozzle Contours for Minimum Particle-Lag Loss," AIAA J., Vol. 1, pp. 2793-2801, 1963.

(105) Hoffman, J. D. and Thompson, H. D., "A General Method for Determining Optimum Thrust Nozzle Contours for Gas-Particle Flows," AIAA J., Vol. 5, pp. 1886-1887, 1967.

(106) Elsbernd, A. A. and Hoffman, J. D., "Maximum Thrust Nozzles for Gas-Particle Flows," AIAA J., Vol. 12, pp. 283-288, 1974.

(107) Rannie, W. D., "Perturbation Analysis of One-Dimensional Heterogeneous Flow in Rocket Nozzles," Detonation and Two-Phase Flow, S. S. Penner and F. A. Williams, Editors, Academic Press, New York, pp. 117-144, 1962.

(108) Rudinger, G., "Addition of Heated Solid Particles to a Gas Flowing in a Pipe," Trans. ASME, J. Basic Engng., Vol. 94D, pp. 81-88, 1972.

(109) Tabakoff, W., Hamed, A. and Hussein, M. F., "Experimental Investigation of Gas-Particle Flow Trajectories and Velocities in an Axial Flow Turbine Stage," ASME Paper 72-GT-57, 1972.

(110) Moon, L. F., "High Power Laser Mixing and Reacting Flow Characterization," Section D1 by G. Rudinger, Bell Aerospace Co., Report No. 9500-920309, 1973.

(111) Rudinger, G., "Penetration of Particles into a Constant Cross Flow," AIAA J., Vol. 12, pp. 1138-1140, 1974.

(112) Brandt, A. and Perini, L. L., "Particle Injection into a Uniform Flow," J. Spacecraft, Vol. 7, pp. 880-881, 1970.

(113) Otterman, B., "Motion of Particles Injected from the Surface into Stagnation Point Flow," AIAA J., Vol. 10, pp. 1079-1081, 1972.

(114) Liu, J. T. C., "Flow Induced by the Impulsive Motion of an Infinite Flat Plate in a Dusty Gas," Astronautica Acta, Vol. 13, pp. 369-377, 1967.

(115) Hamed, A. and Tabakoff, W., "Solid Particle Demixing in a Suspension Flow of Viscous Gas," Trans. ASME, J. Fluids Engng., Vol. 971, pp. 106-111, 1973.

(116) Hamed, A. and Tabakoff, W., "Analysis of Nonequilibrium Particulate Flow," AIAA Paper 73-687, 1973, see also Synoptic: "Some Effects Caused by Solid Particles in Flows," AIAA J., Vol. 12, pp. 581-582, 1974.

(117) Liu, J. T. C., "Flow Induced by an Oscillating Infinite Flat Plate in a Dusty Gas," Phys. Fluids, Vol. 9, pp. 1716-1720, 1966.

(118) Singleton, R. E., "The Compressible Gas-Solid Particle Flow Over a Semi-Infinite Flat Plate," J. Appl. Math. Phys. (ZAMP), Vol. 16, pp. 421-449, 1965.

(119) Otterman, B. and Lee, S. L., "Particle Migrations in Laminar Mixing of a Suspension with a Clean Fluid," J. Appl. Math. Phys. (ZAMP), Vol. 20, pp. 730-749, 1969.

(120) Marchildon, E. K., Clamen, A. and Gauvin, W. H., "Drag and Oscillatory Motion of Freely Falling Cylindrical Particles," Canad. J. Chem. Engng., Vol. 42, pp. 178-182, 1964.

(121) Marchildon, E. K., Clamen, A. and Gauvin, W. H., "Oscillatory Motion of Freely Falling Disks," Phys. Fluids, Vol. 7, pp. 2018-2019, 1964.

(122) Christiansen, E. B. and Barker, D. H., "The Effect of Shape and Density on the Free Settling of Particles at High Reynolds Numbers," AIChE J., Vol. 11, pp. 145-151, 1965.

(123) Panton, R., "Flow Properties for the Continuum View Point of a Nonequilibrium Gas-Particle Mixture," J. Fluid Mech., Vol. 31, pp. 273-303, 1968.

12. ACKNOWLEDGEMENTS

The author wishes to express his thanks to Dr. Robert O. Dietz, Director of Technology, Arnold Air Force Station, for the invitation to prepare this review for AGARD. The work was made possible through the support of Bell Aerospace Company; the Office of Naval Research, U.S. Department of the Navy, under Contract No. N00014-67-A-0226 (Project SQUID); and the Air Force Office of Scientific Research (AFSC), U.S. Air Force, under Contract No. F44620-70-C-0116.

The United States Government is authorized to reproduce and distribute reprints for governmental purposes notwithstanding any copyright notation hereon.

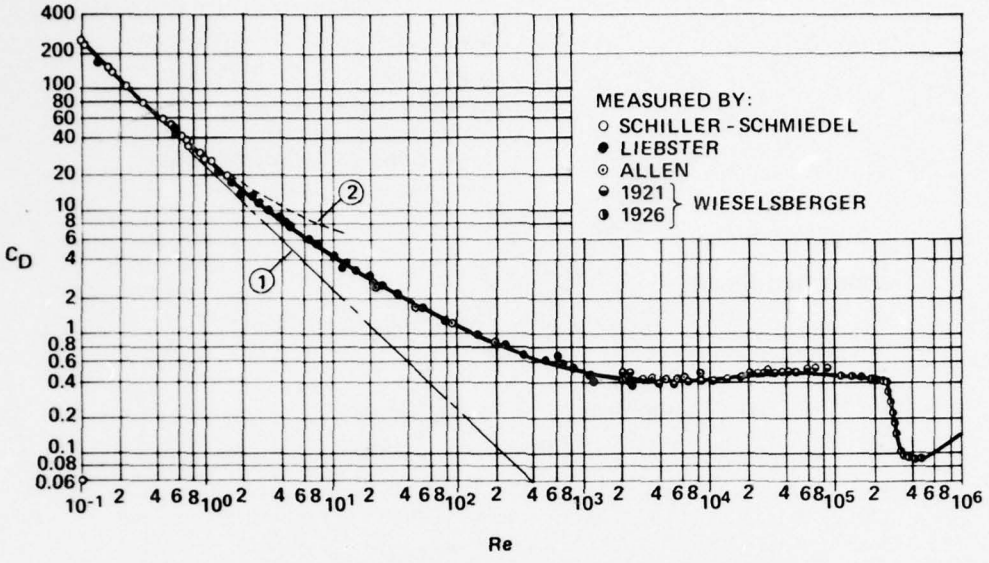

Figure 1 Standard drag coefficient for spheres, after Schlichting (58). (Reprinted with permission of McGraw-Hill Book Co.)

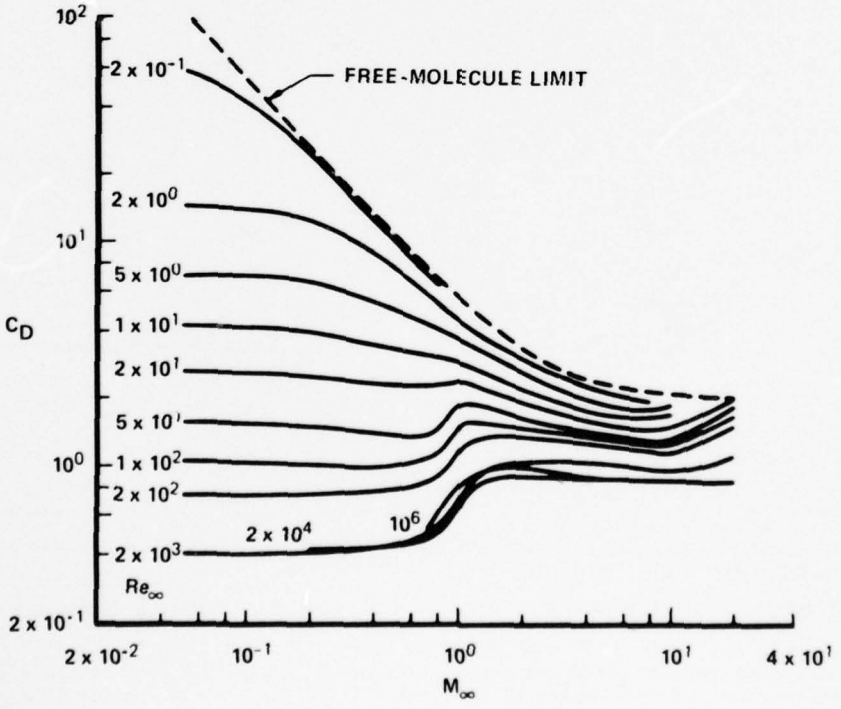

Figure 2 Summary of sphere drag coefficients. Ballistic-range data of Bailey and Hyatt (65). (Reprinted with permission of AIAA)

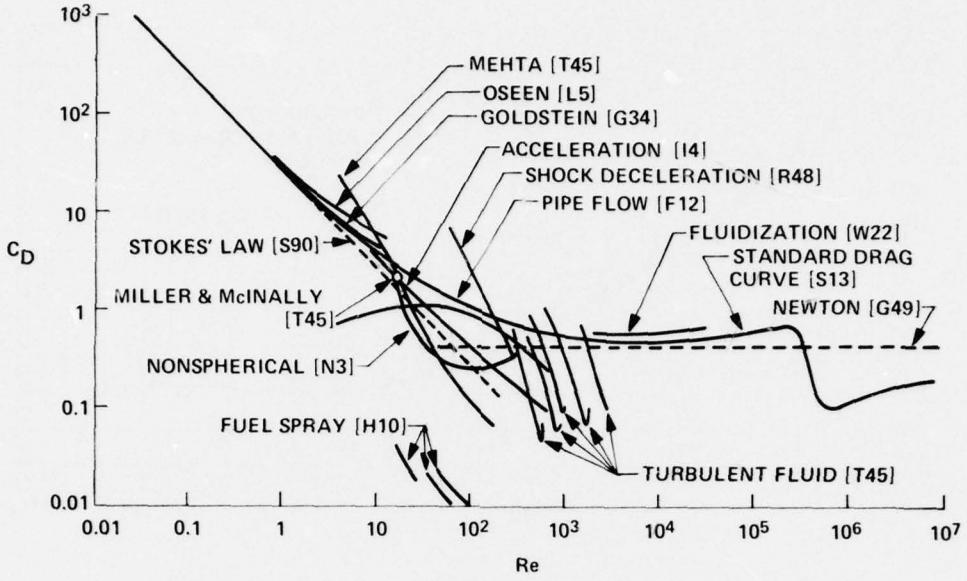

Figure 3 Drag coefficients obtained by several investigators for various flows, after Soo (2). (Reprinted with permission of Ginn and Co., Xerox Corp.)

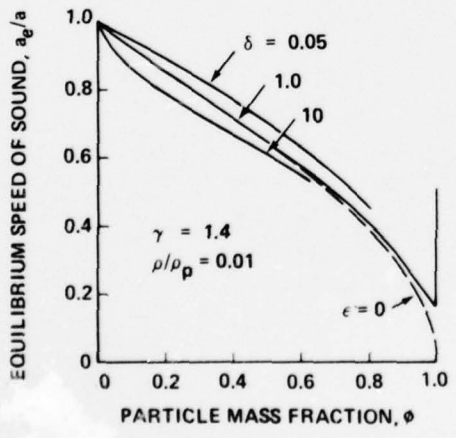

Figure 4 Equilibrium speed of sound for gas-particle mixtures, after Rudinger (82). (Reprinted with permission of Marcel Dekker, Inc.)

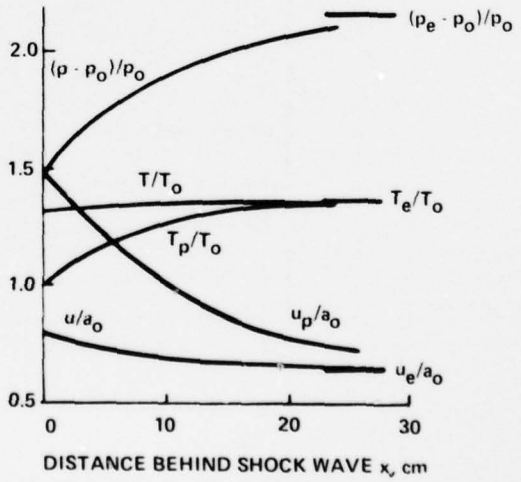

Figure 5 Relaxation zone behind a shock front for 10-μm glass spheres in air at standard temperature and pressure, for η = 0.2 and M_f = 1.50, corresponding to δ = 1.125, γ_M = 1.20, a_{eo}/a_o = 0.88 and M_e = 1.70; based on Ingebo's drag Eq. (13), and Nu = 2, after Rudinger (53). (Reprinted with permission of Marcel Dekker, Inc.)

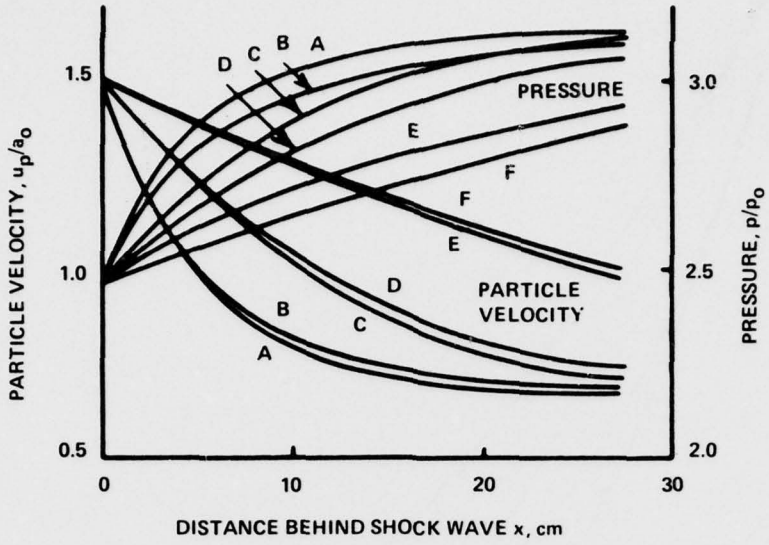

Figure 6 Effect of different assumptions for drag and heat transfer on pressure and particle velocity for the same mixture and shock strength as for Figure 5, Rudinger (53). (Reprinted with permission of Marcel Dekker, Inc.)

Drag Coefficient	Nusselt number Nu = 2	Nusselt number Eq. (16)
Standard	A	B
Ingebo, Eq. (13)	C	D
Stokes, Eq. (6)	E	F

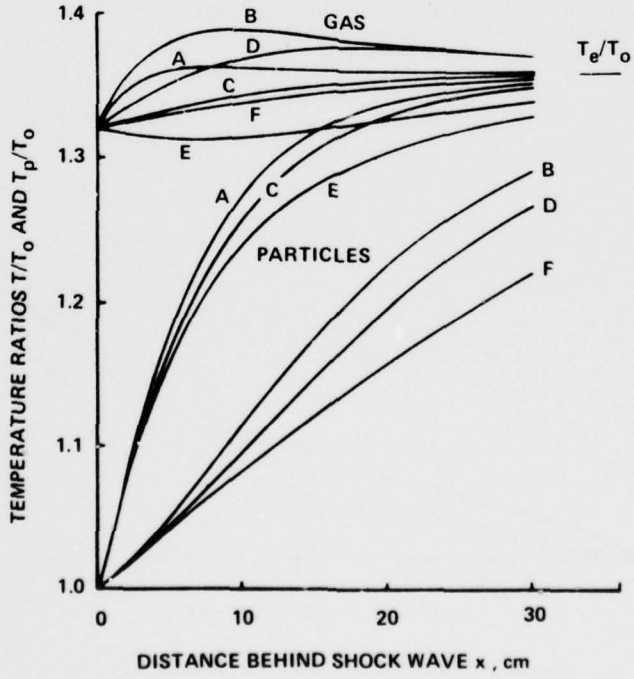

Figure 7 Effect of different assumptions for drag and heat transfer on the gas and particle temperatures for the same conditions for Fig. 6, Rudinger (53). (Reprinted with permission of Marcel Dekker, Inc.)

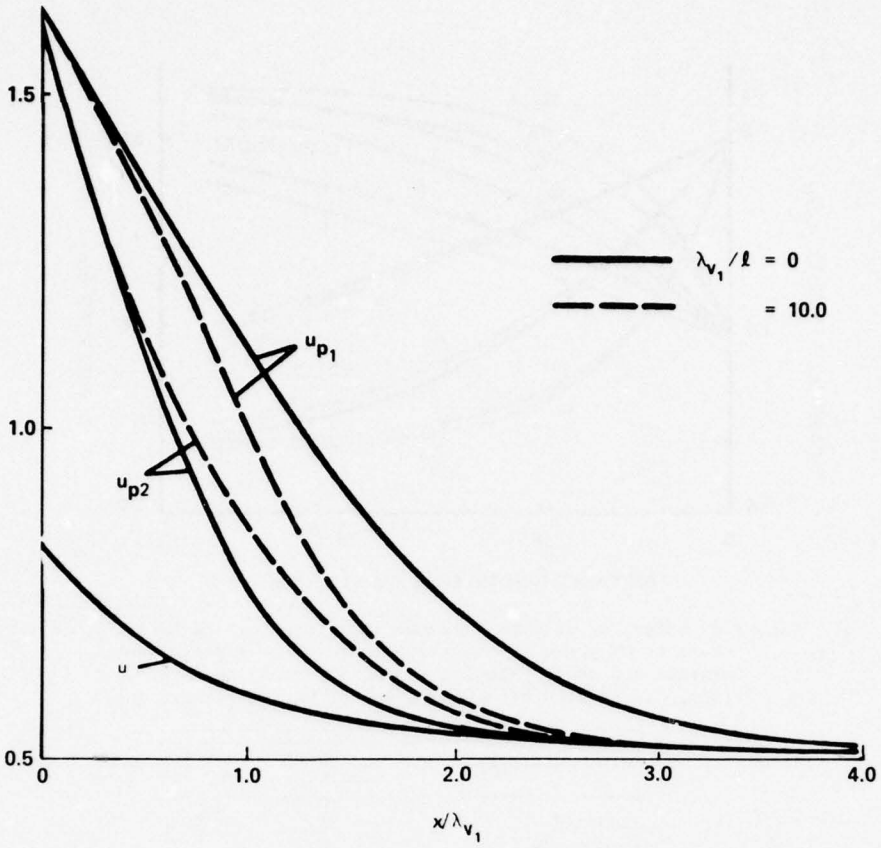

Figure 8 Velocity distribution behind a shock front. Solid lines indicate flow without particle collisions, broken lines with collision; $M_f = 1.6$, $\gamma = 1.4$, $\eta_1 = \eta_2 = 0.25$, $\tau_v/\tau_T = 1$, $D_1/D_2 = 1.5$, $\lambda_v = a\tau_v$, after Marble (29); a misprint in the identification of the lines has been corrected. (Reprinted with permission of Annual Reviews, Inc.)

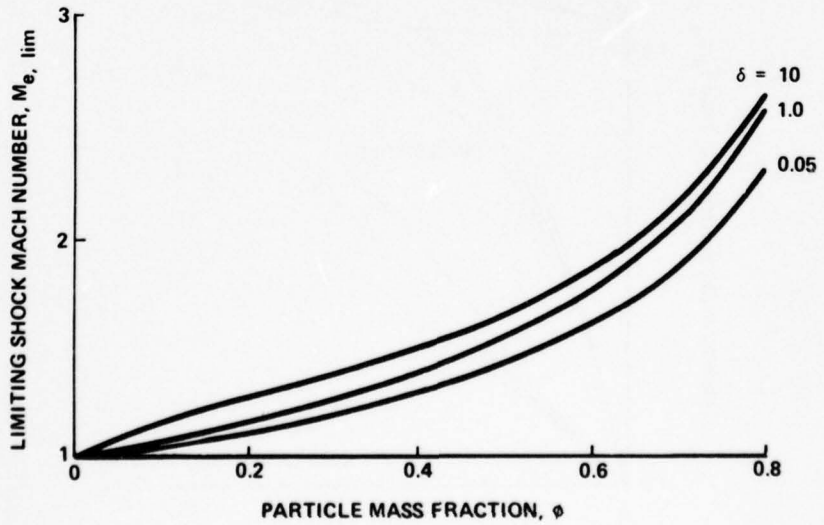

Figure 9 Limiting (minimum) shock Mach number for a discontinuous shock front, after Rudinger (53). (Reprinted with permission of Marcel Dekker, Inc.)

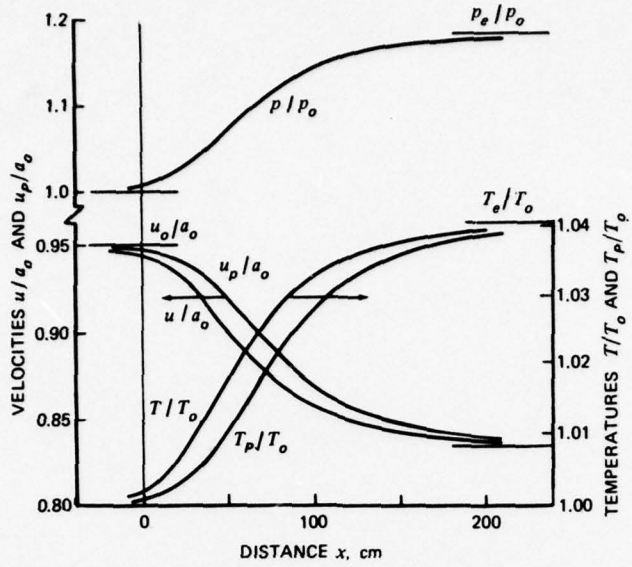

Figure 10 Dispersed shock wave computed for the same conditions as for Fig. 5 but for $M_f = 0.95$ corresponding to $M_e = 1.08$, after Rudinger (53). (Reprinted with permission of Marcel Dekker, Inc.)

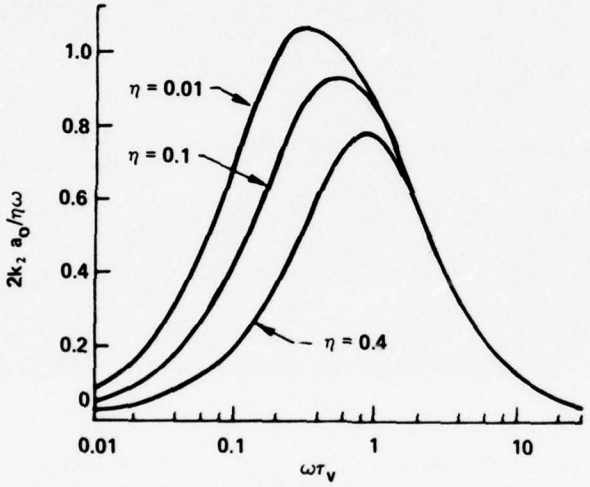

Figure 11 Attenuation of sound waves by water droplets in air; $\delta = 4.17$, Pr = 0.17, $\gamma = 1.4$, after Temkin and Dobbins, (8). (Reprinted with permission of the American Institute of Physics)

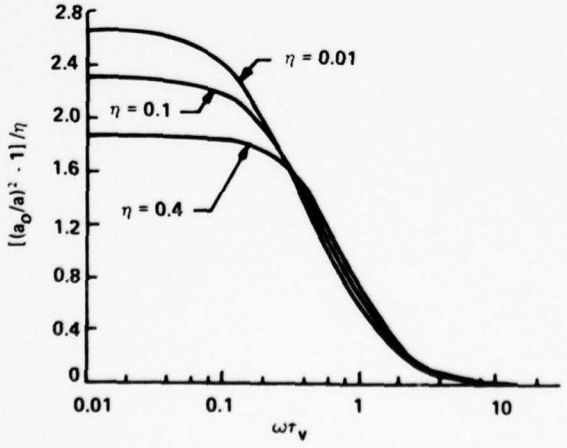

Figure 12 Dispersion of sound waves by water droplets in air for the same conditions as for Fig. 11, after Temkin and Dobbins (8). (Reprinted with permission of the American Institute of Physics)

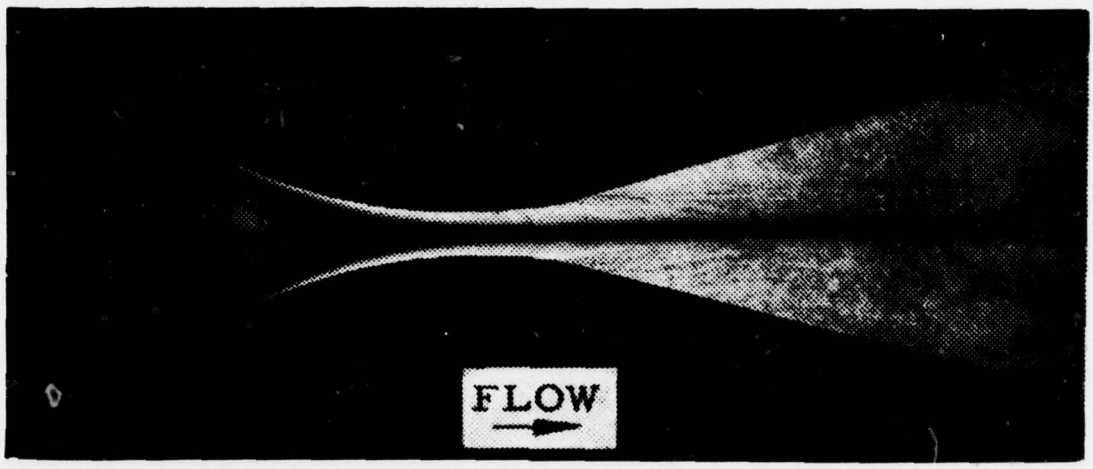

Figure 13 Two-phase flow in a two-dimensional nozzle for nitrogen with 14.4μm glass spheres; $\eta = 0.05$, $u_p/u \approx 0.35$, Gilbert, et al. (102). (Reprinted with permission of AIAA)

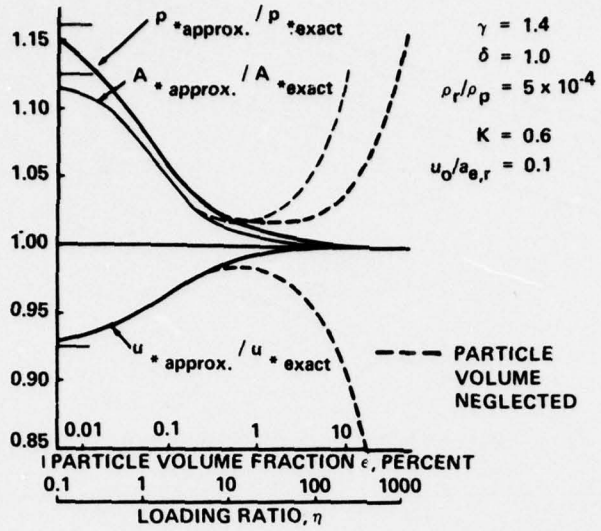

Figure 14 Comparison of the throat conditions based on "exact" and isothermal flow, after Rudinger (53). (Reprinted with permission of Marcel Dekker, Inc.)

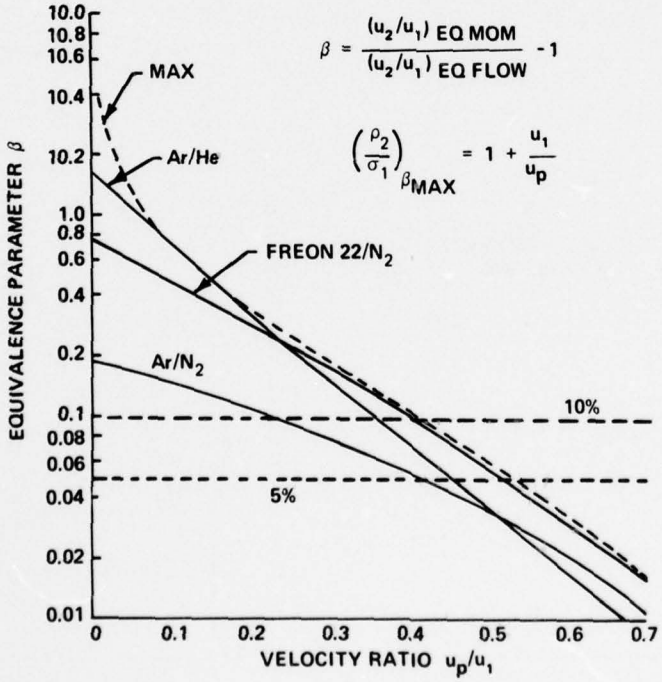

Figure 15 Equivalence between gas jets and gas-particle jets, Rudinger (46). (Reprinted with permission of ASME)

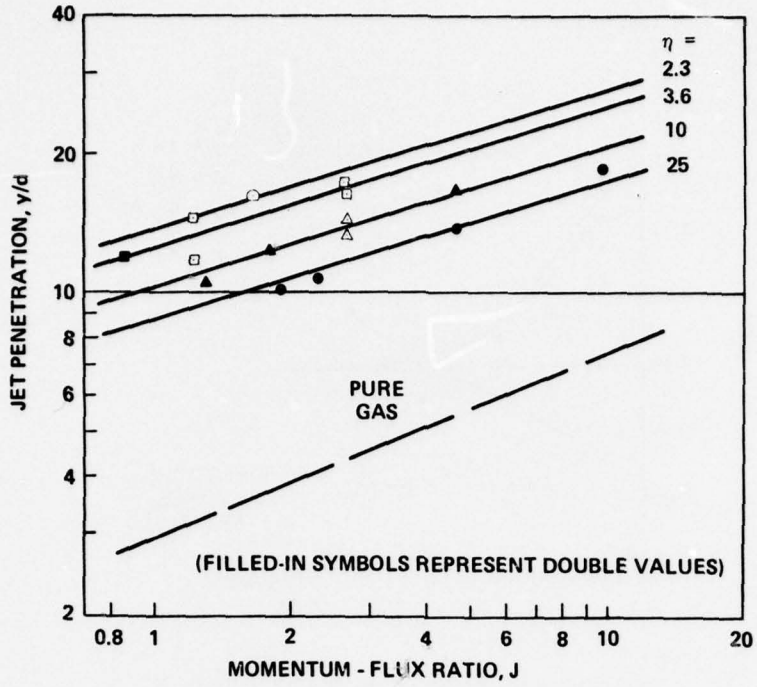

Figure 16 Correlation for the penetration of gas-particle jets into a cross stream, Rudinger (46). (Reprinted with permission of ASME)

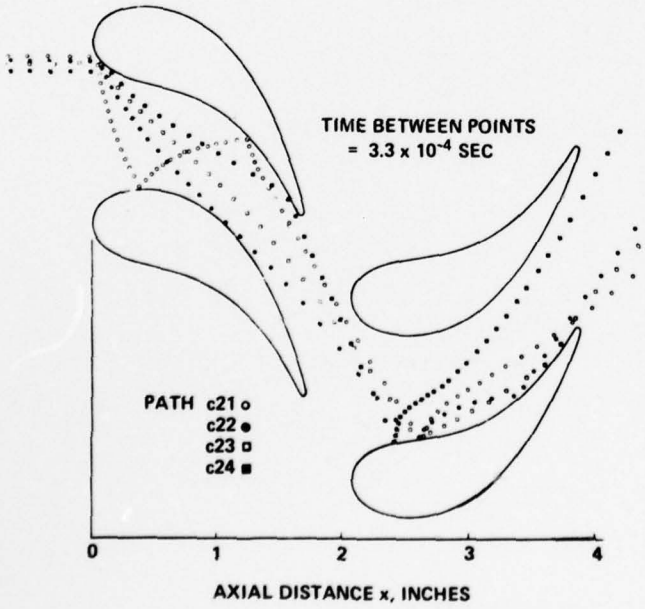

Figure 17 Particle trajectories in an axial-flow-turbine stage, Tabakoff, et al., (109). (Reprinted with permission of ASME)

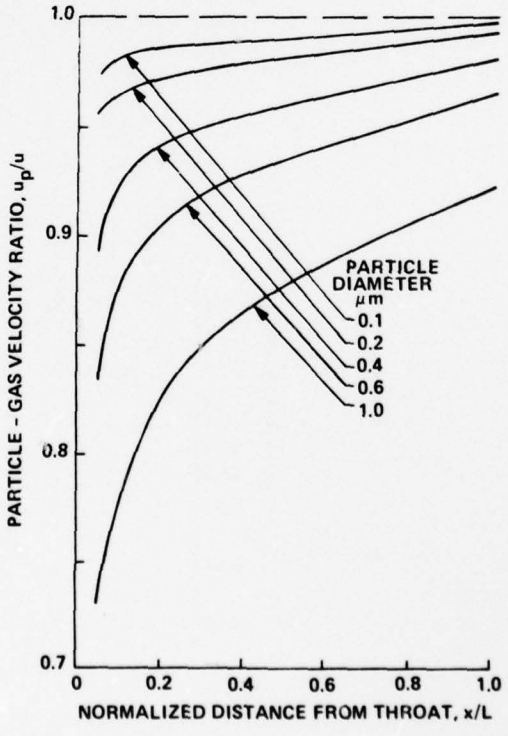

Figure 18 Effect of particle size on the tracking ability of particles in a typical laser nozzle, from Moon (110).

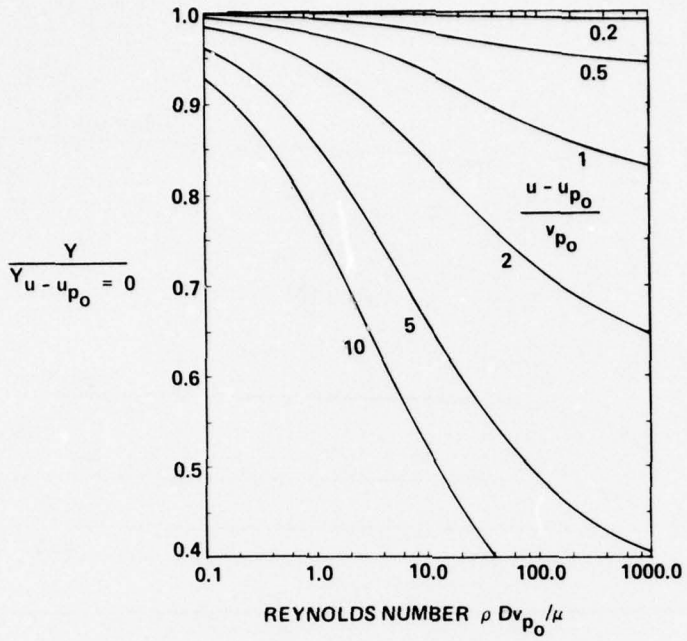

Figure 19 Ratio of the particle penetration into a cross flow to that without cross flow, Rudinger (111). (Reprinted with *permission* of AIAA)

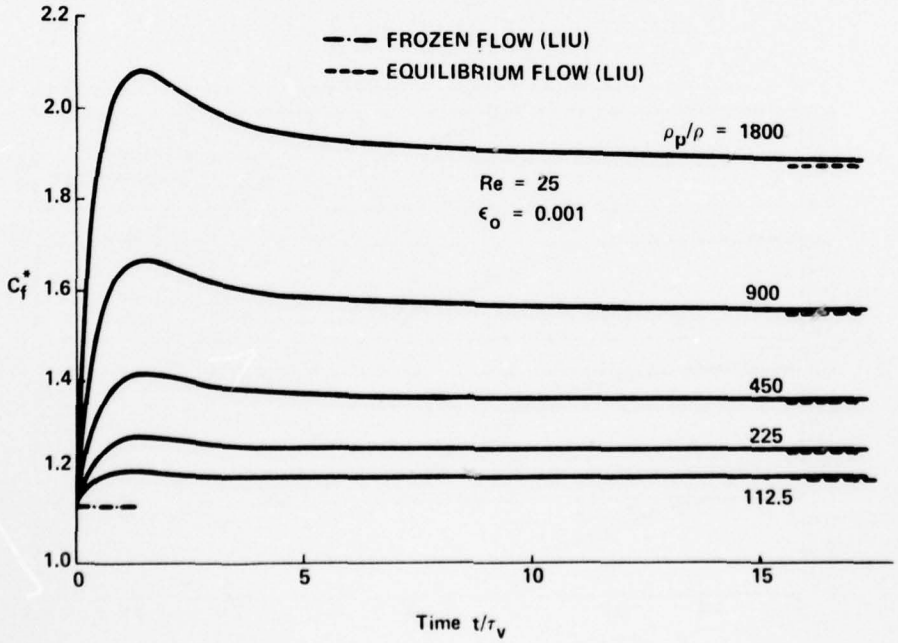

Figure 20 Effect of the particle-to-gas density ratio on the friction coefficient for an impulsively accelerated infinite flat plate, after Hamed and Tabakoff (116). (Reprinted with permission of AIAA)

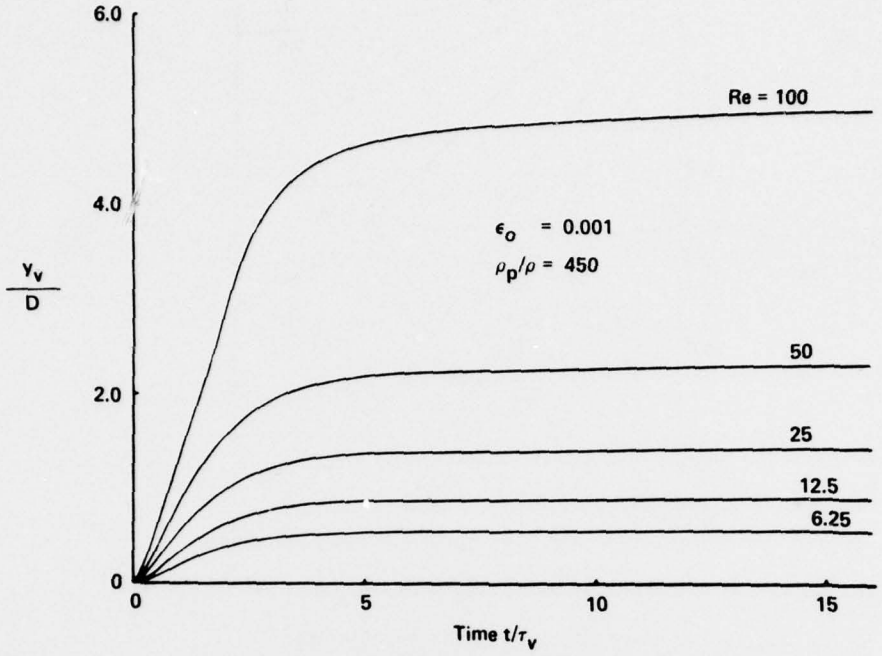

Figure 21 Development of a particle-free layer on an impulsively accelerated infinite flat plate, after Hamed and Tabakoff (115). (Reprinted with permission of ASME)

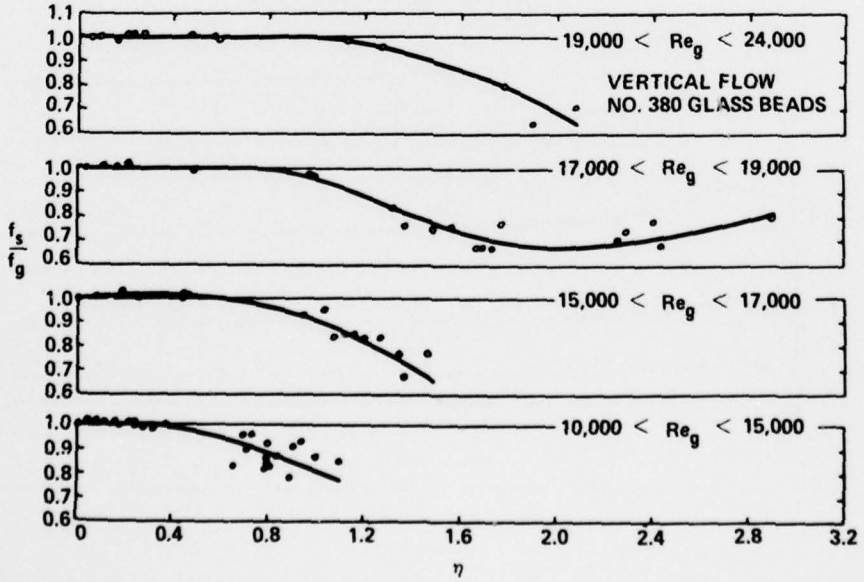

Figure 22 Ratio of friction factor with and without solid particle loading; 36-μm particles, Kane and Pfeffer (50).

INDEX